Sistemas Embebidos. Aplicaciones y Tendencias

Marco Antonio Aceves Fernández
Juan Manuel Ramos Arreguín
José Emilio Vargas Soto
Baldomero Manuel Sánchez Rangel

Primera edición, 2016.

Asociación Mexicana de Mecatrónica A.C.

Sistemas Embebidos: Aplicaciones y Tendencias.

Editado por: Marco Antonio Aceves Fernández, Juan Manuel Ramos Arreguín
José Emilio Vargas Soto y Baldomero Manuel Sánchez Rangel.

Publicado por
Asociación Mexicana de Mecatrónica, A. C.

Primera edición, Febrero 2016
Impreso en Querétaro, México.

ISBN 978-607-9394-05-9

En coloración con

Asociación Mexicana de Software Embebido A.C.

AMESE

y el
2do Congreso Internacional de Software
Embebido y Mecatrónica

Mensaje del presidente

Bienvenidos una vez más a nuestro congreso internacional de Sistemas Embebidos ICESM 2016. Es una satisfacción enorme ser parte de algo tan grande, para mi como primer presidente de la Asociación que fundamos varios colegas de Universidades, Empresas e Instituciones es casi como otro de mis hijos; lo vi nacer, está sano y sigue creciendo, me ha causado muchas alegrías, he pasado noches insomnes y me ha dado uno que otro dolor de cabeza. Al final de cuentas y después de todo, quiero a la Asociación.

Ha sido un año de trabajo arduo, con nuevas empresas afiliadas que nos tuvieron la confianza para poder lograr algunas de sus metas de manera conjunta. También tenemos capítulos estudiantiles nuevos, fruto de la sed de aprendizaje de jóvenes estudiantes de varias universidades, lo que personalmente me da una gran satisfacción.

En esta ocasión, hemos intentado varias cosas nuevas, siempre esperando que los asistentes, ya sean estudiantes, profesionistas, empresas, miembros de Universidades como profesores, coordinadores, etcétera, pueda serles de ayuda el esfuerzo de este gran equipo. Durante todo el año se estuvo escuchando las voces de nuestros profesionistas jóvenes y estudiantes principalmente. También se tuvo en cuenta los comentarios de las empresas que recientemente se afiliaron y las que nos tuvieron la confianza desde el principio que fundamos la Asociación Mexicana de Software Embebido.

Uno de los principales retos que pudimos escuchar de voz de los estudiantes son las oportunidades laborales terminando sus estudios, por lo que nos dimos a la tarea de traer empresas de clase mundial para que pudieran platicar con los alumnos acerca de las habilidades que estas empresas necesitan, al mismo tiempo que se les pudiera ofrecer puestos de empleo a los egresados y oportunidades de estancia para los que aún están estudiando. También hay más conferencias magistrales de líderes en su área, acreditaciones internacionales en los concursos y más artículos técnicos, a la vez de un “show room” de empresas líderes donde pudieran mostrar las innovaciones que han venido desarrollando. Así mismo, incluimos talleres de punta para que pudieran tener experiencia práctica en las nuevas tecnologías y desarrollos.

No puedo terminar este mensaje sin agradecer a nuestros anfitriones, el Tec de Monterrey campus Guadalajara, principalmente al Dr. César Cárdenas, Director del Centro de Diseño Electrónico del Tec, quién además es miembro fundador de la Asociación. Detrás de mi, hay también un grupo de estudiantes y profesionistas talentosos que me ayudaron en las diversas actividades, no sólo durante el congreso sino tomando de su tiempo previo al Congreso, mismo que le dieron a la Asociación desinteresadamente.

Les agradezco a todos la oportunidad de permitirnos llevarles a ustedes todo esto con el único objetivo de que les sean de provecho las actividades de este congreso, esperando que nos sigan acompañando a congresos posteriores. !Bienvenidos!

Dr. Marco Antonio Aceves Fernández

Asociación Mexicana de Software Embebido

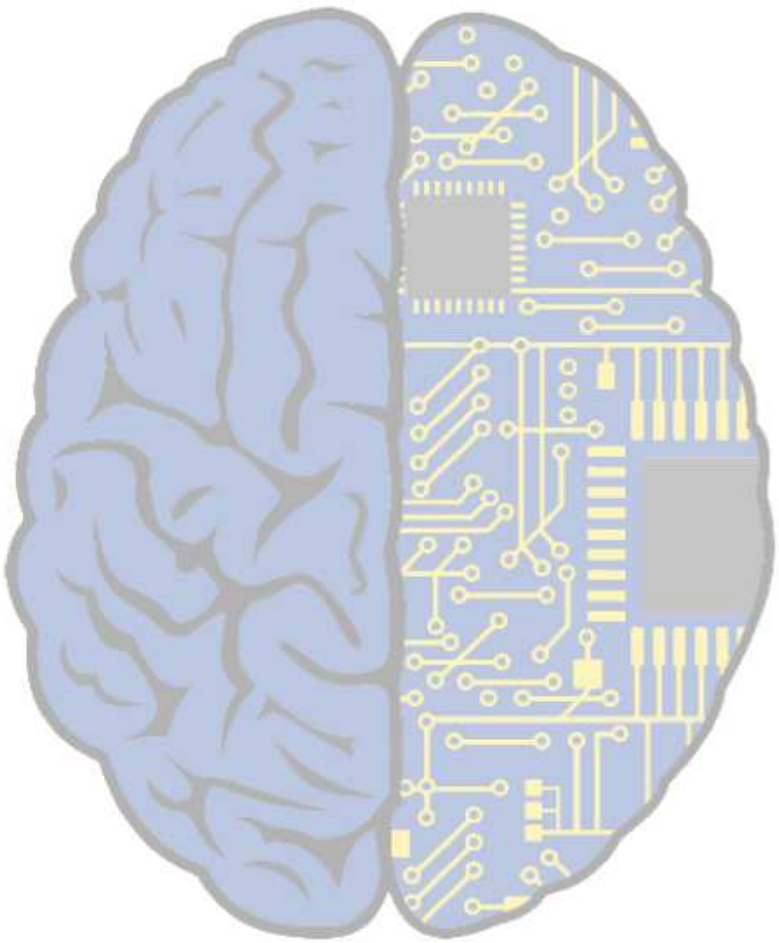

ASOCIACIÓN MEXICANA DE SOFTWARE EMBEBIDO

AMESE

COMITÉ ORGANIZADOR

Marco Antonio Aceves Fernández
Presidente
Universidad Autónoma de Querétaro

Roberto de Jesús García García
Coordinador del Comité Editorial
Universidad Autónoma de Querétaro

Arturo Trujillo Muñiz
Capítulo Estudiantil AMESE-UAQ

Samuel Santiago Mejorada Torres
Capítulo Estudiantil AMESE-UAQ

Uriel Guzmán Sánchez
Capítulo Estudiantil AMESE-UAQ

Itzel Gabriela Morales Carrizal
Capítulo Estudiantil AMESE-UAQ

Jose Eduardo Campa Ferrusca
Capítulo Estudiantil AMESE-UAQ

Ricardo Eusebio Hurtado Dominguez
Capítulo Estudiantil AMESE-UAQ

COMITÉ ORGANIZADOR

Guadalupe Briseño Rodríguez
Capítulo Estudiantil AMESE-UAQ

Edgar Iván de Santiago Olguin
Capítulo Estudiantil AMESE-UAQ

Diego Arellano Briseño
Capítulo Estudiantil AMESE-UAQ

Jose Raul Aviña Galvan
Capítulo Estudiantil AMESE-UAQ

Oscar Alejandro Martínez Mancilla
Tec de Monterrey Campus Guadalajara

Diego Eduardo Bores Ríos
Tec de Monterrey Campus Guadalajara

Oscar Jaureguí Neri
Tec de Monterrey Campus Guadalajara

Gabriel Iván Zepeda Aguirre
Tec de Monterrey Campus Guadalajara

COMITÉ ORGANIZADOR

Jorge Abraham Palomino González
Tec de Monterrey Campus Guadalajara

Iván Godofredo Díaz Tenorio
Tec de Monterrey Campus Guadalajara

Irma Mieko Nagatome Sameshima
Tec de Monterrey Campus Guadalajara

Xicotencatl Lugo Sánchez
Tec de Monterrey Campus Guadalajara

Hector Hugo Reyes Torres

Ana Isabel Quintana Gutierrez

Edson Moreno de Santiago

Juan Xocoyotzin Velazquez Vazquez

COMITÉ EVALUADOR CIENTÍFICO / TECNOLÓGICO

Dr. Marco Antonio Aceves Fernández
Presidente
Universidad Autónoma de Querétaro

Dr. Saúl Tovar Arraiga
Universidad Autónoma de Querétaro

Dr. Jesús Carlos Pedraza Ortega
Universidad Autónoma de Querétaro

Dr. Efrén Gorrostieta Hurtado
Universidad Autónoma de Querétaro

Dr. José Emilio Vargas Soto
Universidad Autónoma de Querétaro

Dr. Juan Manuel Ramos Arreguín
Universidad Autónoma de Querétaro

Dr. Girlberto Ochoa Ruiz

Dr. Luis Corral Velázquez

El comité organizador agradece a los evaluadores su apoyo desinteresado y noble para evaluar y revisar el contenido de los artículos que se sometieron al congreso. Gracias a su valiosa ayuda se logra mantener una alta calidad de las artículos y el contenido del congreso.

PATROCINADORES

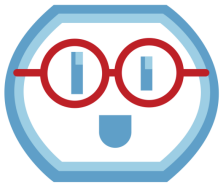

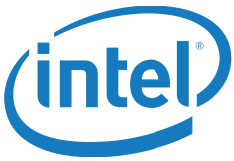

CONTENIDO

ARTÍCULOS

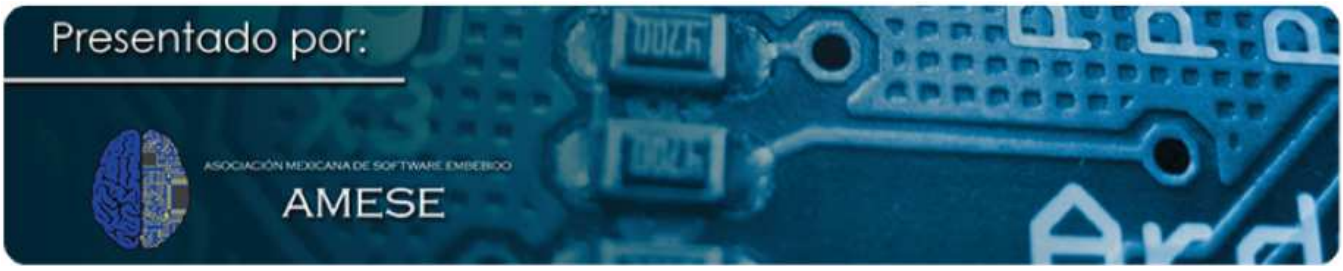
Presentado por:
ASOCIACIÓN MEXICANA DE SOFTWARE EMBEBIDO
AMESE

Capacidades de desarrollo de sistemas embebidos en México para la industria automotriz

Jesús Cienfuegos
Escuela de Ingeniería
Tecnológico de Monterrey
Av. H. Colegio Militar 4700
Chihuahua, Chi 31300, México
jesus.cienfuegos@itesm.mx

Gerardo Méndez
Manager
Centro Técnico de Visteon
Av. H. Colegio Militar 4701
Chihuahua, Chi 31105, México
gmendez@visteon.com

***Abstract* -- Los sistemas embebidos demandan una gran cantidad de personas con conocimientos y habilidades específicos. Existe una brecha entre lo aprendido en la Universidad y los conocimientos y habilidades requeridos por ésta industria. Basado en ofertas de trabajo, el presente estudio generó una matriz de conocimientos técnicos y de habilidades personales requeridas para el área de sistemas embebidos. Se revisó con algunas universidades cuántos de estos conocimientos y habilidades eran cubiertos por las carreras de nivel licenciatura. Se identificó la cantidad de estudiantes que potencialmente podrían cubrir los puestos requeridos. Se obtuvo la brecha en conocimientos y habilidades. La brecha no es cuestión de cantidad, sino de calidad. Para reducir la brecha se requiere el planteamiento de estrategias con la participación de las empresas, universidades y el gobierno. El presente estudio propone algunas estrategias de corto, mediano y largo plazo que podrían implementarse.**

***Index Terms*-- Sistemas embebidos, brecha, conocimientos técnicos, habilidades, estrategia.**

I. Introducción

Se estima que para el año 2020 existirán cerca de 40,000 millones de dispositivos embebidos [1]. Esto será equivalente a 5 dispositivos embebidos por cada ser humano que habite en el planeta y el mercado de tecnología embebida (software y hardware) se ubicará alrededor de los 200,000 millones de dólares [2].

La información referente al desarrollo de sistemas embebidos en México se encuentra asociada a diferentes industrias como la electrónica, informática, electrodomésticos, automotriz y aeronáutica entre otras.

En el año 2014, ProMéxico publicó un reporte completo de la industria electrónica en México. En dicho reporte destaca la oportunidad de inversión en software embebido para televisores por un monto de 678 millones de dólares.

Por su parte, el Diagnóstico para la fundamentación de la maestría en sistemas embebidos establece que en México, "las áreas de aplicación de sistemas embebidos son en su mayoría la automotriz, le sigue la electrónica de consumo y la aeronáutica. En la categoría de otras se mencionaron alimentos, transporte urbano y cinematografía"[3].[1]

El World Economic Forum (WEF) identifica a México como un país en transición, de un enfoque centrado en la eficiencia hacia un enfoque centrado en la innovación [4]. De acuerdo a este reporte, comparando a México con América Latina, el tamaño del mercado mexicano es significativamente mayor en relación al promedio latinoamericano, sin embargo en cuanto a la educación superior estamos por debajo del promedio.

II. Los sistemas embebidos y la industria automotriz

Hace casi 40 años que se hizo la primera implementación de un sistema embebido dentro del automóvil y éste se utilizó para controlar el encendido. Hoy en día, se estima que el 40% de los costos de producción de un carro se deben a la electrónica y software [5]. La tendencia del automóvil autónomo sigue manteniéndose y aunque en el corto plazo no vayamos a observar cambios substanciales, es un hecho que en los próximos años veremos resultados significativos en este aspecto. Lograr que esas funcionalidades sean una realidad será un reto no solamente técnico sino también humano, por ejemplo, la legislación actual en el mundo no está preparada para lidiar con situaciones donde no existe un ser humano al volante.

A. Conocimientos y habilidades requeridos por la industria

El presente estudio realizó el análisis de 20 ofertas de trabajo para el área de sistemas embebidos, de 16 compañías diferentes. La carrera más solicitada por las empresas para cubrir estos puestos es electrónica o ingeniería computacional, seguida por ingeniería en sistemas computacionales, ingeniería de software, mecatrónica, mecánica, maestría en ciencias e incluso se considera a los licenciados en Matemáticas y en Física como candidatos a ocupar posiciones relacionadas a los sistemas embebidos. En la Tabla I se muestran los 10 conocimientos técnicos más

[1] El "Estudio para evaluar las capacidades de desarrollo de sistemas embebidos en México para la industria automotriz" fue desarrollado en colaboración entre el Tecnológico de Monterrey y Visteon.

solicitados en las ofertas de trabajo así como la frecuencia en que fueron solicitados. Fuerte conocimiento del lenguaje C para sistemas embebidos y conocimiento de las arquitecturas de los microcontroladores es lo más solicitado.

TABLA I
LOS 10 CONOCIMIENTOS TÉCNICOS MÁS SOLICITADOS

CONOCIMIENTO	FRECUENCIA
Sólido conocimiento de C para sistemas embebidos	13
Arquitectura de Microcontroladores 8/16/32/ARM	10
Desarrollo de Software Embebido	9
Herramientas de desarrollo de software	7
Procesos de desarrollo de software	7
CMMI	6
RTOS	6
C++ deseable	6
QNX, Linux	6
SPICE	5

Las capacidades técnicas son importantes para cualquier industria, sin embargo, cuando se trata de desarrollo profesional de las personas, siempre están presentes las habilidades personales o mejor conocidas hoy en día como "soft skills". En la Tabla II se muestran las cinco "soft skills" que fueron solicitadas con mayor frecuencia por las empresas analizadas.

TABLA II
LAS 5 HABILIDADES SOLICITADAS CON MAYOR FRECUENCIA

HABILIDAD	FRECUENCIA
Excelente habilidad para comunicarse (oral y escrita)	8
Excelente habilidad para trabajar en equipo	6
Excelente habilidad para trabajar bajo presión	4
Inglés fluido (hablado, escrito y leído)	4
Entender las necesidades y problemas de los clientes	4

III. LAS CAPACIDADES ACADÉMICAS

El conocimiento y la destreza son indispensables para dominar una tecnología. El conocimiento puede ser enseñado mediante exposiciones orales realizadas por un instructor, pero la destreza tiene que ser aprendida a través de la práctica. Un importante estándar de evaluación para una metodología educativa es determinar si efectivamente puede transformar el conocimiento en destreza [6].

Son pocas las universidades que tienen un programa académico de nivel profesional especializado únicamente en sistemas embebidos. Por lo general, quien hoy en día está trabajando como especialista en sistemas embebidos proviene de las carreras de Electrónica o Computación, principalmente.

Dada esta situación se tomó como base a las carreras relacionadas con el área de software (tales como Ingeniero en Sistemas Computacionales, Ingeniería de Software, Ingeniero en Ciencias Computacionales, Tecnologías de Información y Comunicaciones), así como a las relacionadas con el área de Electrónica (tales como Ingeniero Electrónico, Ingeniero en Electrónica y Comunicaciones, Ingeniero en Tecnologías Electrónicas, Ingeniero en Sistemas Digitales) y también a las relacionadas con Mecatrónica y otras áreas que cursan materias de software o electrónica (como por ejemplo Ingeniero Biomédico, Ingeniero Electromédico, Ingeniero en Comunicaciones) y a partir de estas carreras se hizo un análisis del talento humano que potencialmente existe en el país para ocupar posiciones en el área de sistemas embebidos.

Se consideró información obtenida de la Asociación Nacional de Universidades e Instituciones de Educación Superior (ANUIES) para los ciclos escolares 2010-2011, 2011-2012, 2012-2013 y 2013-2014 referentes a las carreras afines a las áreas antes mencionadas.

A. Análisis de la matrícula

En la Fig. 1 se observa que la matrícula de las carreras relacionadas al área de sistemas embebidos es ligeramente superior al 10% de la matrícula total nacional y es una tendencia que se ha mantenido por los 4 años analizados.

Fig. 1. Comparativo de la matrícula nacional de alumnos en nivel licenciatura (fuente: ANUIES)

En la Fig. 2 se muestran los 10 estados que en el ciclo 2013-2014 tuvieron la mayor cantidad de matrícula en carreras profesionales relacionadas a los sistemas embebidos.

Fig. 2. Los 10 estados con mayor cantidad de alumnos en carreras afines a sistemas embebidos. (fuente: ANUIES)

B. Análisis de los egresados

Similar al análisis realizado con los alumnos inscritos se hizo otro para los alumnos egresados de las carreras afines a sistemas embebidos. En la Fig. 3 se muestran todos los alumnos que egresaron de las carreras profesionales en los 4 ciclos escolares anteriores y se compara contra los que egresaron de las carreras relacionadas a los sistemas embebidos. Se observa que cuando se refiere a los egresados de las áreas relacionadas a los sistemas embebidos, el porcentaje de egresados es ligeramente menor al 10% del total de egresados en el país.

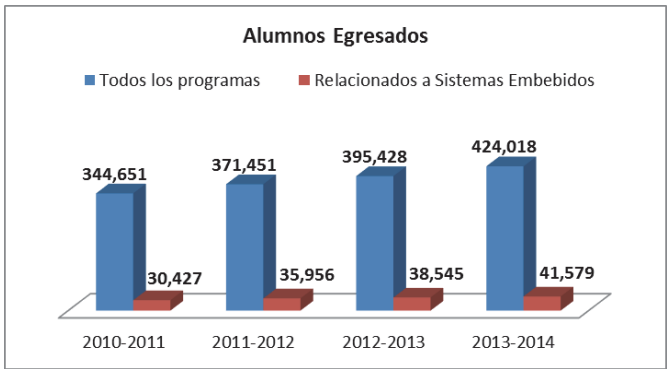

Fig. 3. Comparativo del egreso nacional de alumnos en nivel licenciatura (fuente: ANUIES)

IV. La brecha entre la industria y la academia

El inicio de la brecha entre la industria y la academia empieza desde la forma en que se organizan. Las universidades se organizan en escuelas o facultades (Ingeniería, Derecho, Negocios, Humanidades, Medicina, entre otras) donde se agrupan los maestros de acuerdo a su especialidad, con la intención de a su vez especializar a los estudiantes en sus respectivas áreas de estudio. Dependiendo del programa de estudio, alumnos de una determinada escuela o facultad estarán tomando clases que se encuentran bajo la administración de otra. Sin embargo por lo general, las materias de una escuela o facultad se encuentran desvinculadas de las demás y es común encontrar que los proyectos desarrollados en ingeniería por los alumnos no consideren proyecciones de costos o bien cuidar los flujos de efectivo para no salirse de un presupuesto.

Las empresas por su parte, se organizan regularmente de acuerdo a su modelo de negocio. De esta forma, encontramos que una determinada área o departamento cuenta con técnicos e ingenieros de diferentes especialidades (mecánicos, electrónicos, industriales, mecatrónicos entre otros) y dependiendo de las necesidades del negocio es factible que todos se encuentren interactuando entre sí con un objetivo común, proveer soluciones que satisfagan los requerimientos de los clientes y que a su vez sean rentables para la empresa.

El desarrollo de sistemas embebidos involucra tanto hardware como software. Las universidades tradicionalmente tienden a separar estas dos áreas en electrónica y computación. En consecuencia, por un lado la investigación en ciencias computacionales ha ignorado a los sistemas embebidos y ha creado abstracciones que no consideran las restricciones físicas de los elementos, por otro lado, el diseño de sistemas embebidos va más allá del entendimiento tradicional de la electrónica, porque la computación y el software son partes integrales de los sistemas embebidos [7].

Existe una brecha entre los conocimientos adquiridos durante la formación académica y los conocimientos requeridos por la industria. En los Estados Unidos, los empleadores cada vez más dicen que los alumnos que se gradúan de la universidad no están listos para los lugares de trabajo, solamente el 40% de los empleadores creen que sus nuevos empleados tienen los conocimientos y habilidades necesarios para ser exitosos [8].

De acuerdo a la "Encuesta de escasez de talento 2015" realizada por Manpower, el 35% de los empleadores encuestados dijo que los candidatos no cumplen al 100% el perfil y el 34% dijo que no tenían las habilidades técnicas necesarias [9].

Basado en los conocimientos técnicos solicitados en las ofertas de trabajo analizadas, se aplicó una encuesta a universidades en la ciudad de Chihuahua para ver cuántos de estos conocimientos cubrían en las carreras profesionales relacionadas a las carreras de sistemas embebidos. De 67 capacidades técnicas, las universidades dijeron cubrir 39 de ellas. En la Fig. 4 se muestra un resumen de las capacidades técnicas que las universidades en Chihuahua especificaron transmitir a sus alumnos a través de clases. Los valores de frecuencia indican cuantas universidades respondieron afirmativamente que transmitían dicho conocimiento.

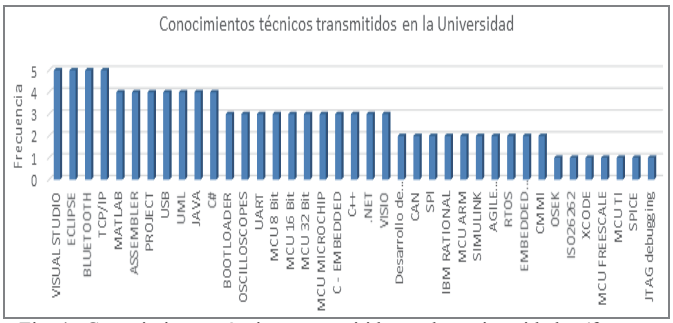

Fig. 4. Conocimientos técnicos transmitidos en las universidades (fuente: Estudio para evaluar las capacidades de desarrollo de sistemas embebidos en México para la industria automotriz)

En la Tabla III se muestra el resumen global de las 5 "soft skills" solicitadas con mayor frecuencia por las empresas y como fueron evaluadas por las universidades en Chihuahua. Se evaluó con 1 si el grado de obtención era bajo, con 2 si era medio y con 3 si el grado de obtención de dicho skill era alto.

TABLA III
LAS 5 HABILIDADES SOLICITADAS CON MAYOR FRECUENCIA POR LAS EMPRESAS Y SU EVALUACIÓN EN LAS UNIVERSIDADES

Habilidad	Evaluación
Excelente habilidad para comunicarse (oral y escrita)	2.5
Excelente habilidad para trabajar en equipo	2.5
Excelente habilidad para trabajar bajo presión	2.75
Inglés fluido (hablado, escrito y leído)	2.25
Entender las necesidades y problemas de los clientes	1.75

La brecha entre la academia y la industria tiene diversas consecuencias, sin embargo, a pesar de que exista ésta situación se deben de cubrir las necesidades de talento humano que tengan las empresas. Cuando se trata de reclutar personal para el área de sistemas embebidos las empresas se inclinan por contratar ingenieros en electrónica sobre los de informática, ya que los primeros tienen conocimientos sólidos para poder trabajar en el diseño y desarrollo de sistemas embebidos [10]. De alguna forma se les facilita más a las empresas compensar las carencias en desarrollo de software de estos profesionistas que compensar las carencias del

conocimiento de hardware que pudieran tener otro tipo de perfiles profesionales.

Los conocimientos técnicos solicitados por las empresas se agruparon en 10 grandes áreas y se compararon contra las respuestas que dieron las universidades. En la Fig. 5 se muestra una gráfica de radar donde se puede observar la brecha entre lo solicitado por las empresas y lo transmitido en la universidades.

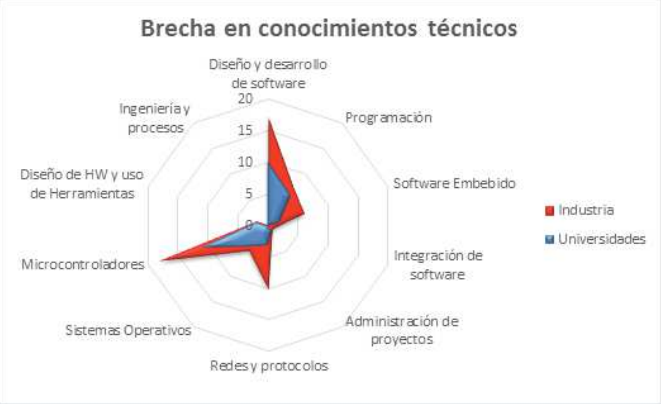

Fig. 5. Brecha de conocimientos técnicos entre las empresas y la academia (fuente: Estudio para evaluar las capacidades de desarrollo de sistemas embebidos en México para la industria automotriz)

A la brecha en las capacidades técnicas se le suman las habilidades personales o "soft-skills". Erick Zuñiga en su artículo "Urgen ingenieros tecnológicos con estas 10 habilidades" identifica cuatro habilidades de negocios: negociación, finanzas básicas, cultura de calidad y metodología de ventas; cuatro habilidades personales: gestión del tiempo, innovación-creatividad, comunicación y valores; y dos habilidades generales: inglés y experiencia profesional.

En el presente estudio se identificaron 15 "soft-skills" en base a las ofertas de trabajo analizadas. Se realizó una evaluación con diferentes universidades a través de una encuesta. La evaluación consideró valores de 1 a 3, donde 1 era que se contaba con la habilidad en un bajo grado y 3 en un alto grado, ver Fig. 6.

Fig. 6. Brecha de habilidades personales entre las empresas y la academia (fuente: Estudio para evaluar las capacidades de desarrollo de sistemas embebidos en México para la industria automotriz)

V. La respuesta actual y posibles estrategias

Las Universidades han reconocido el gap existente entre la academia y la industria y no se han quedado estáticas.

En la Universidad de Alabama, Tuscaloosa, se ha restructurado el programa de estudios de la carrera Computer Engineering para darle un enfoque hacia los sistemas embebidos basados en las recomendaciones del modelo especificado por la IEEE/ACM para esta carrera.

La Universidad Nacional Cheng Kung en Tainan, Taiwan, diseñó un programa de maestría para transmitir los conocimientos relacionados a sistemas embebidos en el primer año de estudio.

En Japón, un grupo de maestros del sistema nacional de tecnología llamado KOSEN, llevó a cabo actividades encaminadas a fortalecer los conocimientos en sistemas embebidos de sus alumnos, ellos reportan haber tenido una efectividad de los 80%, basados en una encuesta realizada a sus alumnos.

El Holon Academic Institute of Technology en Israel, desarrolló un programa académico en sistemas embebidos para nivel universitario y la Universidad Software College of BeiHang en Beijing, China, desarrolló un programa de maestría para proveer desarrolladores de software embebido mejor calificados.

Aquí en México, las universidades han reaccionado creando una diversa cantidad de opciones para compensar esta carencia. En general, las instituciones de educación superior manejan tres modelos para enseñar los conocimientos relacionados a sistemas embebidos: 1) grupo de materias ofrecidas dentro de los programas académicos tradicionales de electrónica y computación; 2) Programas de maestría especializados; 3) educación continua y programas de entrenamiento a la industria.

Los datos obtenidos por el presente estudio nos indican que en México existen suficientes egresados que eventualmente podrían ocupar los puestos requeridos en la industria. Tan solo de las carreras afines a sistemas embebidos, egresaron en el país 41,579 alumnos en el ciclo escolar 2013-2014. Para el 2020 el pronóstico de alumnos egresados de carreras afines a sistemas embebidos en el país es de 63,600.

Con la diversidad tan grande de programas de estudio en el país (203 programas académicos afines a sistemas embebidos), con la cantidad tan grande de universidades que los ofrecen (761 universidades y tecnológicos), ubicados en 425 de los casi 2,000 municipios del país, los estudios realizados siguen mostrando que existe una brecha entre lo aprendido en la universidad y los conocimientos y habilidades requeridos por la industria, además de que las empresas tienen dificultad para conseguir el talento humano que cubra sus necesidades.

Entonces esto nos lleva a la misma conclusión que otros estudios a nivel mundial: no es cuestión de cantidad, sino de calidad.

Es necesario hacer un replanteamiento no solo de la oferta académica, sino de la forma misma en que se hace dicha oferta, incluso involucrando a mas actores. Sabemos que los cambios no se dan de un día para otro, pero también sabemos que si no empezamos a hacer algo es un hecho que nada va a

cambiar y la brecha se hará más grande.

Cuando queremos propiciar un cambio, lo primero que necesitamos es tener conciencia de lo que queremos cambiar y después tener la voluntad para cambiar. Los cambios por definición nos incomodan porque nos sacan de nuestro status-quo y entre mayor sea la incomodidad mayor es el cambio, o expresado como una función matemática, el cambio es directamente proporcional a la incomodidad que provoca.

Debemos de tener cuidado de no hacer cambios solo porque no podemos quedarnos como estamos, porque entonces eso no asegura que vayamos a obtener los resultados deseados. Para realizar un cambio esperando obtener los resultados deseados, necesitamos un objetivo tangible, medible y alcanzable y a partir de ahí un plan para cumplir dicho objetivo. Resulta que en ocasiones hacemos primero el plan y luego definimos un objetivo que se adapte al plan.

VI. OBJETIVO Y PLAN PROPUESTOS

La propuesta de objetivo es: reducir en un plazo de 5 años el 90% de la brecha que existe entre los conocimientos y habilidades adquiridos en la universidad y los mínimos requeridos por la industria. Con este objetivo de que estamos hablando:

1) Reducir la brecha de conocimientos técnicos en un 90% significa asegurarnos de incorporar alrededor de 20 skills en los alumnos en los próximos 5 años, esto es un promedio de 4 skills por año. Podríamos esperar que los egresados para el 2016 tuvieran 4 skills adicionales a los del 2015, y así sucesivamente hasta lograr que los egresados en el 2020, tengan 20 skills adicionales a los que tenían los egresados en el 2015.

2) En el caso de los soft-skills sería asegurarnos de mejorar lo que se hace en la actualidad y que para el 2020 el promedio de los soft-skills sea de 2.7.

Esto sería el objetivo y su dimensión, pero faltaría el plan. Cada actor (academia, industria, gobierno) que desee participar deberá desarrollar un plan propio, sin embargo, existen acciones que es conveniente realizar de forma conjunta.

A continuación se mencionan algunas posibles acciones que podrían realizarse de forma conjunta entre la academia, la industria y el gobierno.

A. En el corto plazo (1 a 3 años)

1) Definir una política gubernamental que apoye, con capacitación y herramientas tecnológicas, el desarrollo de talento humano en el área de sistemas embebidos específicamente dentro de los sectores: automotriz, electrodomésticos, aeroespacial, dispositivos médicos y agrario. Para poder evaluar los resultados de dicha política, es necesario que se considere un periodo de tiempo mínimo de 10 a 15 años y que sea independiente del partido que esté en el gobierno.

2) Que exista una figura legal y un programa de trabajo entre los 3 principales actores.

3) Fortalecer las especialidades en sistemas embebidos considerando los requerimientos de la industria nacional.

4) Continuar con el esquema de proyectos académicos, asegurando que cada proyecto al menos reduzca 4 conocimientos técnicos de la brecha.

5) Crear un equipo de trabajo academia-industria para desarrollar un programa a 3 años, donde se considere la participación de profesores, personal de la industria y alumnos y que involucre actividades relacionadas a los sistemas embebidos tanto dentro, como fuera del salón de clase. Estas actividades pueden ser, exposiciones, talleres, seminarios, conferencias, retos y concursos, entre otros.

6) Clases "team-teaching" pero con profesores y personal de la industria. Sería ideal tener "periodos sabáticos" de empleados en las universidades. Esto es, empleados que su empresa los responsabilizó de un proyecto y se van a la universidad a desarrollar el proyecto asignado por su propia empresa con el apoyo de maestros y alumnos.

B. En el mediano plazo (5 años)

1) Ofertar la carrera de sistemas embebidos, donde el software y el hardware sean especialidades de esta carrera y no al revés. La definición de esta carrera debería contar con una fuerte participación de la industria en la definición de los conocimientos a transmitir y considerar periodos de conceptualización cortos (1 año) combinados con prácticas en la industria, para poder interiorizar la teoría aprendida e incluso obtener conocimientos adicionales

2) Contar con laboratorios de sistemas embebidos totalmente equipados, donde los alumnos realicen prácticas basadas en necesidades de la industria, usando procesos y herramientas que se utilizan en la propia industria.

3) Asegurar que el talento humano que se haya capacitado en sistemas embebidos tenga oportunidades laborales en el país para que no tenga que emigrar.

4) Proyectos fondeados por las empresas.

C. En el largo plazo (más de 5 años)

Crear un ecosistema que fomente el desarrollo de proveedores y la creación de nuevas empresas de base tecnológica dedicadas al diseño y desarrollo de sistemas embebidos.

Como mencionamos, la brecha no es cuestión de cantidad sino de calidad. Seguramente muchas de las acciones propuestas ya se están realizando o en proceso de realizarse. Es importante reflexionar nuevamente sobre dichas acciones porque al día de hoy las empresas continúan manifestando que no encuentran el talento humano adecuado para ocupar las posiciones laborales.

RECONOCIMIENTO

Agradecemos a los colegas del Tecnológico de Monterrey Campus Chihuahua y Campus Monterrey, Instituto Tecnológico de Delicias, Universidad Autónoma de Chihuahua, Instituto Tecnológico de Chihuahua, Instituto Tecnológico de Chihuahua II y Universidad Tecnológica de Chihuahua, que se dieron a la tarea de recolectar y

proporcionar información, así como, a todas las personas y amigos que a través de pláticas, entrevistas y encuestas contribuyeron con el estudio.

REFERENCES

[1] ARTEMIS Joint Undertaking. (s.f.). Obtenido de ARTEMIS Web Site: http://www.artemis-ju.eu/embedded_systems.

[2] *Embedded Systems: Technologies and Markets*. (Septiembre de 2014). Obtenido de BCC Research: http://www.bccresearch.com/market-research/information-technology/embedded-systems-report-ift016e.html

[3] Tellez Mosqueda, J., & Avila Muñoz, P. (Febrero de 2014). Diagnóstico para la fundamentación de la maestría en sistemas embebidos. Obtenido de Infotec: https://www.infotec.mx/work/models/infotec/biblioteca/15/15.pdf

[4] The Global Competitiveness Report 2014-2015. (2014). Obtenido de World Economic Forum: http://www3.weforum.org/docs/WEF_GlobalCompetitivenessReport_2014-15.pdf

[5] Broy, M. (Mayo de 2006). Challenges in Automotive Software Engineering. *ACM Library*, págs. 33-42.

[6] Jing, L., Cheng, Z., Wang, J., & Zhou, Y. (Agosto de 2011). A Spiral Step-by-Step Educational Method for Cultivating Competent Embedded System Engineers to Meet Industry Demands. IEEE Transactions on Education, págs. 356-365.

[7] Henzinger, T. A., & Sifakis, J. (Octubre de 2007). The Discipline of Embedded Systems Design. IEEE Computer Society, págs. 32-40.

[8] Bryant, J., & Sarakatsannis, J. (July de 2015). Why US education is ready for investment. Obtenido de McKinsey & Company: http://www.mckinsey.com/insights/social_sector/why_us_education_is_ready_for_investment?cid=other-eml-alt-mip-mck-oth-1509....

[9] ManpowerGroup. (2015). Encuesta de escasez de talento 2015. Obtenido de ManpowerGroup: http://www.manpowergroup.com.mx/uploads/estudios/Escasez_Talento_2015.pdf

[10] Tellez Mosqueda, J., & Avila Muñoz, P. (Febrero de 2014). Diagnóstico para la fundamentación de la maestría en sistemas embebidos. Obtenido de Infotec: https://www.infotec.mx/work/models/infotec/biblioteca/15/15.pdf

Embedded CAD/CAM module to assist in the design and manufacture of nanostructures

M. Guadalupe Cisneros D., Ramón Díaz de León Z.,
Efrén Flores G., Ismael Lara V.
División de Estudios de Posgrado e Investigación
Instituto Tecnológico de San Luis Potosí
San Luis Potosí, México

Javier González Contreras
Centro de Ciencia y Tecnología de Terahertz
Universidad Autónoma de S.L.P.
San Luis Potosí, México

***Abstract*— An embedded CAD/CAM module to assist researchers in the design and manufacture of nanostructures by CAD using the Finite Element Method (FEM) was successfully implemented. The resulting geometry is fabricated with CAM by using the Photolithographic Method. Three commercial computer programs were used to build the interface module to improve the functionalities, and for reduce learning, design and manufacturing times (COMSOL, MATLAB and LabView). The module was implemented and tested for the design and manufacture of nanoantennas and another nanostructures.**

Keywords*—** Embedded ***CAD/CAM; Finite Element Method; nanostructures; nanoantennas.

I. Introduction

The design of nanostructures is a task that involves the knowledge of some physical phenomena that are still in research like plasmonic resonance, Seebeck effect, etc. [1-5] and they reveal aspects that can be used to develop new structures for a wide range of applications, from solar energy harvesting to the diagnostic of diseases and wireless communications at Tera Bytes per second (TBs) [2, 6, 7].

On the other hand, fabrication of those nanostructures requires specialized equipment and their associated calculation complexity is only achievable by computer aided also in electron beam photolithography method for nanostructure fabrication[5, 8, 9].

The design and the fabrication of a nanostructure are two topics that have been considered independent aspects, each one with a particular way to aboard the solution or implementation processes. In this work there were designed and implemented an interface which can be used to design and manufacture nanostructures making the main process fully automated.

II. Method

COMSOL Multiphysics® was selected as the CAD software because of their native capabilities for solve optics, thermal and mechanical problems by the Finite Element Method which permits a reliable and fast method for design; also this computer program is fully compatible with Matlab® which will be used for pre processing geometry and COMSOL's data returned analysis [10]. It is necessary to have installed the LiveLink for Matlab package (in COMSOL) to take advantage of this interaction capability between both programs.

With the Matlab computer program [8] was implemented a genetic algorithm which helps in determine the geometry that conveniently resolves the necessities of design for nanostructures to be manufactured and also does the calculations to be passed to the CAM stage.

For the particular case of nanoscale structures to be used as antennas, some constants or quantities must be revised as a consequence of certain properties that cannot be obviated at macro scale. For instance, in nanoantennas cannot be neglected the radius of the transmission line, or cannot be ignored the plasmonic resonance effect.

One of those quantities that is included in this CAD/CAM module is for the refractive index whose behavior at optical frequencies was experimentally obtained by [11] as a quantity in function of the frequency (THz). For illustrative purposes, Eq. 1 depicts the refractive index in function of the frequency for gold (Au), for other materials consult the suggested bibliography.

$$n = -0.5097680004322286-(3.0508946281044503*10^40)/(f^3)+(8.694327295404505*10^27)/(f^2)+7.071831942548983*10^13/f+j*(-0.8507140979084992+3.494475566745883*10^39/f^3-5.767704394113701*10^27/f^2+2.209462903239641*10^15/f) \quad (1)$$

Another advantage founded in the module is the implementation of a genetic algorithm whose population is randomly generated and initialized with values given by the user.

Each member of the population represents a little piece of the whole nanostructure and is then calculated a health level called 'fitness' for that individual. The fitness value is calculated by how well it fits with our desired requirements (given by the researcher).

Discarding unhealthily population by evaluating the fitness function allows discard the bad designs by keeping only the best individuals in the population. This process also permits to

find the best nanostructure's shape for the objectives that the researcher wants to achieve like the direction or shape of the electromagnetic field.

During crossover process, it creates new individuals by combining aspects of that selected individuals. The goal is that by combining certain traits from two or more individuals, will be created an even 'fitter' offspring which will inherit the best traits from each of it's parents but mutations are needed to add a little bit randomness into the populations' genetics otherwise every combination of solutions that can be created would be in the initial population being impossible to find the desired solution.

An example of a nanostructure created with this procedure is shown in Fig. 1; the shape for this example was selected to accentuate the non conventional but fully compliant performance for the nanostructure which was designed as a nanoantenna that can concentrate their whole electromagnetic field to only one half of the dipole. Note that the voltage source is at the middle of the dipole.

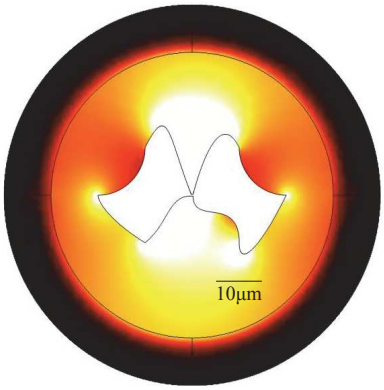

Fig. 1. Nanostructure created by genetic algorithm into Matlab and simulated with COMSOL.

Can be seen in Fig. 2, that classical dipole geometry is less efficient in concentrate electromagnetic field than those generated by Genetic Algorithm.

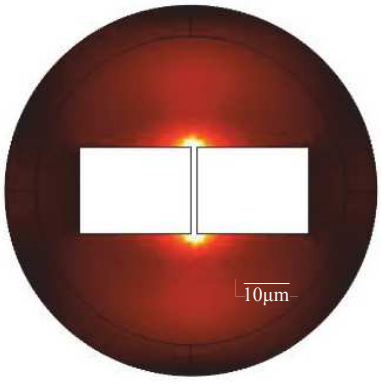

Fig. 2. Classical dipole geometry revealing less electromagnetic field concentration.

The manufacturing machine for the designed nanostructures stage is the "Inspect F50 Scanning Electron Microscope (SEM)". An overview of their main components are shown in Fig. 3, also as can see in the figure, the control of the microscope can be achieved by local area network [12].

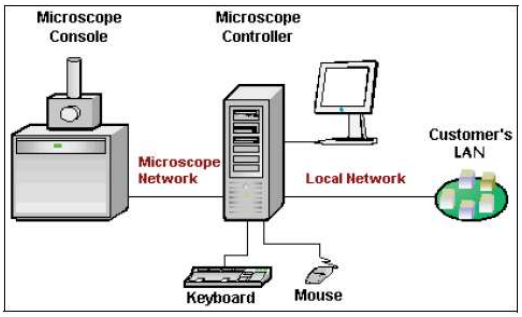

Fig. 3. Inspect F50 Scanning Electron Microscope schematic.

The SEM will be controlled through LabView® computer program by sending or making accessible (depending on the user's choice) via local network the file that contain the manufacture instructions.

It was taken advantage of the embedded Local Area Network (LAN) capabilities of LabView software to implement the computer control and communications stage. Fig. 4 shows an actual segment of the implemented solution with LabView for illustration purposes.

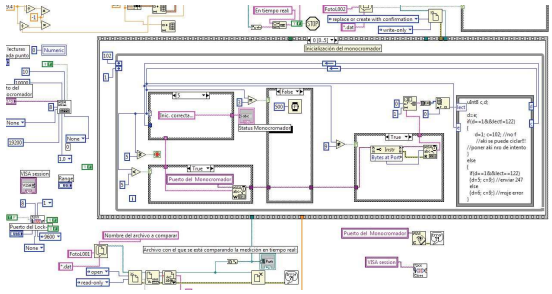

Fig. 4. screenshot for LabView depicting the interface between CAD and CAM stages (for illustrating purposes only).

Fig. 5 shows the flowchart depicting the whole automation process where three main software programs and other important components are included.

Depending on kind of nanoantenna or the fabrication specifications for other nanostructures, must be necessary some human intervention in the processes, for example when the nanostructure is designed to be a Seebeck Nanoantenna, where each side (normally symmetric) of the geometry, requires different material to take advantage of the Seebeck effect. For this particular case, it must be necessary to extract the substrate where geometry was partially drawn, deposit the first material,

reinsert substrate in SEM and repeat the process for the second part of geometry.

The CAM stage makes a storage and mark recognition sub-process to permit continuing the drawing process without mistakes or dislocations.

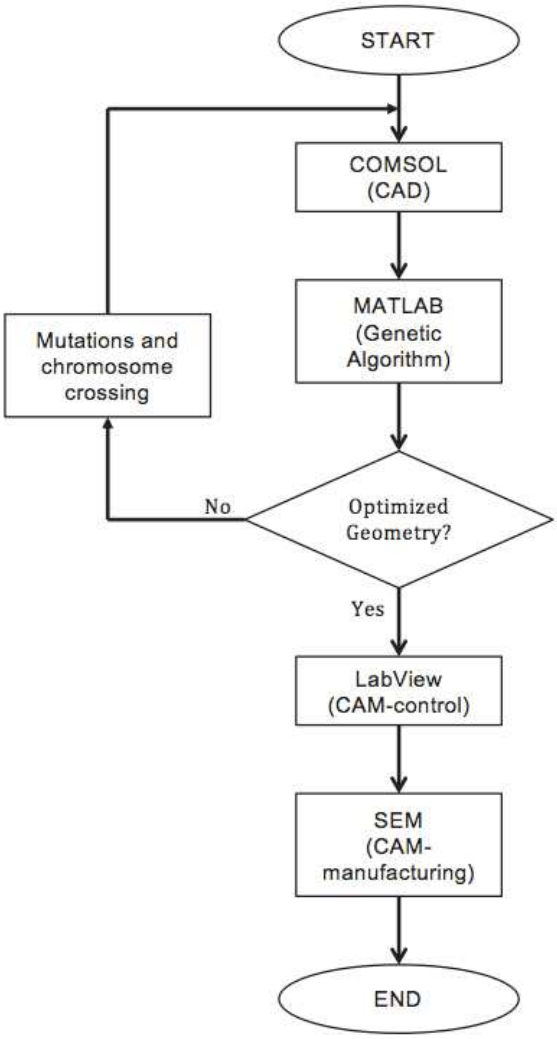

Fig. 5. CAD/CAM module flowchart.

III. Results

An automation process from the design stage to the manufacture of the nanostructure was implemented with the help of three main computer programs (COMSOL Multiphysics, Matlab and LabView) making that process more accurate by reduction of the human error between stages and more easy to use with only one interface to manage all the three computer programs with a friendly user interface.

Fig. 6 shows a comparative graphic between classical dipole geometry and those generated by Genetic Algorithm. Note that electromagnetic field is stronger and have more bandwidth in GA than classical geometry.

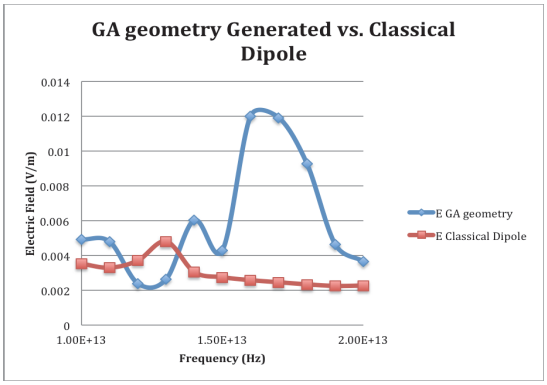

Fig. 6. Electromagnetic field collected by nanostructures. Line blue represents the GA generated geometry. Line red represents the rectangular classsical geometry.

Fig. 7 shows a nanoantenna designed and simulated with the use of the CAD stage of the module. The simulation demonstrates the capability of nanostructure to convert electromagnetic waves on thermal energy which, from Seebeck effect can be obtained DC current so that can be stored in batteries [13-16].

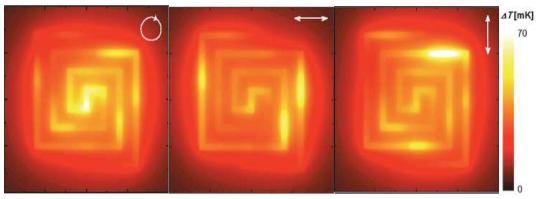

Fig. 7. Actual example of a nanostructure designed and simulated by the CAD module [13].

Fig. 8 shows a nanoantenna fabricated with the use of the CAM stage of the module, sending directions and geometry to the SEM for its fabrication by LAN.

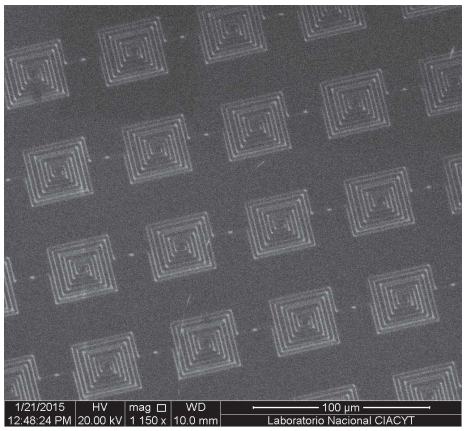

Fig. 8. Actual example of a nanostructure manufactured with the CAM module.

IV. Conclusions

Researchers with interest in nanotechnology may need or require time for learning about three different software programs to achieve their goals in design and fabrication, situation which can distract them for the essential objectives or making them dependent of other persons to assist them in that particular issues.

With this proposal, researchers will need to learn only one computer program and they will find support inside the software during the whole process, from design to manufacture, also reducing the human error inherent in each stage before the implementation of this embedded process.

The module proposed is still working and it has been in use in the recently created National Laboratory of Science and Technology of Terahertz (Laboratorio Nacional de Ciencia y Tecnología de Terahertz).

Acknowledgment

This work was supported by the project "Centro Mexicano de Innovación en Energía Solar" from "Fondo Sectorial CONACYT-Secretaría de Energía-Sustentabilidad Energética through project number 32", by the "Centro de Ciencia y Tecnología de Terahertz" from the Universidad Autónoma de San Luis Potosí, and the "Electrical, Electronic and Mechatronic Department" from the Instituto Tecnológico de San Luis Potosí.

Authors thanks to M.C. Javier Mendez Lozoya for the SEM images obtained as part of their Ph. D. work.

References

[1] Tuccio S, Alabastri A, Razzari L, Toma A, Liberale C, Zaccaria R P, De Angelis F, Das G and di Fabrizio E Terahertz Resonant Dipole Nanoantennas
[2] Tonuchi M 2007 Cutting-edge terahertz technology. In: *Nature Photonics,* (Japan: Nature Publishing Group) pp 97-105
[3] Federico S and O. T J 2012 Generación y medición de radiación con frecuencia de terahertz empleando pulsos de luz ultracortos *ANALES AFA* **23** 6
[4] Ho-Jin S and Tadao N 2011 Present and Future of Terahertz Communications *IEEE transactions on terahertz science and technology* **1** 8
[5] Vieu C and al. e 2000 Electron beam lithography: resolution limits and applications *Applied surface science* **164** 111-7
[6] Blin S, Thome L, Nouvel P, Pénarier A, Coquillat D, Knap W, Ducournau G, Lampin J-F, Bollaert S, Hisatake S and Nagatsuma T 2014 THz wireless communications using plasma-wave detectors. (Francia: Université Montpellier) p 2
[7] Taminiau T H, Stefani F D, Segerink F B and Van Hulst N F 2008 Optical Antennas direct single-molecule emission *Nature Photonics* **2** 4
[8] Hahn B and Valentine D 2013 *Essential Matlab* (U. S. A.: Academic Press)
[9] Lukas N and Niek v H 2011 Antennas for light *Nature photonics* **5** 88-90
[10] AB C 2014 Introduction to Comsol Multiphysics. (United States of America: COMSOL AB) p 116
[11] González F J, Alda J, Simón J, Ginn J and Boreman G 2009 The effect of metal dispersion on the resonance of antennas at infrared frequencies *Infrared Physics and Technology* **52** 4
[12] Dufek M 2010 The Inspect F50 User Operation Manual. (USA: FEI Company)
[13] Briones E, Cuadrado A, Briones J, Díaz de León R, Martínez-Antón C, McMurty S, Hehn M, Montaigne F, Alda J and González F J 2014 Seebeck nanoantennas for the detection and characterization of infrared radiation *Optics Express* **22** 9
[14] F. A I, Miquel J J and Chong H 2014 Terahertz band: Next frontier for wireless communications. In: *Physical Communication*: Elsevier) pp 16-32
[15] Gonzalez F J 2005 Thermal-impedance simulations of antenna-coupled microbolometers *Infrared physics & technology* 4
[16] Kim R and S. L M 2011 Computational Study of the Seebek coefficient of one-dimensional composite nano-structure Journal of Applied Physics 10University Science, 1989.

Development of a Mechatronic Device for Arm Rehabilitation

With Medical Infrared Thermography Evaluation

Teth Azrael Cortés Aguilar
Departamento de Ingeniería Electrónica
Instituto Tecnológico Superior de Zapopan
Zapopan, Jalisco, México
teth.cortes@itszapopan.edu.mx

Bruno Vergaray Manrique
Departamento de Ingeniería Electrónica
Instituto Tecnológico Superior de Zapopan

Jorge Arturo Torrejon
Departamento de Ingeniería Electrónica
Instituto Tecnológico Superior de Zapopan

***Abstract*— Arm injuries usually involve a long and costly rehabilitation period. However, a suitable treatment can reduce the duration and negative impact of the rehabilitation period. In this paper, we propose a mechatronic device for arm rehabilitation to improve the efficacy and performance of physics therapies. The Mechatronic Device for Arm Rehabilitation uses an electronic embedded system to set up the rehabilitation routine parameters. Also we propose the use of Medical Infrared Thermography as a method to evaluate the recovery health process. In elbow rehabilitation results, the thermal images show temperature increase as evidence of exertion in muscles and blood vessels.**

Keywords*— *Therapy Robot; Embedded System; Mechatronic Device; Medical Infrared Thermography.

I. NOMENCLATURE

COECYTJAL	Consejo Estatal de Ciencia y Tecnología de Jalisco
GEAR	Gannon Exoskeleton for Arm Rehabilitation
IR	Infrared Radiation
LWIR	Long Wavelength Infrared
MIT	Medical Infrared Thermography
MWIR	Medium Wavelength Infrared
SEAT	Simulation Environment for Arm Therapy
WREX	Wilmington Robotic Exoskeleton

II. INTRODUCTION

Traumatic injuries usually involve a long, costly rehabilitation period. High-quality treatment can reduce the duration and negative impact of the rehabilitation period. It is well known that richly vascularized areas heal faster compared to poorly vascularized areas.

Use of mechatronic rehabilitation therapy is associated with minimizing the time, expense and inconvenience of receiving rehabilitative care; additionally, it contributes to the meaningful improvement in patients' physical and cognitive functioning as well as health related quality of life.

This work was partially sponsored by COECYTJAL and Tecnológico Nacional de Mexico- campus Zapopan.

Medical Infrared Thermography (MIT) is a non-radiating and contact-free technology used to monitor physiological functions related to skin temperature control. Detecting an inflamed area may provide substantial additional feedback to medical personnel to determine exactly where the injured area is located, and to determine which recovery health process ensures the most effective treatment.

In this paper we propose a Mechatronic Device for Arm Rehabilitation with an electronic embedded system to set up the rehabilitation routine parameters. Also, we propose the use of Medical Infrared Thermography as a method to evaluate the recovery health process in physical therapy.

A. Rehabilitation robots used in physical therapy

A therapy robot is used during a rehabilitation program for a certain period to increase an individual's ability to regain the capability of movement. These robots are part of human–machine interactions that are often considered robotic therapy aids to assist handicapped patients. The principle goal in the rehabilitation robots field is to develop executable and implementable technologies that can be simply used and managed by patients, engineers, therapists and clinicians, hence increasing the ease of activities in the daily lives of patients with motor impairments by improving the efficacy and performance of clinician's therapies. The first rehabilitation robots were developed for upper limbs during the 1990s, followed by supporting devices for lower limbs and the entire body. In general, they provide some form of physical support and mobility in case the affected limb is no longer functional or has been amputated; they also aid rehabilitation exercises when the limb is still functional but with limitation such as in a stroke patient [7].

B. Mechatronics in the rehabilitation of the arm

By using traditional methods with motor rehabilitation therapy in daily clinical routines, the frequent and intensive training guided manually by the physiotherapists is time consuming and requires significant labor. Robotic training devices are widely used in rehabilitation therapy for

the improvement of the upper-limb of patients [13]. Such is the case of the robots: a) The device ARMin-II helps in repetitive training with patients who have suffered paralysis in their arms because of possible damage to the central nervous system [3], b) The Driver's Simulation Environment for Arm Therapy (SEAT) is a prototype rehabilitation device developed by Rehabilitation Research & Development Center to test the efficacy of patient-initiated bimanual exercise to encourage active participation of the hemiplegic limb [15], c) T-WREX is an adult-sized version of Wilmington Robotic Exoskeleton (WREX), which is a five degrees-of-freedom orthosis that counterbalances the weight of the arm using elastic bands [18], and d) The Gannon Exoskeleton for Arm Rehabilitation (GEAR) is a machine the aids in the rehabilitation of primary functional movements of the arm. When seated, the patient is connected to the device via a padded cuff strapped onto the elbow. A set of springs is used to maintain the system stability and help the lifting of the arm [5].

Use of therapy robots was associated with minimizing the time, expense, and inconvenience of receiving rehabilitative care, along with contributing to the meaningful improvement in patients' physical and cognitive functioning as well as health related quality of life [2]. Assisting robotic therapy strategies reduces movement errors. However, a recent randomized study showed that patients with incomplete spinal cord injury only obtained marginal improvements in simulated walking speed after 12 weeks of robotic assisted training. A possible explanation for why conventional therapist-assisted training seems to outperform robotic rehabilitation is the inability of the controllers to adapt to the patients special needs [14].

C. *Benefits of physical therapy in recovery health*

Daily sessions of therapy lasted about 45 min, 1000 movements. An analysis of a relatively small sample of patients (58 patients) suggests that a one-month period of intensive upper limb rehabilitation results in significant improvements in patients with moderate to severe motor impairments [11].

A post-rehabilitation change task related brain activation. Two different neuroplastic patterns were observed in recovery of motor function following rehabilitation of chronic upper extremity motor deficits; the two different patterns of brain activation change were as follows: 1) an increase in volume of brain activation; and 2) a more focused volume of activation [21].

Exercise is one of the most commonly used treatments in elbow management by physiotherapists, especially progressive stretching exercises. A small study was conducted over a duration of 6–8 weeks, in which patients underwent a trial of exercises including both stretches and ultrasound. The results showed a favorable effect on pain but not maximal grip strength, concluding that progressive exercise therapy was more effective than ultrasound therapy [24].

D. *Infrared Thermography*

Infrared thermography, also generally known as thermography or thermal imaging, captures the temperature variations emitted by a body using a radiation detector, which is normally a high speed infrared camera. The captured radiation is analyzed to retrieve information about the material subsurface, which is then used to understand its internal configuration. In thermography, the subsurface anomalies are detected by monitoring the surface temperature and the regions where the heat flow is modified due to the anomalies identified [22].

Heat transfer by radiation is an energy transport mechanism that occurs in the form of electromagnetic waves. Via this heat transfer mode, energy can also travel in vacuum and may be partially absorbed and reflected by a body, or even pass through it. By denoting with $\propto_r$ the radiation fraction being absorbed by the body, with ρ_r the fraction being reflected by it and with τ_r the fraction being transmitted (which passes through), energy conservation requires:

$$\propto_r + \rho_r + \tau_r = 1 \quad (1)$$

Where $\propto_r$, ρ_r and τ_r are, respectively called absorptivity, reflectivity and transmissivity coefficients of the body under consideration. Radiation is emitted by all bodies at an absolute temperature T>0 and, for non-transparent bodies $\tau_r = 0$, it originates from their surface only. The body which emits the greatest amount of energy at a given temperature is called black body [8]. The law that prescribes the energy flux (energy rate per unit body area) per wavelength (spectral hemispherical emissive power) $I^b(\lambda)$ $[W/m^3]$, which is emitted by a black body in the hemisphere outside its surface, is the Planck's law of radiation:

$$I^b(\lambda) = \frac{C_1}{\lambda^5(e^{C_2/\lambda T}-1)} \quad (2)$$

Where λ is the radiation wavelength (m), T the absolute black body temperature (K) and C_1 and C_2 the first and the second universal radiation constants, respectively equal to $3.7418 \times 10^{-16}\ Wm^2$ and $1.4388 \times 10^{-2}\ mK$. The equation shows that I^b goes to zero for both $\lambda \to 0$ and $\lambda \to \infty$. The electromagnetic spectrum is roughly divided into a number of wavelength intervals called bands. The infrared spectral band, of interest within the present context, is generally sub-divided into four lesser bands with arbitrarily chosen boundaries: near infrared (0.75–3 μm), middle infrared (3–6 μm), far or long infrared (6–15 μm) and extreme infrared (15–1,000 μm). Most currently used IR camera detectors are sensitive in the middle (MWIR) and the long (LWIR) spectral bands, but the band between ~5 and ~7.5 μm is seldom used

because of its rather high atmospheric absorption [8]. According to Wien's displacement law, the wavelength λ* at which the black body emits its maximum spectral emissive power is a function of the absolute black body temperature according to: λ*T = 2,897.8 μm-K. The total (over all wavelengths) hemispherical emissive power E^b (W/m^2) also depends on the absolute black body temperature alone, according to:

$$E^b = \sigma T^4 \quad (3)$$

Where σ is the Stefan–Boltzmann's constant, it is equal to 5.6704×10^{-8} W/m^2K^4. However, since infrared camera detectors capture only a limited band of the whole electromagnetic spectrum, while making measurements with IR thermography, Planck's law rather than Stefan–Boltzmann's law must be applied. Real objects almost never comply with the laws described above, even if they may approach the black body behavior in certain spectral bands and conditions. In equation (2), the Planck's law of radiation can be rewritten for real bodies:

$$I(\lambda) = \varepsilon(\lambda)\frac{C_1}{\lambda^5(e^{C_2/\lambda T}-1)} \quad (4)$$

Bodies that have emissivity independent of λ are called gray bodies. Kirchhoff's law states that the spectral emissivity coefficient is equal to the spectral absorptivity coefficient $\alpha_r(\lambda)$, which is the absorbed fraction of the radiation of wavelength λ. Therefore, for non-transparent bodies, such as those generally used in infrared thermography, (1) becomes

$$\varepsilon(\lambda) + \rho_r(\lambda) = 1 \quad (5)$$

Real objects almost never emit in a diffusive (isotropic) way, the emissivity coefficient ε being dependent also on the angle θ (directional emissivity) between the direction of emission and the normal to the emitting surface (viewing angle) [8]. Most of the diagnostic imaging modalities in medicine utilize portions of the electromagnetic spectrum. However, in contrast to other medical devices, MIT uses non-ionizing radiation, thus allowing an unconstrained and harmless application in patients. Using infrared radiation, infrared cameras generate thermal images based on the amount of heat dissipated at the surface. Roughly 80% of the emitted infrared radiation of human skin is within the wavelength range of 8-15μm. Human skin, with an emissivity of 0.98, is almost equal to a black body radiator [12].

E. Medical Infrared Thermography

Medical Infrared Thermography (MIT) is a non-radiating and contact-free technology used to monitor physiological functions related to skin temperature control. The efficiency, safety and low cost of MIT make it a useful auxiliary tool for detecting and locating thermal abnormalities characterized by increases or decreases in skin surface temperature, Fig. 1. Research suggests that the most beneficial application of MIT is the diagnosis of injuries [4].

Fig. 1. Medical Infrared Thermography a) thermal image, b) Flir E-50 thermographic camera.

The association between changes in temperature and disease is almost as old as medicine itself. Hippocrates stated, "Should one part of the body be hotter or colder than the rest, then disease is present in that part". A new generation of high-resolution cameras, appropriate software and standardized protocols have been developed for medical imaging, resulting in improved diagnostic capability and reliability. In 1987, the American Medical Association recognized MIT as a feasible diagnostic of injuries. The following worldwide thermography organizations promote the proper application of medical thermal imaging: a) International Academy of Clinical Thermography, b) International Thermography Society, c) American Academy of Medical Infrared Imaging, d) European Association of Thermology, e) Northern Norwegian Centre for Medical Thermography, f) German Society of Thermography and Regulation Medicine [4].

Some studies shows that infrared thermography is a sensitive, objective, investigational procedure for the assessment of unilateral and bilateral tennis elbow [6], gastroesophageal reflux disease [9] and anti-inflammatory treatment efficacy [20]; it also serves as a noninvasive imaging technique of tissue stiffness changes and stiffness values associated with a pathology or as a result of therapy [23]. The various advantages of thermography include: a) noninvasive technique, b) easy seating examination, c) minimal examination time (2-3 minutes), d) non-expensive technique, e) obvious difference in color changes (gradient – 0.05°C) and f) its real time enables very fast scanning of stationary targets and capturing of fast changing thermal patterns.

The physics of heat radiation and the physiology of thermoregulation in the human body make the reliability and validity of thermal images difficult. Skin temperature regulation is a complex system that depends on blood-flow rate, local structures of subcutaneous tissues and the activity of the sympathetic nervous system. However, there is evidence that the sympathetic nervous system is the primary regulator of blood circulation in the skin, and therefore, is the primary regulator of thermal emission. Vasoconstriction and

vasodilation of the blood vessels function to regulate blood flow in the skin. Thermoreceptors in the skin, also known as Ruffini corpuscles, recognize the environmental temperature. Increasing the temperature results in vasodilation, leading to increased blood flow through the skin, whereas vasoconstriction occurs by a decrease in temperature and results in reduced blood flow through the skin. These physiological processes combine with heat transfer and thermoregulation in convection, conduction, radiation and sweat evaporation. Heat transfer by radiation is of great value in medicine [16]. With continuing exercise, the body core temperature begins to rise. When internal temperature increases toward a threshold, a regulating system starts to stimulate thermo sensitive neurons in the central nervous system. This triggering of cutaneous vasodilation ensures the transfer of metabolic heat from the core to the skin. The vasoconstrictor mechanism at the beginning of the exercise occurs primarily in the skin blood vessels, whereas the perforator vessels are less affected. As exercise duration increases, it contributes to the rewarming of the skin. The identification of a skin thermic map of perforator vessels that includes its perfusion area can be important to define individual anatomy of certain tissues. Normal findings in human body skin temperature are a symmetrical distribution, and injury or exercise can affect this thermal symmetry [19].

The infrared measurements are highly sensitive to thermal differentials. Healthy people exhibit symmetric thermal patterns. Research has shown that an asymmetry of 1° C is abnormal. Detecting an already inflamed area may provide substantial additional feedback to medical, scientific, and coaching personnel as to exactly where the injured area is, and the extent to which the tissue is damaged. Thermal imaging in the detection and treatment of injury relies on the underlying physiology of temperature differentials. [25].

Traumatic injuries usually involve a long, costly rehabilitation period. High-quality treatment can reduce the duration and negative impact of the rehabilitation period. It is well known that richly vascularized areas heal faster compared to poorly vascularized areas. MIT may give information about the state of vascularization and the on-going healing process to ensure the most effective treatment and to provide recovery information [1].

III. METHODOLOGY

Fig . 2 shows a diagram of the mechatronic system. The embedded system Arduino UNO receives the following user signals: starting angle, end angle, and speed and number of repetitions. LCD screen 16x2 is the interface between the user and the machine. The embedded system communicates with stepper motor driver and the stepper motor moves a gear system on a rotating table where the accessory arm rehabilitation is installed.

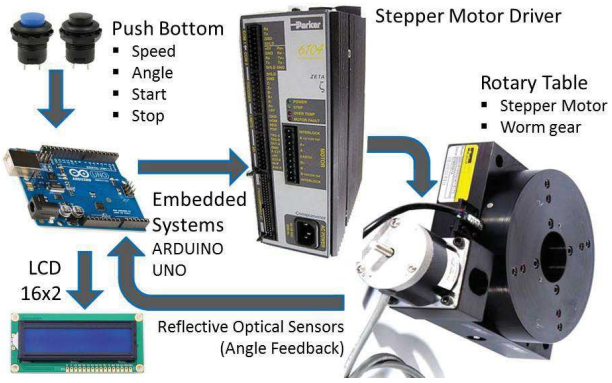

Fig. 2. *S*chematic diagram of mechatronic system

A stepper motor can be a good choice when a controlled movement is required. This is because stepper motor is an open loop system with no feedback required, making it simpler and less costly to control. Stepper motor can generate holding torque when energized and can be stalled without damage. It is widely used for accurate positioning machines and robotics [10]. Stepper motor is an electromechanical device which converts electrical pulse into discrete mechanical movements. It rotates in discrete step when electrical command pulses are applied to it. The direction of the motor rotation is related to the sequence of the pulses applied and the speed of the rotation is directly related to the frequency of the input pulses.

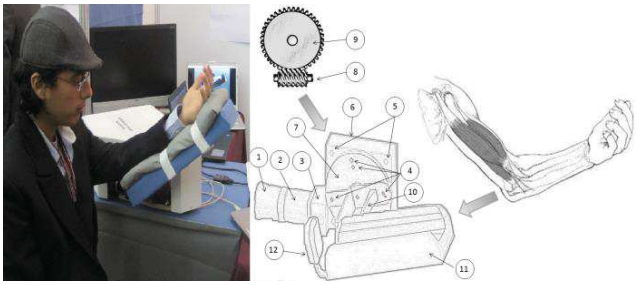

Fig. 3. Mechatronics device. Elbow rehabilitation routine

The elbow is a hinge joint between the radius and ulna of the forearm and the humerus of the upper arm. The bones are held together by ligaments. The primary ligaments of the elbow include the medial collateral ligament on the inside of the elbow and the lateral collateral ligament on the outside. Several muscles surrounding the joint are responsible for movement. In order to assess the pain threshold from pressure exerted it is necessary to quantify the pressure [26]. The tendons attach the muscle to the bone, the cartilage covers and protects the ends of the bones, and bursa sacs provide lubrication and protection around the joint. The causes of some of the most common elbow pain include: Arthritis, Osteoarthritis, Rheumatoid arthritis, sprains and strains,

dislocation, elbow fractures, Olecranon bursitis, cubital tunnel syndrome, lateral epicondylitis and medial epicondylitis [17].

Fig . 3 displays elbow routine rehabilitation. The forearm lies on the accessory (Part. No. 11 and 12), which is connected to the rotary table (Part No. 5,6,7,4 and 10) and delivers an adequate torque from worm gear (Part No. 8 and 9) and stepper motor (Part No. 1,2 and 3).

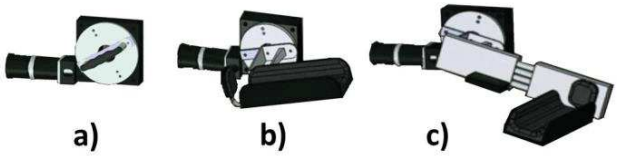

Fig. 4. Asscesories of the mechatronic device for arm rehabilitation. a) wrist, b) Elbow, and c) shoulder.

Arm rehabilitation also includes wrist and shoulder exercise routines. The wrist rehabilitation requires a rotary movement and the shoulder rehabilitation requires up and down lifting movements.

TABLE I. PARTS DESCRIPTION OF ELBOW ACCESSORY

	Part No.	*Description*
Arm	11	Forearm support
	12	Elbow support
Stepper motor	1	Hand-crank motor
	2	Stepper motor
	3	Motor coupling
Rotary table	4	Screws
	5	Clearance holes
	6	Gear case
	7	Rotary disk
	8	Worm shaft (inside gear case)
	9	Worm gear (inside gear case)
	10	Mechanical joint connection

Table I shows a list of mechatronic device parts used in elbow rehabilitation accesory. In addition, we design accessories for wrist and shoulder rehabilitation, see Fig 4. However, in this paper we report results of Medical Infrared Thermography evaluation only for elbow routine. For future work we have considered engaging in applied research with MIT evaluation about relations between pain, recovery health and injury diagnostic using wrist and shoulder accessories of Mechatronics Device for Arm Rehabilitation.

IV. RESULTS

In Medical Infrared Thermography evaluation we used a camera FLIR E50. The red area in Fig 5 shows temperature increase after routine completion. Image a) refers to temperature increase in exercised muscles and b) refers to temperature increase in skin blood vessels.

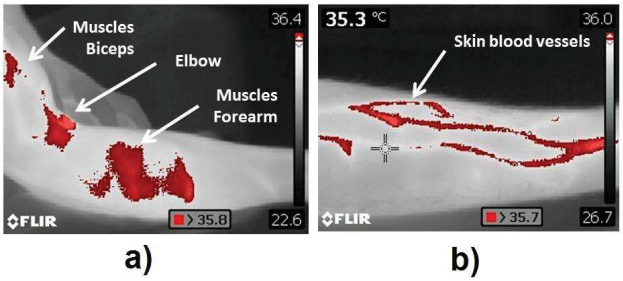

Fig. 5. Medical Infrared Thermography. a) Temperature increase in exercised muscles, b) Temperature increase in skin blood vessels

Infrared images in Fig. 5 are evidence of exertion in the muscles and the circulatory system. The mechatronic device rehabilitates the patients' arms with elbow injury.

V. CONCLUSION

The Mechatronic Device for Arm Rehabilitation was proposed using a stepper motor to move a worm gear inside a rotary table, where accessories for rehabilitation of elbow, shoulder and wrist can be screwed. The control and user interface are provided by the embedded system to setup the routine parameters: start angle, end angle, speed and number of repetitions.

Thermal images allow us to evaluate routine elbow rehabilitation and recovery through temperature increase in muscles and blood vessels. Application of Medical Infrared Thermography is an evaluation method, which has the following benefits: efficiency, safety and low cost for the diagnosis of injuries in mechatronic rehabilitation therapy.

VI. ACKNOWLEDGMENT

The authors gratefully acknowledge the help and support of F. Schick, L. Escobar Hernandez, R. Gomez Lee, H. E. Salgado Rodriguez.

VII. REFERENCES

[1] A. J. Singer, R. A .F. Clark, R.A.F. "Cutaneous wound healing". *The New England Journal of Medicine*, vol. 341, no.10, pp. 738-746, 1999.

[2] C. E. Levy, E. Silverman, H. Jia, M. Geiss, D. Omura, "Effects of physical therapy delivery via home video telerehabilitation on functional and health-related quality of life outcomes", *The Journal of Rehabilitation Research and Development*, vol. 52, pp. 361-370, 2015.

[3] C. H. Guzmán Valdivia, A. Blanco Ortega, M.A. Oliver Salazar, "Entendiendo la Mecatrónica en la Rehabilitación", *X Congreso Internacional sobre Innovación y Desarrollo Tecnológico*, Cuernavaca, México, 2013.

[4] C. Hildebrandt, K. Zeilberger, E. F. John Ring, C. Raschner, "Sports Injury The Application of Medical Infrared Thermography in Sports Medicine", *in An International Perspective on Topics in Sports*

Medicine and Sports Injury, K. R. Zaslav, Ed. Croatia: InTech, pp. 357-274, February 2012.

[5] D. Piovesan, Y. Arumugam, C. Jackson, S. Kumar Shanmugam, A. Restifo, K. Legters, "Gannon Exoskeleton for arm Rehabilitation (G.E.A.R)", *Proc. Of the ASME*, Houston, USA, 2015

[6] D. Thomas, G. Siahamis, M. Marion, C. Boyle, "Computerised infrared thermography and isotopic bone scanning in tennis elbow", *Annals of the Rheumatic Diseases*, vol. 51, pp. 103-107, 1992

[7] F. Yakub, A. Zahran, M. Khudzairi, Y. Mori, "Recent trends for practical rehabilitation robotics, current challenges and the future", *International Journal of Rehabilitation Research*, vol. 37, no. 1, pp. 9-21, March 2014.

[8] G. M. Carlomagno, G. Cardone, "Infrared thermography for convective heat transfer measurements", *Experiments in Fluids*, vol. 49, pp. 1187-1218, 2010.

[9] H. J. Park, J. S. Nah, H. Y. Zhang, Y. E. Cho, S. I. Lee, In S. Park, "Digital Infrared Thermographic Imaging in Patients with Gastroesophageal Reflux Disease", *Journal of Korean Medical Science*, vol. 13, pp. 291-291, February 1998.

[10] H. M. Nasab, "Speed control driver of stepper motor", *Science Road Journal*, vol. 1, no. 1, pp. 1-5, 2013

[11] J. Nilson, G. Maffi, B. Tommolillo, G. Grioni, "Robot-aided neurorehabilitation: Monitoring the effect of robot- assisted training on hand and elbow-shoulder movements by means of quantitative robot derived kinematic measurements", *30th International Congress of Clinical Neurophysiology*, Berlin, Germany, 2014

[12] J. Steketee, "Spectral emissivity of skin and pericardium". *Physics in Medicine and Biology*. vol. 18, no. 5, pp. 686-694, 1973

[13] J. Wang, Y. Li, "A Cooperated-Robot Arm Used for Rehabilitation Treatment with Hybrid Impedance Control Method", *Intelligent Robotics and Applications*, vol. 6425, pp 451-462, 2010

[14] L. M. Crespo, J. Schneider, L. Jaeger, R. Riener, "Learning a locomotors task: with or without errors?", *Journal of NeuroEngineering and Rehabilitation,* vol. 11, no, 25, pp. 17-21, 2014

[15] M. J. Johnson, H.F.M. Van der Loos, C.G. Burgar, L. J. Leifer "Design and Evaluation of Driver's SEAT: Simulation environment for upper limb stroke therapy", *Robotica*, vol. 21, pp. 13-23, 2003

[16] N. Charkoudian, "Skin blood flow in adult human thermoregulation: how it works, when it does not and why". *Mayo Clinic Proceedings*, vol.78, no.5, pp. 603-612, 2003

[17] Orthopaedic & Rheumatologc Institute, *Treatment Guide Understanding Elbow Pain*, Doc. 866.275.7496, Cleveland Clinic, 2015

[18] R. Sanchez, D. Reinkensmeyer, P. Shah, J. Liu, S. Rao, R. Smith, S. Cramer, T. Rahman, J. Bobrow, "Monitoring Functional Arm Movement for Home-Based Therapy after Stroke", *Proc. of the 26th Ann. Int. Conf. of the IEEE EMBS*, San Francisco, CA, USA, 2004

[19] R. Vardasca, "Symmetry of temperature distribution in the upper and lower extremities". *Thermology International*, vol.18, no.4, pp. 154-155, 2008.

[20] S. D. Sikdar, A. Khandelwal, S. Ghom, R. Diwan, F. Debta "Thermography: A new Diagnostic Tool in dentistry", *Journal of Indian academy of oral medicine and radiology*, vol. 22, no. 4, pp. 206-210, 2010.

[21] S. Pundik, J. P. McCabe, K. Hrovat, A. E. Fredrickson, C. Tatsuoka, J. Feng, J. Daly, "Recovery of post stroke proximal arm function, driven by complex neuroplastic bilateral brain activation patterns and predicted by baseline motor dysfunction severity", *Frontiers in Human Neuroscience*, vol. 9, no. 394, July 2015

[22] S. Vedula, "Infrared Thermography and ultrasonic inspection of adhesive bonded structures, overview and validity", M.S. thesis, Clemson University, USA, 2010

[23] T. Varghese, J. A. Zagzebski, G. Frank, E. L. Madsen, "Elastographic Imaging Using a Handheld Compressor ", *Ultrasonic Imaging*, vol. 24, pp. 25-35, 2002.

[24] V. A. L. Jones "Physiotherapy in the management of tennis elbow: a review", *Shoulder & Elbow Journal*, vol. 1, pp. 108-113, 2009

[25] W. A. Sands, J. R. McNeal, M. H. Stone, "Thermal Imaging and gymnastics injuries: a means of screening and injury identification", *Science of Gymnastics Journal*, vol. 3, no. 2, pp. 5-12, 2011.

[26] W. Y. Lau, A. J. Blazevich, S. S. X. Wu, "Assessment of Muscle Pain Induced by Elbow-Flexor Eccentric Exercise", *Journal of Athletic Training*, vol. 50, no. 11, 2015

Electronic implementation for an elemental unit of a FitzHugh neural network

L.J. Ontañón-García, M.T. Ramírez-Torres
Coordinación Académica Región Altiplano Oeste
Universidad Autónoma de San Luis Potosí
Salinas de Hidalgo, San Luis Potosí, México
luis.ontanon@uaslp.mx;marcotulio_rmz@hotmail.com

R.E. Lozoya-Ponce, M. García-Martínez
Departamento Académico de Mecatrónica y
Tecnologías de Información.
Escuela de Ingeniería y Ciencias
Tecnológico de Monterrey
ricardo.lozoya@itesm.mx,
moises.garcia85@gmail.com

***Abstract*—The printed circuit board (PCB) of an elemental neural network is implemented from the mathematical model described by FitzHugh. This model represents the excitable oscillatory behavior of the membrane potential and the refractoriness of the potential of a single neuron. The system is electronically implemented by means of operational amplifiers connected in multiplier, adding and integrating configurations. The designed circuit can be implemented in a coupling scheme suitable for analog neural networks communication, avoiding the discretization of the commonly digital schemes.**

Keywords—Physical Design and PCB, mathematical models, biological systems, neuron, synchronization, neural network.

I. Introduction

In the middle of the last century, the advances in the electronic and circuits theory made possible the implementation and study of biological systems. One of the most relevant examples of this was on the measure of the membrane potential of the axon of the giant squid. This experiment developed by Hodgkin and Huxley [1] result in the first mathematical model of the neuron. The model described the electrical excitation and propagation through the axon of the giant squid by the voltage-clamp technology through a four dimensional system of ordinary differential equations. The publication of this model resulted in a new trend which focuses on the study and development of biological mathematical models in different areas of science. For example, a decade later FitzHugh [2] using an approximation based on the Van der Pol equation for a relaxation oscillator, successfully reduced the Hodgkin and Huxley model in the number of equations. This reduced model describes the electrical behavior of a neuronal membrane and the ion currents which are involved in the process. After this model was published, a great number of experiments concerning the study of the electrical activity in neurons were developed [see [3] and the references within]. However there is a greater number of equations in the subsequent systems, making the FitzHugh-Nagumo model the most reduced neuron model.

The electronic implementation from which the printed circuit board (PCB) was generated here [4] is based on analog continuous-time computation methods [5-8], in which operational amplifiers (op-amps) are connected in different forms in order to obtain summations, integration and multiplication effects on the signals. This methods study real life problems which are difficult to be analyzed through dynamical systems. The idea is to use their exact solutions instead of their approximate responses using numerical integration methods which are limited by discretization and memory limitations. Throughout this analog processes, axons and neural cells have been correlated in order to describe certain types of computation and decision-making processes [9-10]. Furthermore, the presented circuit of the neuron is implemented in a bidirectional coupling method which can be extended in a neural network communication scheme.

The aim of this project lies in the analog signal handling from the neuron model. Since in other models, for example the hypothetical nervous system called a perceptron, which was proposed by Frank Rosenblatt [11], only binary signals were discussed. The handling of analog signals opens a new panorama; and just as there is digital and analog electronics, this paper proposes the revision of a continuous system which can further complement the theory of discrete neural networks, in a future work.

This article is organized as follows: Section II presents the general theory that envelops the mathematical model of the neuron; Section III introduces the circuit design of the biological system; Section IV describes the coupling between two neurons and the communication scheme. Section V describes the electronic implementation and the PCB. And finally conclusions are drawn in Section VI.

II. Mathematical Model of the FitzHugh Neuron

The two dimensional model considered for the network, was described by FitzHugh. This model is based on the Van der Pol equation for a relaxation oscillator which is generalized by the addition of terms to produce a pair of non-linear differential equations with either a stable singular point or a limit cycle oscillator [2], resulting in the following set of equations:

$$\begin{aligned} \dot{x_1} &= x_1 - \tfrac{1}{3}x_1^3 - y_1 + I, \\ \dot{y_1} &= \tfrac{1}{c}(x_1 + a - by_1); \end{aligned} \tag{1}$$

where x and y are the state variables, x stands for the membrane potential and its excitability, while y represents the accommodation and refractoriness of the potential. The parameters $a, b, c \in \boldsymbol{R}$, while the term $I \in \boldsymbol{R}$ corresponds to the

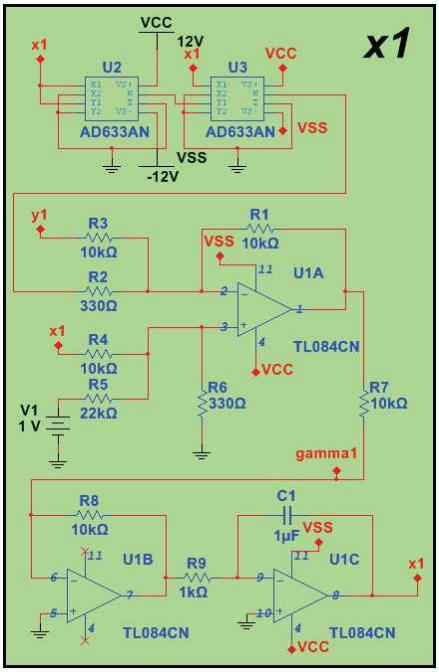

Figure 1: Schematic diagram of the x_1 state given by (1).

the stimulus intensity depicted by the membrane current in the Hodgkin and Huxley model. The systems electrical activity changes oscillating regarding to a cathodal shock of the membrane current [2]. The common values of the parameters in which the system presents oscillations are $I = 0.5, a = 0.7, b = 0.8, c = 12.5$.

III. The Electronic Implementation

The design of the system described here presents some variations with respect to the electronic implementation described in [4]. Here the values are arranged to consider commercial resistor values. The use of analog components considering the technic based on the op-amps was first proposed by Orponen in [4]. The main advantage of this technique, is that these electronic devices are not affected by the loss of information in an analog to digital conversion.

The process of conversion from the differential equation of a system throughout the configurations of the amplifier will be consider as described in [4] and [12].The state x given by (1) along with its corresponding set of parameters will be integrated with respect of time from both sides of the equation, resulting in $x_1 = \int (x_1 - \frac{1}{3}x_1^3 - y_1 + I)dt$. From this equation one can easily implement the configurations of the op-amps (inverting amplifier, differential amplifier and inverting integrator) as the Figure 1 depicts.

If standard node analysis technique is applied to the circuit in the output terminal of U1C, it will result in an equation that

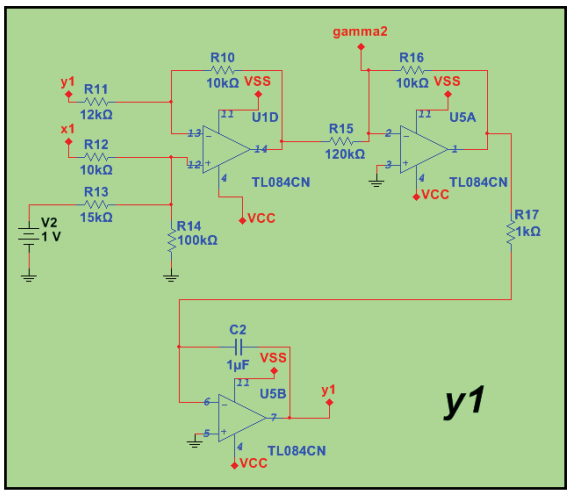

Figure 2: Schematic diagram of the y_1 state given by (1).

governs the behavior of the output voltage of the voltage follower in the U1C component. Therefore the resulting state will be given by:

$$x1 = \frac{R8}{R7}\int \left(-\frac{R1}{R3}y1 - \beta_{1x}\left(\frac{x^3}{100}\right) + \beta_{2x}x1 + \beta_{3x}V1\right)dt + V_{c1_0}, \quad (2)$$

where the terms $\beta_{1x}, \beta_{2x}, \beta_{3x}$ are given as follows:

$$\begin{aligned} \beta_{1x} &= R1/R2, \\ \beta_{2x} &= \frac{(R5\|R6)(R1+R2\|R3)}{(R2\|R3)(R4+R5\|R6)}, \\ \beta_{3x} &= \frac{(R4\|R6)(R6+R2\|R3)}{(R2\|R3)(R5+R4\|R6)}. \end{aligned} \quad (3)$$

The notation "‖" represents the equivalent resistor in parallel in the following way $RA \parallel RB = (RA \cdot RB)/(RA + RB)$. By the substitution of the corresponding commercial resistor values of R1-R6 depicted in Figure 1, the gains of the U1A Op-Amp will result in $\beta_{1x} = 30.3030$; $\beta_{2x} = 1.0172$; $\beta_{3x} = 0.4624$. Therefore x_1 will become $x_1 = \int (x_1 - 0.30303x_1^3 - 1.0172y_1 + 0.4624)dt$ which still are oscillating parameters of the neuron [2].

The cubic term was implemented through the four quadrant multiplier AD633AN depicted as the U2 and U3 components. In this case the U1A is arranged in the difference amplifierconfiguration, U1B corresponds to the inverting amplifier, and the integration is carried out by U1C. If the values of the resistors are replaced as the diagram of Figure 1 depicts, the equation (2) will result in the same form as the one in the variable state in Eq. (1). The term V_{C1_0} corresponds to the initial voltage in the capacitor C1.

Similar considerations can be made to the state y of the equation (1). The integration of both sides will result in $y_1 = \frac{1}{c}\int (x_1 + a - by_1)dt$, which implemented with the op-amp configuration will result in the circuit of Figure 2. Considering the node analysis in the output of U5B, the voltage will result in the following equation:

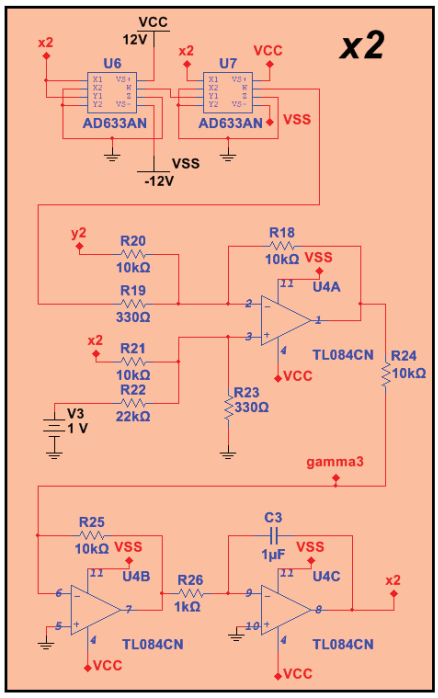

Figure 3: Schematic diagram of the x_2 state of system 2.

$$y1 = \frac{R16}{R15}\int\left(-\frac{R10}{R11}y1 + \beta_{1y}x1 + \beta_{2y}V2\right)dt + V_{c2_0}, \quad (4)$$

where the terms β_{1y}, β_{2y} are given as follows:

$$\begin{aligned}\beta_{1y} &= \frac{(R13\|R14)(R10+R11)}{(R11)(R12+R13\|R14)},\\ \beta_{2y} &= \frac{(R12\|R14)(R10+R11)}{(R11)(R13+R12\|R14)};\end{aligned} \quad (5)$$

Which if substituted with the corresponding commercial resistor values of Figure 2 will result in $\beta_{1y} = 1.0377, \beta_{2y} = 0.7233$, and then $y_1 = \frac{1}{c}\int(1.0377x_1 + 0.7233 - 0.8333y_1)dt$ corresponding also to oscillating values of the neuron.The values of the resistors and voltages are depicted in the schematic from Figure 2. The term V_{C2_0} corresponds to the initial voltage of the capacitor C2.

The schematics from Figure 1 and 2 corresponds to the states of a single neuron. In order to present an elemental unit of a neural network at least two coupled systems are needed. The second system will take the exact same form as the equation (1) with the values obtained from (3) and (5). The schematics of the system are described in Figure 3 and Figure 4 for the x_2 and y_2 states, respectively.

IV. Coupling of the Systems

In order to synchronize both neuron circuits a coupling method is required. Since the systems are identical (at least from the diagram without considering the real tolerance in resistors) an effective synchronization method comes from the

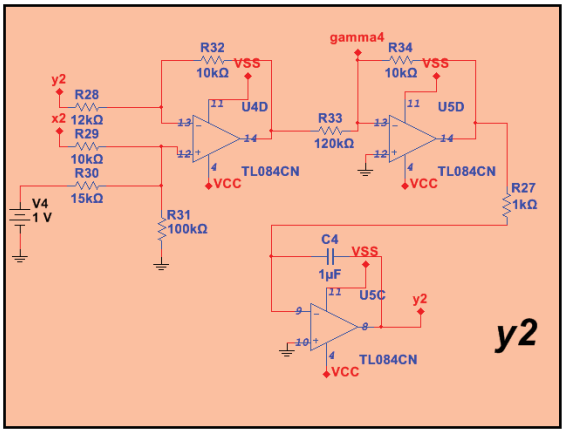

Figure 4: Schematic diagram of the y_2 state of system 2.

bidirectional coupling. The idea is to couple both states x_1 and y_1 with their respective of system 2, i.e., x_2 and y_2, respectively. The coupled systems will result in the following set of equations:

$$\begin{aligned}\dot{x_1} &= x_1 - \frac{1}{3}x_1^3 - y_1 + I + \gamma_1;\\ \dot{y_1} &= \frac{1}{c}(x_1 + a - by_1) + \gamma_2;\\ \dot{x_2} &= x_1 - \frac{1}{3}x_1^3 - y_1 + I + \gamma_3;\\ \dot{y_2} &= \frac{1}{c}(x_1 + a - by_1) + \gamma_4;\end{aligned} \quad (4)$$

where $\gamma_i, i = 1, \dots, 4$ correspond to a bidirectional coupling which takes the following form:

$$\begin{aligned}\gamma_1 &= \alpha_1(x_2 - x_1);\\ \gamma_2 &= \alpha_2(y_2 - y_1);\\ \gamma_3 &= \alpha_3(x_1 - x_2);\\ \gamma_4 &= \alpha_4(y_2 - y_1).\end{aligned} \quad (5)$$

The parameter $\alpha_i \in \boldsymbol{R}, i = 1, \dots, 4$ corresponds to the coupling force. Notice that synchronization can be achieve if $\lim_{t\to\infty}(x_2 - x_1) \to 0$ and $\lim_{t\to\infty}(y_2 - y_1) \to 0$. The coupling can be generated throughout the circuit depicted in Figure 5 for $\gamma_1, \dots, \gamma_4$. The signals $gamma1, \dots, gamma4$ will be connected through the 10KΩ resistors (R51, …, R54) in the following inverting inputs: 6 of the U1B in Figure 1, 2 of the U5A in Figure 2, 6 of the U4B in Figure 3 and 13 of the U5D in Figure 4, respectively. This will result in the following values for coupling strength:

$$\begin{aligned}\alpha_1 &= \frac{R8}{R51};\\ \alpha_2 &= \frac{R16}{R52};\\ \alpha_3 &= \frac{R25}{R53};\\ \alpha_4 &= \frac{R34}{R54};\end{aligned} \quad (6)$$

With the resistor values marked as 10KΩ, the values of the coupling strength will result in $\alpha_i = 1, i = 1, \dots, 4$. If this values are to increase the respective resistor R51, …, R54 can be modified according to the equation (6).

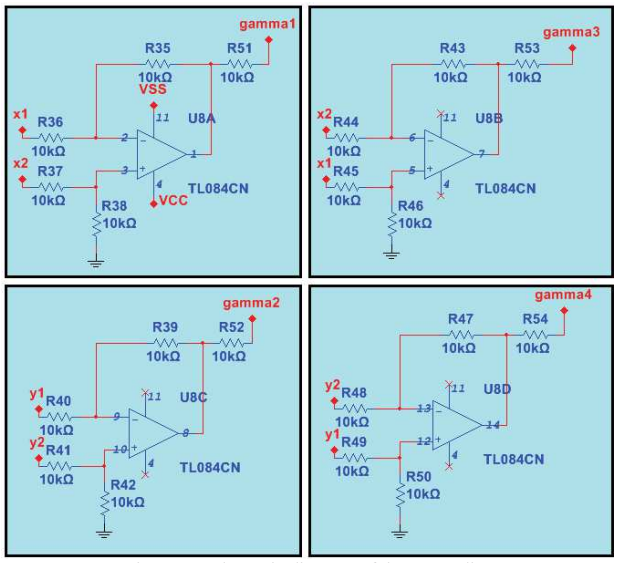

Figure 5: Schematic diagram of the γ coupling.

V. PCB OF THE ELECTRONIC IMPLEMENTATION

The PCB was designed in order to contain both neuron into the board without the coupling. The purpose of this is to avoid limitations with respect to the number of neurons to be further include in the network. Since for each neuron system included two signals (x_n and y_n, respectively) must be considered for the inputs of the coupling Op-Amps. The coupling depicted in Figure 5 represents a bidirectional coupling, however different types of couplings can be implemented in different experiments. As mentioned before, the capacitors and resistors were adjusted in to the circuit to match commercial resistor values. The PCB design can be appreciated in Figure 6.

VI. EXPERIMENTAL RESULTS

The experimental results of theelemental unit of the FitzHugh neural network are depicted in Figure 7. Where it can be appreciated the two autonomous states for both systems in Figure 7 a) and b) for x_1, x_2, and y_1, y_2, respectively. Notice between the signals that the signal in red$math = x_2 - x_1 \neq 0$, meaning that both systems are not synchronizedsince the two neurons oscillate autonomously with different trajectories. On the other hand, after adjusting the bidirectional coupling from Figure 5 both systems synchronize their states as it is depicted in Figure 7 c) and d) for x_1, x_2, and y_1, y_2, respectively. The signal $math = x_2 - x_1 \approx 0$ meaning that both systems oscillate synchronously. The measurements for the peak to peak voltage and the oscillating frequency are depicted on each corresponding measure of the Figure 7.

VII. CONCLUSIONS

Although analog computing was thought to be not suitable for all applications, even obsolete in the digital revolution, now a days there have several studies proving the opposite. One of the main advantage of analog devices as mentioned before, is the characteristic of presenting non-discretized or approximate signals from their outputs. This results in a mayor advance in

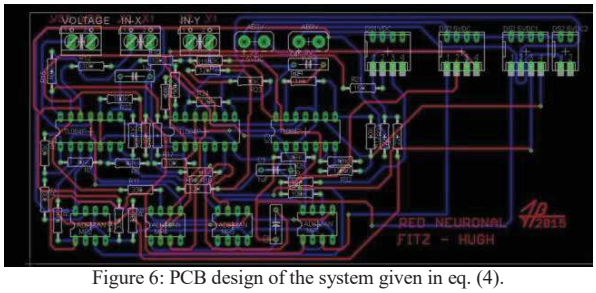

Figure 6: PCB design of the system given in eq. (4).

electronic bio-inspired systems, since analog circuits assimilate a more natural response than their digitalized versions.

In this case the PCB and physical implementation of the elemental unit of the FitzHugh neural network probe to be suitable for bidirectional coupling, resulting in a synchronizing behavior in their states, which is a fundamental characteristic in biological systems working in clusters. The synchronization that the system depicted was present even by the variation of the original parameter values. In which the systems oscillate adequately resulting in a feasible option to develop units of a larger FitzHugh neural network.

With this electronic design new coupling methods can be implemented with different number of systems in order to study the mutual interaction of systems in a more tangible way. Also, the technique described here can be extended to several biological systems in order to help biologist with a low cost alternative to develop new methods in the research of cures for diseases, for example in pancreatic beta cell, which are biological systems that are known to produce the insulin hormone only in synchronized cluster in the Langerhans islets.

The studies of this researches along with the results of the neural network can be reported elsewhere.

ACKNOWLEDGMENS

L.J.O.G. acknowledges the financial support through the following projects PRODEP/DSA/103.5/15/6988 and C15-FAI-04-80.80.

REFERENCES

[1] Hodgkin, A. L., & Huxley, A. F. (1952). The dual effect of membrane potential on sodium conductance in the giant axon of Loligo. The Journal of physiology, 116(4), 497-506.

[2] FitzHugh, R. (1961). Impulses and physiological states in theoretical models of nerve membrane. Biophysical journal, 1(6), 445.

[3] Hindmarsh, J. L., & Rose, R. M. (1984). A model of neuronal bursting using three coupled first order differential equations. Proceedings of the Royal Society of London B: Biological Sciences, 221(1222), 87-102.

[4] Ontañón-García. L.J, Soubervielle-Montalvo C. & Campos-Cantón, E., Analog circuit implementation of a neuron with applications to communications. Memorias del XVI Congreso Nacional de Control Automático CNCA 2015, Octubre 14-16, 2015. Cuernavaca, Morelos, México.

[5] Orponen, P. (1997). A survey of continuous-time computation theory. In Advances in algorithms, languages, and complexity (pp. 209-224). Springer US.

[6] Siegelmann, H. T., & Fishman, S. (1998). Analog computation with dynamical systems. Physica D: Nonlinear Phenomena, 120(1), 214-235.

[7] Horio, Y., & Aihara, K. (2008). Analog computation through high-dimensional physical chaotic neuro-dynamics. Physica D: Nonlinear Phenomena, 237(9), 1215-1225.

[8] Xue, Y. (2015). Recent Development in Analog Computation-A Brief Overview. arXiv preprint arXiv:1504.00450.

[9] Cabessa, J., & Villa, A. E. (2015). On Super-Turing Neural Computation. In Advances in Cognitive Neurodynamics (IV) (pp. 307-312). Springer Netherlands.

[10] Scarpellini, B. (2003). Two undecidable problems of analysis. Minds and Machines, 13(1), 49-77.

[11] Rosenblatt, F. (1958). The perceptron: a probabilistic model for information storage and organization in the brain. Psychological review, 65(6), 386.

[12] Ontañón-García. L.J, Campos-Cantón, E. & Campos-Cantón, I., Electronicimplementation of a pancreatic beta cell. Memorias del XVICongreso Latinoamericano de Control Automático, CLCA 2014, Octubre14-17, 2014. Cancún, Quintana Roo, México.

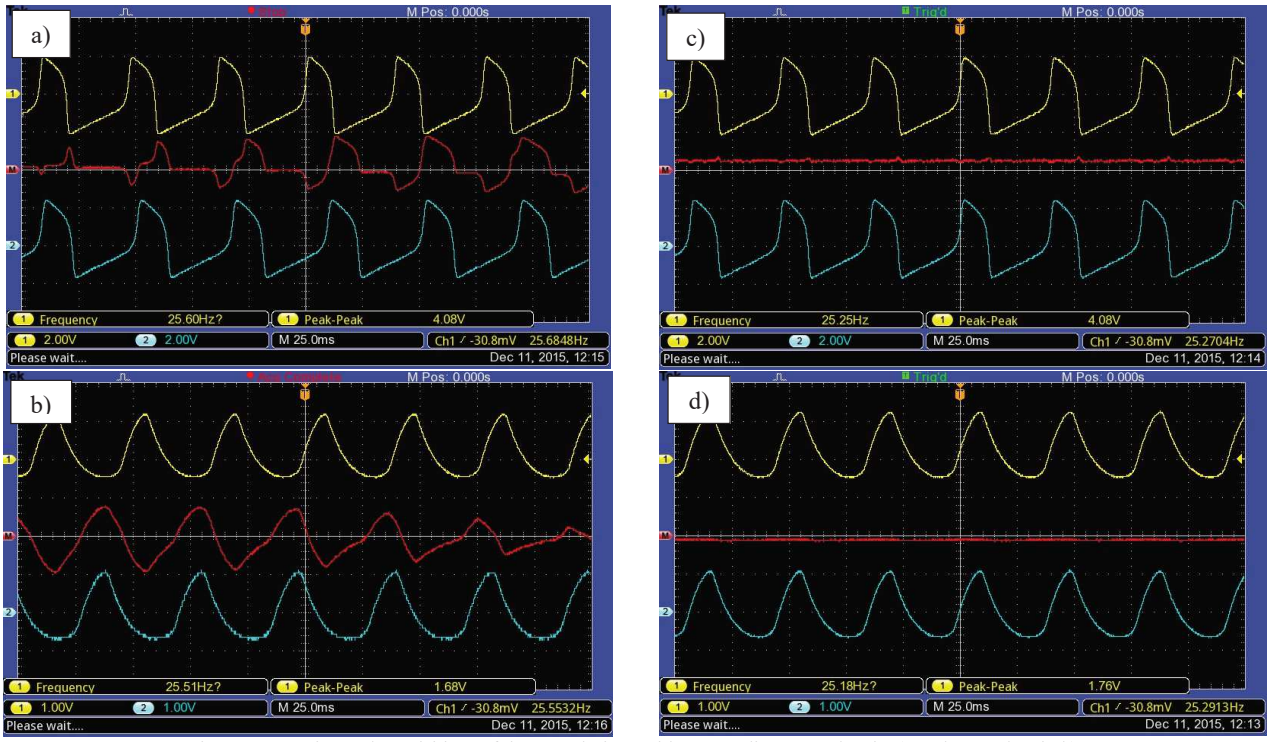

Figure 7: Experimental acquisitions of the PCB design. Without coupling: x_1 and x_2 in a) and y_1 and y_2 in b).
With the coupling from Figure 5: x_1 and x_2 in c) and y_1 and y_2 in d).

Quadcopter trajectory tracking using visual servoing

Pablo Valencia Bibian, Amparo Dora Palomino Merino, Sergio Vergara Limon,
María Aurora Diozcora Vargas, Jaime Julián Cid Monjaraz.
Benemérita Universidad Autónoma de Puebla, Facultad de Ciencias de la Electrónica, Edificio 1FCE76, Ciudad Universitaria
Av. San Claudio y 18 Sur, Colonia Jardines de San Manuel, Puebla, Puebla Tel, (222) 229 55 00 ext. 7405
pablovale2000@yahoo.com.mx, palomino@ece.buap.mx .

***Abstract*— This work exhibits the quadcopter mobile robot control over the yaw movement using visual servoing. To achieve the goal it was adjusted using sensors. At first, mobile robot will remain at a constant height. The images are gotten by the camera and then sent to the computer via wireless where they're processed, it also gets (position and velocity) information, calculates error for subsequent feedback to the microcontroller and thereby moves towards a new desired position.**

The prototype structure (frame) is a modified racing model with a flight controller Multiwii 2.4 to which adjustments were made to go through the use of the computer. Open CV was used for image processing, Arduino software was occupied for microcontroller programing using camera on hand mode configuration and a visual servoing control based on the position, mention should be made of practical applications at industrial and research levels of this control type as it can be used locating faults or damages to tanks and pipelines by detecting image changes.

Keywords—camera, quadcopter, visual feedback.

I. INTRODUCTION

The visual servoing refers to a closed loop system that uses visual information (commonly get by a camera) to control a robot movement [1], the term was initiated by Hill and Park in 1979 [2]. We can also classify the visual servoing by the camera position: using stand by camera mode: in this configuration the camera is placed in the robot and it allows to watch the robot movement in first person based on the environment observation that surrounds the robot.

Also we can classify the visual servoing according as how we get information included into the position based visual servoing (PBVS) and based on image (IBVS). At first, the main image features are obtained and its position is estimated with respect to the camera using these values, a signal error is generated between the robot current position and the position you want to reach (desired position).

At the second error signal is defined directly by the image features it contains [3] [4].

Nowadays the UAV's (Unmanned Aircraft vehicles) are commonly used in many applications. That motivates us to study different types of control aircraft, besides, advanced technology allows cheaper sensor based in the MEM'S (Microelectromechanical systems) used in the IMU (Inertial Measurement Unit), as well as miniaturization wireless cameras. That allows to increase the chances to get a real information in a more reliable way.

One of the advantages of employment cameras is that we venture into unknown environments, for this reason , one of the project objectives is to dispense the GPS (Global Position System) as a position sensor, giving the responsibility to the optic sensor. Likewise a microcontroller based on ATmega2560 (Arduino Mega) was used to control the vehicle because of its versatility and extensive documentation.

A. State of the art:

Nowadays there are several works about quadcopters controlled by visual techniques for location space as for example RANSAC [5], another line of research has as a goal to control the quadcopter through the vision taking to account a circular mark to determine the position of the vehicle [6].

Given the capabilities that the quadcopter has to recognize images, it also exists related jobs with the inspection structure [7], as well as researching and rescuing [8]. Also there are used in development of cartographic plans. These are just some of the applications that visual servoing has in this vehicle type, but it is not only limited to these options since they can be used as anthropomorphic robot manipulators [9].

II. SYSTEM OVERVIEW

The main goal of the work is to control the movement of yaw on the robot. The mobile robot we use is described as an unmanned aerial vehicle with 4 motors coupled in a single plane, also known as quadcopter, it has 6 degrees of freedom, but it only has 4 engines therefore it cannot be defined in the same status an independent value for each degree of freedom [10, 11]. The 4 engines which would be the input variables and they give the quadcopter basic movements (Fig. 1).

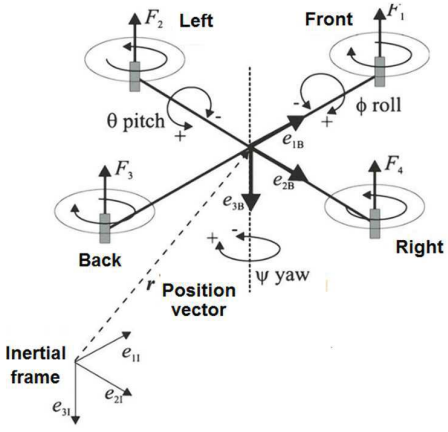

Fig. 1. Basic movements of a quadcopter.

The movement is originated from the changes in each engine speed. The methodology for a simple dynamic model that contains the most important information to facilitate the design of a controller could be found in [12].

A. The movement equations

Given Newton's second law we know that the relationship between forces and accelerations of an inertial system is given by the equation:

$$\sum \overline{F_e} = m \cdot \overline{a_e} \quad (1)$$

Where:

$\overline{F_e}$ = Represents the sum of all forces acting on the center of gravity

m = is the mass of the rigid body

$\overline{a_e}$ = is the acceleration

In the case of non-inertial reference expression is obtained by:

$$\sum \overline{F_b} = \begin{bmatrix} F_x \\ F_y \\ F_z \end{bmatrix} = m(\overline{a}_b + \overline{\omega} \, X \, \overline{v}_b) \quad (2)$$

In a mathematical vector form we can express:

$$\begin{bmatrix} F_x \\ F_y \\ F_z \end{bmatrix} = m \left(\begin{bmatrix} \dot{u} \\ \dot{v} \\ \dot{\omega} \end{bmatrix} + \begin{bmatrix} p \\ q \\ r \end{bmatrix} X \begin{bmatrix} u \\ v \\ \omega \end{bmatrix} \right) \quad (3)$$

Expanding the vector product we have:

$$\begin{aligned} F_x &= m\,(\dot{u} + q\omega - rv) \\ F_u &= m(\dot{v} + ru - p\omega) \\ F_z &= m\,(\dot{\omega} + pv - qu) \end{aligned} \quad (4)$$

From the second law of Euler rotation you have:

$$\sum \overline{M_e} = \frac{dL_e}{dt} = \frac{d(I_e\overline{\omega})}{dt} \quad (5)$$

Which can be expressed in terms of speed, angular accelerations and moments as:

$$\sum M_b = \begin{bmatrix} L \\ M \\ N \end{bmatrix} = I \cdot \dot{\overline{\omega_b}} + \overline{\omega_b} \, x \, (I \cdot \overline{\omega_b}) \quad (6)$$

If the inertia tensor is diagonal, it can simplify the development of the equation 6 to get the 3 equations rigid rotation system:

$$\begin{aligned} L &= I_{xx}\dot{p} + qr(I_{zz} - I_{yy}) \\ M &= I_{yy}\dot{q} + pr\,(I_{xx} - I_{zz}) \\ N &= I_{zz}\dot{r} + pq(I_{yy} - I_{xx}) \end{aligned} \quad (7)$$

B. Yaw Control

The yaw movement is controlled by feedback from ψ; the error in yawE_ψ, It is determined by the difference between the current and the desired value ψ^* (8).

$$E_\psi = \psi - \psi^* \quad (8)$$

The error (8) it's related to the voltage applied to yaw by a control law (9):

$$V_\psi = -(k^a_{p\psi}E_\psi + k^a_{d\psi}E^*_\psi) \quad (9)$$

Where E^*_ψ It's the time derivative of the yaw error, $k^a_{p\psi}$ and $k^a_{d\psi}$ are the control gains.

This is expressed by the block diagram shown in Fig. 2.

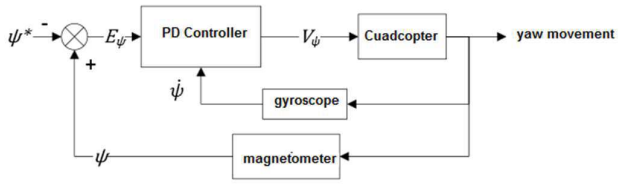

Fig. 2. Yaw motion control.

This movement will provide the vehicle direction. The roll and pitch control is similar. In general, we can describe the quadcopter control as shown in Fig. 3.

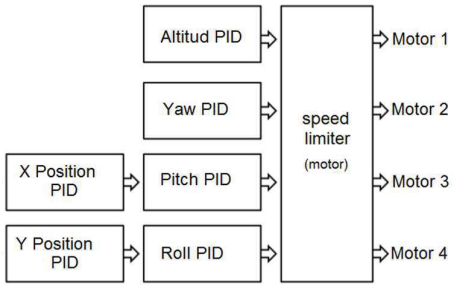

Fig. 3.Description of a quadcopter control.

C. Trajectory tracking

The purpose of trajectory tracking control is to get through a control law that allows the mobile robot to reach and follow the error equal to zero and desired states that vary overtime.

Related to the control strategy, there have been developed a wide variety of algorithms due the fact that the quadcopter model is a multi-variable nonlinear model. Within the proposed algorithms, the Lyapunov based controllers developed by H.Voos [13] and Bouabdallah [14].

III. Visual Servoing

In its simplest form, the goal of any control scheme based on vision is to minimize the error $e(t)$ (Fig. 4) in the manner shown in (10).

$$e(t) = s(m(t), a) - s^* \quad (10)$$

Where $m(t)$ It's a set of measures characteristics of the image (the image coordinates of a point of interest).

$s[m(t), a]$ It is the vector of visual features

a It's a set of additional system parameters (generally the intrinsic parameters of the system).

s^* Refers to the desired values of the visual characteristics.

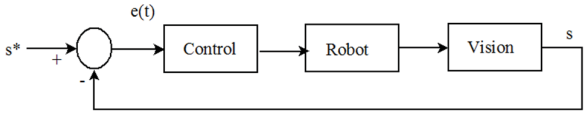

Fig. 4. Basic system of visual control.

A. Optical sensor

Since we will control using vision techniques we require an optical sensor and a wireless camera was used for this purpose, therefore its description and modeled are studied since this sensor will provide us information needed to close the control loop and thanks to that the quadcopter will be positioned in the desired location, this requires to have internal and external necessary parameters to model the camera's system.

B. Pinhole Camera Model

The Pinhole camera model [15] describes the mathematical relationship between the coordinates of a 3D point and its projection on the plane of the 2D image (Fig. 5).

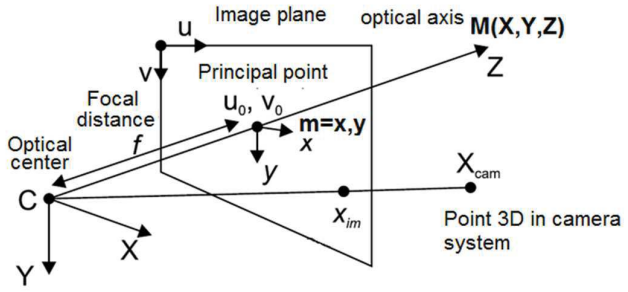

Fig. 5. Pinhole Camera.

The camera performs a projection from a M point in the space to a m point in the image plane through the optical center of the camera, the M point has coordinates (X_c, Y_c, Z_c), It is represented in the image plane by an m point with coordinates (u, v), with reference to a central point of the image (u_0, v_0) where the main point of the camera is found in its own optical axis and at a focal distance f from the center of the sensor (11).

$$\frac{u}{X_c} = \frac{v}{Y_c} = \frac{f}{Z_c} \tag{11}$$

Intrinsic and extrinsic parameters:

The m point can be expressed alternately with reference to the top left edge coordinates x, y (in pixels) through transformation (12).

$$x = u_0 + f_x u \; ; \; y = v_0 + f_y v \tag{12}$$

Which it is expressed in matrix form in (13).

$$\begin{bmatrix} x \\ y \\ 1 \end{bmatrix} = \begin{bmatrix} f_x & 0 & u_0 \\ 0 & f_y & v_0 \\ 0 & 0 & 1 \end{bmatrix} \begin{bmatrix} u \\ v \\ 1 \end{bmatrix} = K \begin{bmatrix} u \\ v \\ 1 \end{bmatrix} \tag{13}$$

Where: K It's the matrix of intrinsic parameters, which is a 3x3 matrix that describes the geometry and the camera optics at the same time; f_x, f_y are the focal lengths in x *and* y respectively.

From (11) we have:

$$\tilde{q} = \frac{1}{Z_c} \begin{bmatrix} X_c \\ Y_c \\ Z_c \end{bmatrix} = (u, v, 1)^T \tag{14}$$

Where $\tilde{q}$ is a point expressed in projective coordinates.

C. Calibration Camera

Through camera's calibration intrinsic and extrinsic parameters are obtained, as well as the distortions of the camera, result of its imperfections (radial and tangential). This calibration record is performed when observing an object of known geometry in which a calibration pattern is printed, the camera parameters are estimated from the relationship between three dimensional coordinates and two-dimensional projections obtained by the image plane, the pattern calibration most widely used is a chessboard [16].

IV. System Description

The experimental platform consists of different elements which are shown Fig. 6.

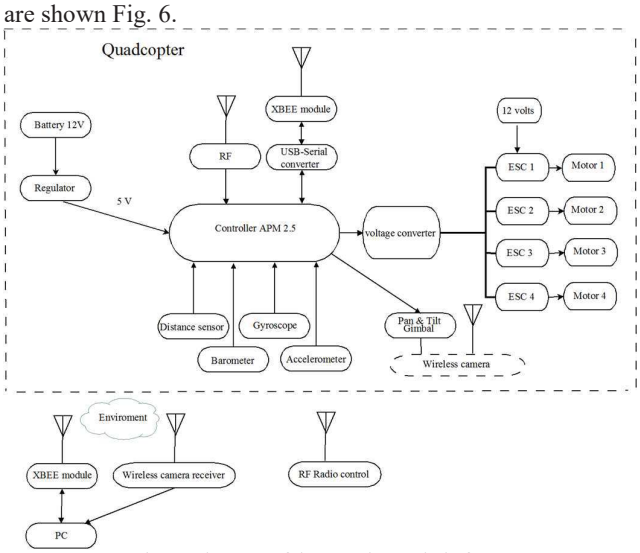

Fig. 6. Elements of the experimental platform.

A. Actuators

4 motors brushless are used 2212 / 13T 1000KV to generate movement of the propellers.

B. Sensors

Inertial Measurement Unit IMU6000 works with 3.3 volts, for communication, it uses an IIC protocol and it also consists of accelerometers and gyroscopes, in total it has 6 DOF (Degrees Of Freedom).

C. APM Controller Card

The controller card is an APM 2.5 (ArduPilot Mega) based on the ATmega2560 chip, it has 54 ports of configurable

entry and output. It's here where the controller is programmed.

D. Electronic Speed Controller (ESC)

Brushless motors are three-phase, ESCs receive the PWM signal provided by the WAP card and based on this it provides the motor energy required.

E. Distance sensor

This sensor is ultrasonic, it operates by emitting an inaudible frequency and getting back to the bounce off versus an object, the sensor measures the time it took to receive the signal from departed and estimates the distance.

F. Power Supply

The energy is provided by a standard LiPo battery of 11.1 volts, with 3-cell 3000mAh. This gives the quadcopter about 10 minutes flight.

G. Pan and tilt system

This mechanic subsystem allows to compensate the quadcopter movement causing the optical axis of the camera will always be perpendicular to the XY plane.

H. Wireless camera

The wireless camera provides images to be processed on a PC and using algorithms and through vision techniques the visual information is obtained.

V. Implementation

On a PC the tests were done in a quadcopter with DJI 450 frame this has an APM 2.6 controller card, the communication is performed by using the MavLink protocol developed by 3D Robotics, it's a color camera and it has a CCD sensor with a 0.3 megapixel resolution (Fig.7).

Fig.7. Quadcopter frame DJI 450.

A. Electrical Diagram

The electronics are connected as shown in Fig. 8.

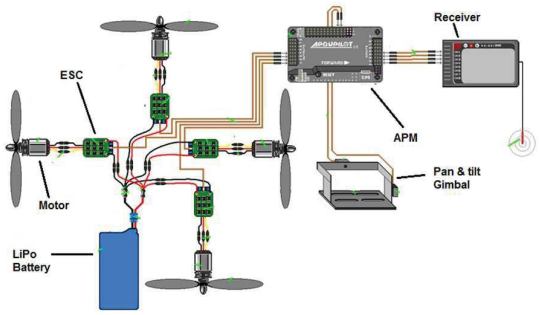

Fig. 8. Electric connections

B. Camera placement

The pinhole camera mounted on a pan & tilt system is shown in (Fig. 9)

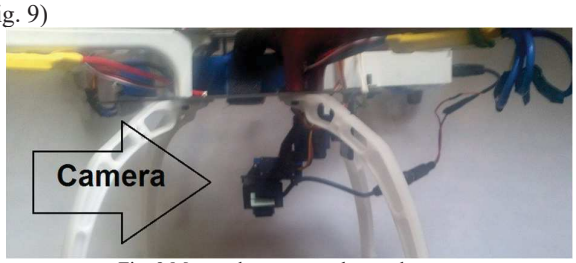

Fig. 9 Mounted camera on the quadcopter.

C. Obtaining parameters

To control properly the quadcopter we must calculate the needed values to rightly stabilize the vehicle, this requires knowing its weight and the gravity center (Fig. 10).

Fig. 10.Center of gravity and weight of the quadcopter.

The obtained mass with all elements is 1,095 kilograms

From a chess board pattern type, extrinsic and intrinsic parameters were obtained (Fig. 11).

Getting the following results (see Table 1).

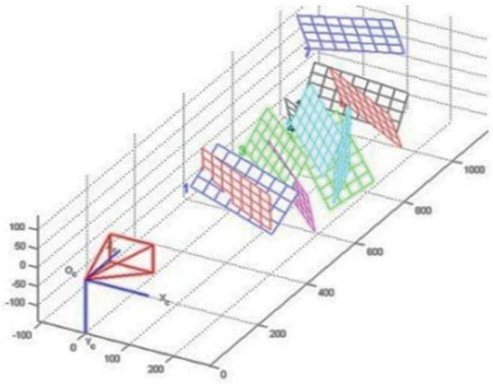

Fig. 11. 3D Parameters representation.

TABLE 1.

Parameter	*Estimation*	*Description*
f_x	935.52100	Focal Distance
f_y	927.38760	Focal Distance
c_x	148.99604	X coordinate of the principal point in the image
c_y	233.26474	Y coordinate of the principal point in the image
$p1$	-.13116	Radial distortion coefficients image
$p2$	-.05587	
$p3$	-.00358	
$t1$	0.0149	Coefficient of tangential lens distortion
$t2$	0.0000	

VI. Results

For this test a follower line program was used, this program looks for a black line on a white background and will get feedback vector rotation when the robot goes out of the way.

A. Simulation Results

The position in z (Fig. 12) and the path followed (Fig. 13) through the following initial conditions:

Since there is no wind and it's a controlled environment without disturbs.

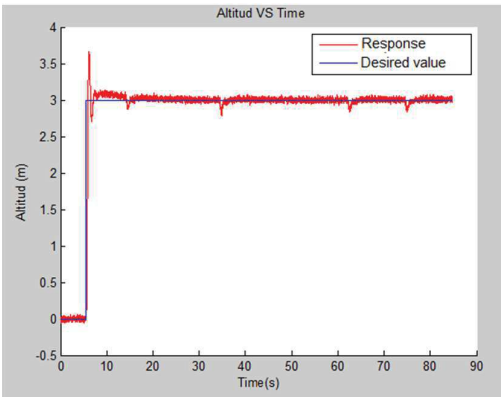

Fig. 12. Response signal about the Z axis.

The (Fig.12) shows the input signal in blue to reach the set height in 3 meters above the Z axis. Once introduced, the signal it´s considered constant. The red signal is the real signal (measure) and it has a minimum values in seconds: 14, 38, 65, and 78, which correspond to the points where the quadcopter rotates.

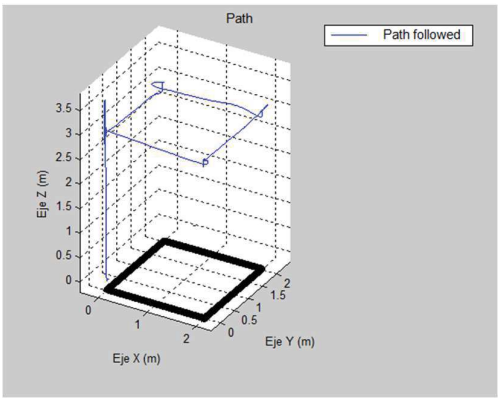

Fig. 13. Path followed.

B. Experimental Results

The same algorithm was implemented in the quadcopter being gotten the following results (Fig. 13).

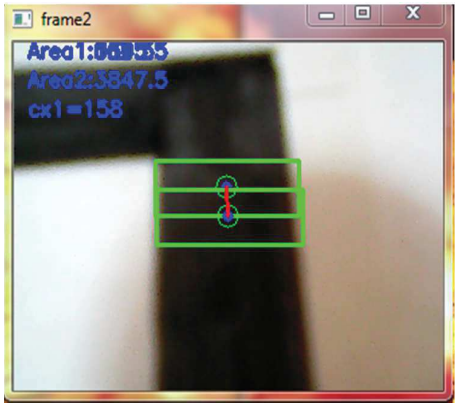

Fig. 14. Image Processing.

Calculated from the images, the necessary information (yaw angle) is extracted to determine the error and to get a new desired position (Fig 14). Finally the robot follows the path. (Fig 15).

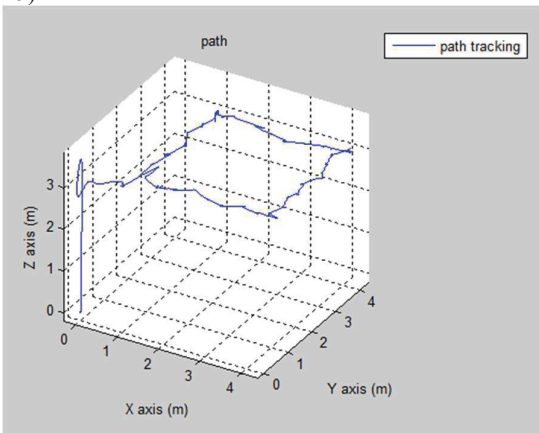

Fig. 15. Path tracking.

VII. Discussion

In order to control the yaw movement is finished and the graphs obtained we can conclude that a vision system is applicable in this kind of robot for familiar environments, and its implementation is possible for all the degrees of freedom of the quadricopter, which will be an improvement from this work in the future. One of the reasons which was based on Arduino Controller and free software such as OpenCV and Python is because this software is lightweight, cross-platform: tests were made with Windows, Linux and in a raspberry Pi system, our aim is that this project can migrate to a small platform so that can have some autonomy to explore unfamiliar environments.

VIII. Conclusions

The main objective has been achieved and can be used as a camera sensor to control direction and height estimation.

The implementation of cameras as sensors has many advantages and disadvantages, as advantages we can mention that it allows us to manipulate robots in familiar environments, not only unmanned vehicles but arms robots that can interact with the environment recognizing objects as well as the work area. As disadvantages we can find that it requires significant processing capacity by the computer, also it has a delay as a result of data transmission and images processing.

The visual servoing allows us to greatly expand the panorama control, because through him we can implement embedded systems that allow vehicle autonomy, for example whether to venture into unknown environments and make a quick decisions required by the robot, the vision techniques open up the possibility to implement them in recognition and reconstruction of 3D environments for cartography applications or search and rescue locating people, there is a wide range of possibilities from image processing control to both location and reconstruction areas. Finally it should be noted that it is not the only vision and technique, it is not necessarily the best, such as, in IBVS is does not required the camera parameters in order to implement this technique, there are other vision techniques applied in industry such as SURF, SIFT, and optical flow, which are currently applied to industrial environments and they don't require an object model reference.

References

[1] S. Hutchinson, G. D. Hager and P. I. Corke, 1996, "A Tutorial on Visual Servo Control". IEEE Trans. on Robotics and Automation , Vol.12, No. 5, October, pp. 651-670.

[2] J. Hill J. and W. T. Park, 1979, Real Time Control of a Robot with a Mobile Camera". In Proc 9th ISIR, Washington, D.C., Mar. pp. 233-246

[3] F. Chaumette, and Boudet, s., "2D vsual servoing", IEEE trans. Robot. Automat., 238-250, 1999.

[4] D. Lingfeng comparison of image-based and position-based robot visual servoing methods and improvements, ISBN:0-612-91991-9

[5] F. Fadri, Desing and Implemetation of a docking station for micro-helicopers, 2011, master tesis, Eidgenossische Technische Hochschule Zurich, Autonomous System Lab.

[6] D. Eberli, D Scaramuzza "Vision Based Position Control for MAVs Using One Single Circular Landmark" J Intell Robot Syst DOI 10.1007/s10846-010-9494-8.

[7] K. Máthé, L. Bu, sonju "Vision and Control for UAVs: A Survey of General Methods and of Inexpensive Platforms for infrastructure Inspection"revista sensors, 15, 14887-14916; doi: 10.3390/s150714887, 2015

[8] R. Guerrero Ochoa, F Coronel "sistema de navegación de un cuadricoptero guiado por el movimiento de las manos para operaciones de búsqueda y rescate "Unive"sidad Politécnica de Salesiana sede Cuenca, tesis, 2013.

[9] F. Reyes cortés "Robótica control de robots manipuladores" Alfaomega, 2013

[10] R. Ragel de la Torre, "Modelado, control y simulacion de un quadricoptero equiparo con un brazo manipulador robótico"proyecto fin de carrera, 2012.

[11] M. Vladimir Peña Giraldo "Modelamiento Dinámic y control LQR de un quadricóptero", revista Avancee de investigación en ingeniería numer 13, 2013.

[12] L. Sevilla Fernández, "Modelado y control de un quadricóptero" tesis ICAI-Universidad Pontificia Comillas, Junio 2014

[13] H. Voos Nonlinear control of a quadcopter micro-uav using feedback-linearization. International conference on mechatronics, Malaga, Spain, April 2009

[14] A. Noth Bouabdallah, S and R. Siegwart. PID vs Lg control techniques applied to an indoor micro quadrotor. Swiss federal institute f Technology, 2004

[15] R. Szeliski "Computer Vision Algorithms and Applications", texts in computer science Springer. 2010.

[16] S. Bennet & Lasenby. J. Chess – Quick and Robust Detection of chessboard features, ArXiv e-print journal. (2013)

Electronic system to monitor the truck route in the Mexico City

Applied with Android mobile devices to display the data in a Google map

Tatiana Leal del Rio[1-a], Gustavo Juarez Gracia[1-b]
Instituto Politécnico Nacional - IPN
Centro de Investigación en Ciencia Aplicada y Tecnología Avanzada - CICATA unidad Legaria
Mexico City, Mexico
mileydy.1125@gmail.com[1-a], agjuarezg@ipn.mx[1-b]

L. Noé Oliva Moreno[2]
Instituto Politécnico Nacional - IPN
Escuela Superior de Computo - ESCOM
Mexico City, Mexico.
loliva@ipn.mx[2]

Abstract—This paper describe the development of an electronic system with electronic components and microcontrollers automotive of the Texas Instruments company, that reduces the energy consumption of the system, is scalable and allow the integration of different electronic embedded modules, thank at the numerous serial communications ports that has, and that are used among other functions, to determine the route traveled for the trucks within Mexico City. Also, in future works, the precision of the GPS commercial modules can be improved with the employ of intelligent algorithms, as well as, a preventive maintenance with the data of the main sensors and actuators of a vehicle or truck can be made.
The system uses a short-range communication such as the Bluetooth, in addition of the development of an Android mobile application that allows to monitor continuously the behavior of the truck in the company. The Global Positioning System (GPS) information of the moving truck is stored every 30 seconds on a Secure Digital (SD) memory card placed in the electronic system. The acquisition of the GPS data is turning on and off according to the schedule of activities of the company in order to save power consumption from the battery of the truck. The hardware is composed of two microcontrollers manufactured by Texas Instruments Company, a Real Time Clock, a Bluetooth module, a GPS module and SD CARD memory, among other components. The validation of the functionality of the prototype was done by making several tours in Mexico City. The Android mobile application was developed in the Eclipse software, version 23 Android Software Development Kit (SDK) and its performance was evaluated by using the GPS positioning data stored in the SD memory card. The application mobile is developed in the Eclipse software with version 23 of the SDK of Android, with a new graphic interface of Android called "Navigation drawer" that consist in a dropdown horizontally menu that contain views of each one of the functions of the application, as the view of Google maps for viewing of the truck route.

Keywords—trucks; embeded system; GPS positioning data; bluetoot communication; Android application.

I. INTRODUCTION

Actually, there are many companies such as CoSoAVL "Automatic Vehicle Localization" or GPS Control, focused exclusively to determine the real-time satellite location of trucks and other vehicles by using GPS technologies and other activities related to the topic. To accomplish this task, the companies install GPS devices in trucks and/or vehicles to monitor them by sending the geographical location information to an internet server. Subsequently, the information is provided to the user in a web application, or sending alarms to a mobile device. With these systems, not only the trucks and/or vehicles position are given, but also it provides additional information such as speed, temperature, opening the fuel tank, engine status, door opening, and security alarm equipment, among others. The growth and development of these electronic systems are based primarily on the design and selection of electronic embedded modules to manage and communicate different automotive communication protocols such as: Controller Area Network (CAN) [1] and On Board Diagnostics (OBD II) [2] to obtain and monitor data of the automotive sensors and actuators from the Engine Control Unit (ECU) [3][4], as well as the adaptation of GPS systems to track and trace the truck route [5][6][7]. This paper is about the development of a scalable electronic system of low energy consumption, designed with electronic components and microcontrollers automotive of the Texas Instruments company, to monitor the route traveled for trucks in the Mexico City and also, to compare the technology used in this work, with other related works and services of positioning geographical that certain companies offering, as well as the future works that can be made with this prototype. Electronic system the geographical positioning data are obtained of a commercial GPS module every 30 seconds by a TM4C123GH6PM microcontroller of Texas Instruments Company that employs an algorithm to determine and store valid GPS positions on a SD memory card. The data are sent to a mobile device with Android through a Bluetooth communication to display the truck route in a Google map.

II. SELECTION OF THE TECHNOLOGY USED IN THE SYSTEM

This section describe some works developed for researchers and companies about of GPS systems that allow to monitor the route of the trucks and vehicles, as well as the technology used in this research to design an electronic system scalable, of low power consumption and low cost in its implementation

that can improve the current systems. A geo referenced system for the locations and register of the route traveled by trucks of a furniture company in Ecuador was made. That system consisted in the development of a web application using ArcGIS for Microsoft SilverLightWPF that allow the user to monitor the trucks, to optimize routes and to generate statistics of the data of geographical positioning stored in the application [8]. The system is interesting, the information is in the web and the algorithm of location is new, but in the market exist companies that offering the same services and with more information. As it mentioned in the introduction, CoSoAVL (www.cosoavl.com) "Automatic Vehicle Localization" is a company focused exclusively to determine the real-time satellite location of trucks and other vehicles by using GPS technologies in addition to the information of speed, temperature, opening the fuel tank, engine status, door opening, and security alarm equipment, among others. This service is good, but the user has to pay more money by the additional information. Therefore, the electronic system proposed in this paper it is focused in to develop a prototype that can bring together all the characteristics of the current GPS systems [5][6][7], to improve the precision of geographical location and to obtain information of the vehicle to develop a preventive maintenance by using own algorithms, whose operation of the design proposed, it can be optimized in future works with the development of this system.

The microcontrollers that will handle all the operations and the performance of the system were selected according to the following aspects:

- High performance of the processor for an optimal execution of all operations of the system.
- Electronic system scalable in hardware with memory capacity for future works that allow improving his operation.
- Low power consumption due to that supply power of the system is provided by the battery of the truck.
- Low cost of implementation for that the system is competitive in the market.
- Microcontroller that implement the CAN communication protocol for automotive applications.

Actually, companies as Microchip, Atmel, Texas Instruments, National Instruments, Intel, among others are some examples of companies dedicated to manufacture microprocessors and microcontrollers in the market with specific characteristics, of low cost with high performance in the processor, for the development of different works. Due to that fact, this project is focused in the development of an electronic system for the automotive area, where it opted to select the microcontrollers of the Texas Instruments (TI) companies, since that TI is a strong company in the develop of automotive technology, and offer to the user an online platform complete (*www.ti.com/lsds/ti/analog/webench/automotive.page*) for the simulations and selection of automotive electronics components in the design of the power supplies, as well as the implementation of the CAN communication protocol in their microcontrollers for the communication of data with the ECU of the vehicles, high performance in the processor, hibernation modules for the low power consumption, among others characteristics, for to reduce the implementation cost of these systems. For examples, companies as Arduino and Microchip that are very commercials in the market, but they don't support the CAN communication in their microcontrollers.

TABLE I. GENERAL CHARACTERISTICS OF THE TM4C123GH6PM MICROCONTROLLER

General Characteristics	Integrated Circuit
	TM4C123GH6PM
Company	Texas Instruments
Supply voltage	3.30 V
Current	300.00 mA
Maximun Power	990.00 mW
Instruction set architecture	ARM Cortex™ –M4F Harvard
Number of instructions	Thumb-2
Data bus width	32 bits
Micro Direct Memory Access (µDMA)	ARM PrimeCell 32-channel configurable µDMA controller
Flash size	256 KB single-cycle
EEPROM size	2 KB
SRAM size	32 KB single-cycle
Internal ROM	Internal ROM loaded
Maximum CPU frequency (MHz)	80 MHz; 100 DMIPS
Numbers of GPIOs	43
UARTs	8
SSI	4 modules
I^2C	4 modules
CAN	2 CAN 2.0 A/B controllers
Universal Serial Bus (USB)	1 (2.00 OTG/Host/Device)
Hibernation module	1 general

TM4C123GH6PM of the Texas Instruments company is the main microcontroller (table I) and it is responsible to manage the different electronic modules (Fig. 1) that implements the system. TM4C123GH6PM is characterized for to implement a high performance ARM Cortex –M4F core based in Harvard architecture. The Cortex –M4F processor implements a Thumb instruction set based on Thumb-2 technology, ensuring high code density and reduced program memory requirements. The instruction set of the processor provides the performance of 32 bits architecture, with high code density of 8 bits and 16 bits microcontrollers. Also, the technology of the processor provides high speed, low latency memory accesses and it implements atomic bit manipulation (it is an independent configuration of bits in a register without setting the entire register) that enables faster peripheral control and it has an optional Memory Protection Unit (MPU) that permits control of individual regions in memory, a single cycle multiply instruction and hardware divide, a maximum frequency of the 80 Mhz operation with 100 Dhrystone Million Instructions Per Second (DMIPS), fast code execution permits slower processor clock or increases sleep mode time, ultra-low power consumption with integrated sleep modes, among other functions [9]. The TM4C123GH6PM microcontroller has a supply voltage of 3.30 V and it includes a Direct Memory Access controller (µDMA). The µDMA provides a way to offload data transfer task from the Cortex M4F processor, allowing for more efficient use of the processor ant the available bus bandwidth, and it can perform data transfers between memory and peripherals and it supports the CAN communication protocol [16].

Now, as TM4C123GH6PM is responsible to manage the different electronic modules of the system, it isn't possible to implement directly the hibernation module (that consist a sleep the processor) in this microcontroller, due to that the TM4C123GH6PM microcontroller is constantly receiving data of the GPS module, and it is storing data in the SD Card memory while the truck is operating during working hours. Therefore, the system can optimize the power consumption in the TM4C123GH6PM microcontroller, if an external signal to the microcontroller, activates or deactivates its hibernation module before and after of the working hours.

The second microcontroller selected to the electronic system, it is the MSP430G2553 microcontroller of the Texas Instruments company. In the table II is seen a comparative of three commercial microcontrollers of different companies [10][11][18][19] in the market. The MSP430G2553 microcontroller is selected according to the following main aspects [18][19]:

- The supply voltage of 3.30 V is equal to the supply voltage of the main microcontroller to reduce cost of implementation.
- It has a RISC processor of the 16 bits with DMA controller that increases performance of the peripherals. The DMA allow to reduce the power consumption by allowing the CPU to remain in a low power mode without having to awaken to move data to or from peripheral.
- Few GPIOs.
- Flash memory is bit-byte, and word addressable and programmable.
- Five software selectable low power modes of operation with an interrupt event that it can wake up the device from any of the low power modes, service the request, and restore back to the lower power mode on return from the interrupt program.

TABLE II. GENERAL CHARACTERISTICS OF DIFERENT COMMERCIAL INTEGRATED CIRCUITS

General Characteristics	**Integrated Circuits of Companies Different**		
	PIC16F87	***MSP430G2553***	***ATmega48a***
Company	Microchip	Texas Instruments	Atmel
Supply voltage	5.00 V	3.30 V	5.00 V
Instruction set architecture	RISC Harvard	RISC with **DMA** Von-Neumann	RISC Harvard
Number of instructions	35	27	131 (*general*)
Data bus width	8 bits	16 bits	8 bits
Flash size	1 KB x 14 bits	16 KB	4 KB
EEPROM size	64 B	------	256 B
RAM size	68 B	512 B	512 B
Maximum CPU frequency (MHz)	20MHz 5 MIPS	16 MHz 16 MIPS	20 MHz 20 MIPS
Numbers of GPIOs	13	16	23
Serial interface (1 per type)	UART, SPI, I^2C	UART, SPI, I^2C	UART, SPI, I^2C
Sleep mode (1 MHz)	YES (0.10 µA-2.00 V)	YES (0.50 µA-2.20 V) with **5 Hibernation module**	YES (0.10 µA-1.80 V)

The PIC16F87 microcontroller is discarded for the supply voltage, the low memory capacity and low performance of the processor compared with the other microcontrollers. The Atmega48a microcontroller is discarded for the supply voltage, numbers of GPIO and low flash memory compared with the MSP430G2553 microcontroller.

III. CONFIGURATION OF THE SYSTEM

Mexico City is the capital of the United Mexican States, which is a country located in North America between the Pacific Ocean and Gulf of Mexico to 19 degrees latitude, 99 degrees longitude and its territory is mathematically represented by the GRS80 Datum [12].

To the development of the electronic system, a car travel was performed in the Mexico City to obtain an experimental database of 73 Recommended Minimum Specific (RMC) sentences GPS [13] through commercial GPS module UBlox Neo 6M [14][15] that is configured to a frequency of 1 Hz in the reception of National Marine Electronics Association (NMEA) sentences with a period of random data acquisition. The electronic system is composed for a TM4C123GH6PM and MSP430G2553 microcontrollers of the Texas Instruments Company, where the TM4C123GH6PM microcontroller [16] is responsible for managing data of commercial modules Bluetooth HC-05, UBlox Neo 6m GPS and Openlog data logger SD card, and the MSP430G2553 microcontroller is responsible for managing data of the DS1307 RTC module. The Bluetooth HC-05 module [17] is configured to operate in Slave mode at the rate 9600 baud with point to point connections, and authentication for security code and Personal Identification Number (PIN) between dispositives. The openlog data logger (https://github.com/sparkfun/OpenLog/wiki/datasheet) is configured at the rate of 9600 baud for sending and receiving data in commands mode with the 26 character in American Stander Code for Information Interchange (ASCII) as output code of the commands mode for to create, delete and edit files in the memory SD card. The MSP430G2553 microcontroller [14][15] is configured to 16 MHz frequency in lower power consumption mode with Inter Interface circuit (I2C) communication protocol for data communication with the RTC DS1307 module [20] at the start or finish of the route, and with the TM4C123GH6PM microcontroller through the Universal Asynchronous Receiver Transmitter (UART) protocol for to communicate data and activate or deactivate the GPS module. Ultimately, other car travel was performed in the Mexico City to validate the electronic system and the mobile application, with a total of the 148 recorded sentences RMC GPS in the memory SD card. The Fig.1 shows the block diagram of the electronic system.

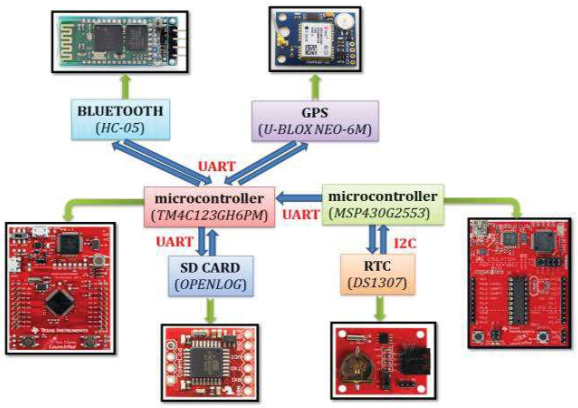

Fig. 1. Block diagram of the electronic system developed.

IV. DESCRIPTION OF THE SYSTEM

We record the route of a truck in the Mexico City taking into account the following aspects:

A. Geographycal description of the Mexico City

Because the earth planet has an irregular shape of earth's surface, there is no single mathematical model that can describe it fully. Therefore, the earth's surface can be represented mathematically by a reference surface called geoid. The geoid is a geometric figure representing the average sea level at the Earth's surface, if the water flows under the continents, but as the geoid has a slightly irregular shape because to the different materials that forming the earth, It is necessary to represent the geoid as a more abstract geometric figure and without irregularities, through reference ellipsoid [21]. The reference ellipsoid is a geometric figure that mathematically represents any geographical area at the earth. The Datum is represented by the geoid and ellipsoid, and is defined as a tangent point to the geoid and ellipsoid where both agree. The United Mexican States are represented mathematically by the GRS80 Datum [12] (table III). The data of the GRS80 Datum, the sampling period and the conversion of the geographical coordinates to Universal Transverse Mercator (UTM), are necessary to calculate the distance between of two points, and determine if the truck is moved from a valid geographical position to another, and store the geographical position in a SD card memory.

TABLE III. REFERENCE DATUM OF THE UNITED MEXICAN STATES

Ellipsoid Parameter		
Parameter	***Nomenclature***	***GRS80***
Semi-major axis	*a*	6387137 m
Semi-minor axis	*b*	6356752.3141 m
Eccentricity	*e*	0.00669438002290
Second eccentricity	*e'*	0.00673949677548
Flattening of the ellipsoid	*f*	0.00335281068118
Polar radius of curvature	*c*	6399593.6259 m

B. Sampling period

The sampling period was determined according to the speed limits and sizes of residential blocks that are allowed in the Mexico City. According to the regulation of metropolitan transit of the Mexico City [23] and to the standard size of residential blocks (100.00 - 150.00 meters), the distance (in meters) that can travel a truck per minute can be seen in the table IV. In this table, it can see that the maximum distance that a truck can go per minute in Mexico City is 1166.67 m at a speed of 70.00 km/h, and that the minimum distance is 333.33 m at a speed 20.00 km/h. Now, if we consider that the maximum distance along a residential block is around 100.00 and 150.00 meters, to consider a time period of 1 minute (60 seconds) between a sample and sample, it could be affecting the accuracy of the route; that is, that when is comparing the distance of 333.33 meters to 100.00 or 150.00 meters from the size of a residential block in special zones were presented that for this time and this speed, the distance is more than double that a residential block, without regard to events where the truck has to make turns between streets. Therefore, to minimize these situations during travel of a truck, it has been proposed that the time period for sampling of the RMC sentences of the GPS module are of half minute (30 seconds).

TABLE IV. SPEED LIMITS IN THE MEXICO CITY.

Speed Km/h	***70 km/h***	***60 km/h***	***40 km/h***	***30 km/h***	***20 Km/h***
Speed (m/min)	1166.67 m/min	1000.00 m/min	666.67 m/min	500.00 m/min	333.33 m/min
Distance (m) per minute (min)	1166.67 m	1000.00 m	666.67 m	500.00 m	333.33 m
Distance (m) per half minute (min)	583.33 m	500.00 m	333.33 m	250.00 m	166.67 m

C. Geographycal coordinate conversion to Universal Transverse Mercator (UTM) and distance calculation

The UTM system is a planar coordinate system (in meters) that is based on the Mercator Transverse projection. This system is characterized by to divide in 6 degrees of longitude to the central meridian from the 84 degrees north to the -80 degrees south of latitude, in 60 zones each 6 degrees of longitude in width [21]. For the map projection and conversion of geographical coordinates to UTM, three factors are important:

- A scale factor of 0.9996 to reduce the lateral distortion along central meridian of each zone UTM.
- The point of origin of each UTM zone is the intersection of the equator and the zone's central meridian, but to avoid dealing with negative numbers, the central meridian of each zone is set at 500,000.00 meters East in the Northern and Southern hemispheres, and the equator is set at 0.00 meters for Northern hemisphere and 10'000,000.00 meters for Southern hemisphere to determine positions.

Now, the geographical coordinates can be converted to UTM by using the mathematical model of A. Coticchia and L. Surace

[24] (table V) that takes into account the three important factors of the UTM system, time zone, the geographic Datum of the coordinates to convert, and other geodetic parameters, where:

- ***a***: Semi-major axis of the ellipsoid under the specified Datum.
- ***b***: Semi-minor axis of the ellipsoid under the specified Datum.
- ***c***: Polar radius of curvature of the specified Datum.
- ***e***: Eccentricity of the specified Datum.
- ***e'***: Second eccentricity of the specified Datum
- ***Huso***: Time zone point to convert.
- ***λ***: Length in radians of the point to convert.
- ***φ***: Latitude in radians of the point to convert.
- λ_0: Length in degrees of the point to convert.
- φ_0: Latitude in degrees of the point to convert.
- ***Δλ***: Distance between the point to be convert and the central meridian of the same.
- ***A, ξ, η, v, ζ, A_1, A_2, J_2, J_4, J_6, α, β, γ, Bφ***: Parameters of A. Coticchia and L. Surace.
- ***X***: X coordinate of the point to convert.
- ***Y***: Y coordinate of the point to convert.

TABLE V. MATHEMATICAL MODEL OF A. COTICCHIA Y L. SURACE TO CONVERT GEOGRAPHIC COORDINATES TO UTM.

Equation	*Number*
$c = \frac{a^2}{b}$	1
$e = \frac{\sqrt{a^2 + b^2}}{a}$	2
$e' = \frac{\sqrt{a^2 + b^2}}{b}$	3
$decimal\ degree = degree + \frac{minutes}{60} + \frac{\frac{seconds}{60}}{60}$	4
$Radians = \frac{decimal\ degree * \pi}{180}$	5
$Huso = integer[\frac{decimal\ degree\ length}{6} + 31]$	6
$\lambda_0 = Huso * 6 - 183$	7
$\Delta\lambda = \lambda - \lambda_0$	8
$A = cos\,\varphi * sen\,\Delta\lambda$	9
$\xi = \frac{1}{2}\ln[\frac{1+A}{1-A}]$	10
$\eta = arc\tan\left(\frac{\tan\varphi}{\cos\Delta\lambda}\right) - \varphi$	11
$v = \frac{c}{(1 + e'^2 * cos^2\varphi)^{1/2}}$	12
$\zeta = \frac{e'^2}{2} * \xi^2 * cos^2\varphi$	13
$A_1 = sen(2 * \varphi)$	14
$A_2 = A_1 * cos^2\varphi$	15
$J_2 = \varphi + \frac{A_1}{2}$	16
$J_4 = \frac{3 * J_2 + A_2}{4}$	17
$J_6 = \frac{5 * J_4 + A_2 * cos^2\varphi}{3}$	18
$\alpha = \frac{3}{4} * e'^2$	19
$\beta = \frac{5}{3} * \alpha^2$	20
$\gamma = \frac{35}{27} * \alpha^2$	21
$B_\varphi = 0.9996 * c * (\varphi - \alpha * J_2 + \beta * J_4 - \gamma * J_6)$	22
$X = \xi * v * \left(1 + \frac{\zeta}{3}\right) + 500{,}000$	23
$Y = \eta * v * (1 + \zeta) + B_\varphi$	24

The equations (23 and 24) allow convert the geographical coordinates of the Mexico City to UTM, and are valid only for the Northern hemisphere, since it assume an East false of 500,000.00 meters and a North false of 0.00 meters for these calculations. To calculate the distance between two points UTM, the Pythagorean Theorem is applied through (25), wherein X_1Y_1 and X_2Y_2 are the Cartesian coordinates of the points in question, and d is the distance to be calculated. To apply this procedure it assumes that the earth is flat, and that the distances are less than 20 km (http://www.movable-type.co.uk/scripts/gis-faq-5.1.html). For this case, the distances traveled by the truck are less the 20 km, due to the maximum speed limit of 70 km/h in the Mexico City and the sampling period set in the electronic system.

$$d = \sqrt{(X_2 - X_1)^2 + (Y_2 - Y_1)^2} \qquad (25)$$

The Pythagorean Theorem will result in an error of:

- Less than 30 meters for latitudes less than 70 degrees.
- Less than 20 meters for latitudes less than 50 degrees.
- Less than 9 meters for latitudes less than 30 degrees.

D. Data Storage

To determine and store valid GPS sentences on the SD card memory, it is taken into account the Circular Error Probability (CEP) of the GPS module to know if the truck has moved since its current geographical position to a new valid geographical position. The Fig. 2 shows the satellite shadow of horizontal position accuracy of 2.50 meters CEP of the UBlox Neo 6m GPS module. The 2.50 meters CEP means that there is a 50% of probability that a geographic position provided by the GPS module is within of a circle of radius 2.50 meters, and a 50% of probability of that geographic position is outside this circle. Now, considering that the geographic position provided by the GPS module is within a circle of 2.50 meters of radius, the next geographic position will be valid, if the truck is moved more than 5.00 meters from its previous position, to avoid that this new circle is intercepted by the circle of the previous position.

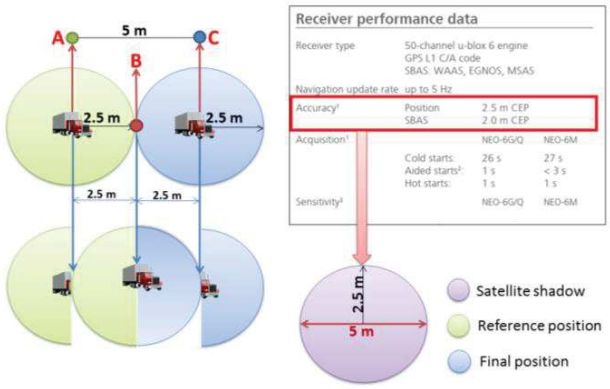

Fig. 2. Horizontal accuracy of the UBlox Neo 6m GPS module.

Of all the NMEA sentences that are provided by the GPS module [13], the RMC sentence is the interest (Fig. 3), but only a part of these sentences have the necessary information to be stored on the SD memory card and the route register of the truck.

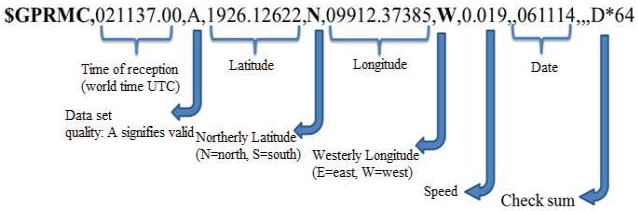

Fig. 3. Description of the RMC data sentence.

Of the RMC sentence only the time of reception, the latitude, the longitude and date will be the data to store on the SD memory card. Therefore, the structure and size of these sentences will be:

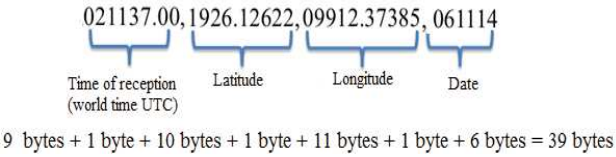

Fig. 4. Size of the sentence that be stored on the SD card memory.

Because Mexico City isn't moved from its geographical position, the latitude will always be in the North at 19 degrees with a size of 10 bytes, and the longitude in the West at 99 degrees with a size of 11 bytes, the time will always have a fixed size of 9 bytes (HHMMSS.SS) and the date a size of 6 bytes (DDMMYY). The time of reception, the latitude, the longitude and the date are separated by a comma, for a total of 3 commas and 3 bytes. Summing all these bytes, the size of the sentence to store on the SD card memory will be of 39 bytes (Fig. 4). Estimating the size of the data that will be stored on the SD memory card for a work period 8 hours continuously per day, by time periods of one day, one week, one month and one year are shown in the table VI.

TABLE VI. ESTIMATED DATA STORAGE TO SD MEMORY CARD

Data storage to SD card (Schedule 8:00 to 16:00)			
Sampling (each 30 seconds)	***Samples per minute***	***Number samples***	***String size in Kbytes***
Samples per day	480.00	960.00	37,440.00
Samples per week (7 days)	3,360.00	6,720.00	262,080.00
Samples per month (30 days)	14,400.00	28,800.00	1'123,200.00
Samples per year (360 days)	172,800.00	345,600.00	13'478,400.00
Storage capacity of SD memory card	4Gbytes with capacity of storing data up to 296.77 years		

Samples per day are calculated taking into account the work period of the truck divided by the sampling period of the electronic system, where 960.00 samples are the maximum number of samples per day, with a memory size of 37,440.00 Kbytes.

8.00 hours ***x*** *360.00 seconds = 28800.00 seconds*
28800.00 seconds / 30.00 seconds = 960.00 samples
960.00 samples ***x*** *39.00 bytes = 37,440.00 Kbytes*

Fig. 5. Maximum size of samples per day.

V. RESULTS

To validate the operation optimal of the electronic system, it was necessary to make several experimental travels in the Mexico City, with different times of acquisition of the positioning geographical of a vehicle to determine the route traveled by it. The general form, two travels were made in the Mexico City. The first travel is made only with a GPS commercial module and a laptop where the acquisition data of the positioning geographical were made of random form. The second travel is made with the complete electronic system. The data of the positioning geographical of each travel were compared with the algorithm of the A. Coticchia and L. Surace implemented in the electronic system, and were validated through graphics made in OriginPro and graphics made in a Google map of the mobile application in Android to validate that the algorithm implemented in the electronic system is correct.

The first travel was made in the Mexico City in November 2014. The travel consisted in the obtaining of NMEA sentences GPRMC where the GPS module was configured to a frequency of 1 Hz, with data capture randomly. Electronic devices used in this travel were: a laptop Lenovo Intel Core i5 of 64-bit and Windows 8, a conventional breadboard, a U-BLOX NEO 6M GPS module, and a signals converter UART to USB. The communication interface between the GPS module and the laptop was made for UART, and the data obtained during the experimental travel were displayed on the Hercules serial interface and stored in a text file called recorrido.txt. The travel

started the 6 of November of the 2014 in the Mexico City at the Calzada Legaria 252 (Miguel Hidalgo delegation) at the 17 hours with 55 minutes, and finished at the 21 hours with 16 minutes of the same day, at the Research Center in Applied Science and Advanced Technology (CICATA) Legaria unit with a total of 73 GPRMC sentences used to developed the mobile application on Android [25].

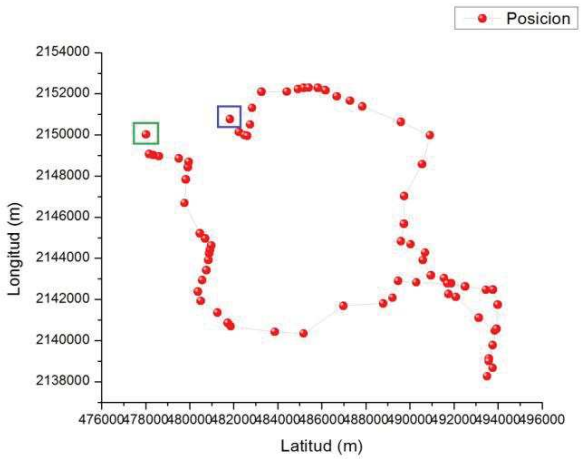

Fig. 8. First path (mathematical model of A. Coticchia and L. Surace) in truck made in Mexico City.

Fig. 9. First path (geographic coordinates in the Android mobile application) in truck made in Mexico City.

Fig.8 shows the graphic in OriginPro of the travel accomplished (in meters) by a truck in the Mexico City, by using the mathematical model of the A. Coticchia and L. Surace. The blue frame indicates the start position, and the green frame indicates the finish position of the route. The Fig. 9 shows the travel accomplished by a truck in a device mobile with Android in the Mexico City using the Google maps API.

The second travel accomplished in the Mexico City was made in July 2015. The travel started at the 15 hours with 12 minutes and finished at the 15 hours with 49 minutes at the Research Center in Applied Science and Advanced Technology (CICATA) Legaria unit the first of July of the 2015, with a total of 148 GPRMC sentences. Electronic equip used to register the travel were: a U-BLOX NEO 6M GPS module, a Openlog data logger SD card, a HC-05 Bluetooth module and TM4C123GH6PM Launchpad. The data were obtained in time periods of 30 seconds and storage on the SD memory card if the distance traveled between the current position and previous position is equal or longer than 5 meters. The Fig. 10, the blue frame indicates the start and finish position of the travel.

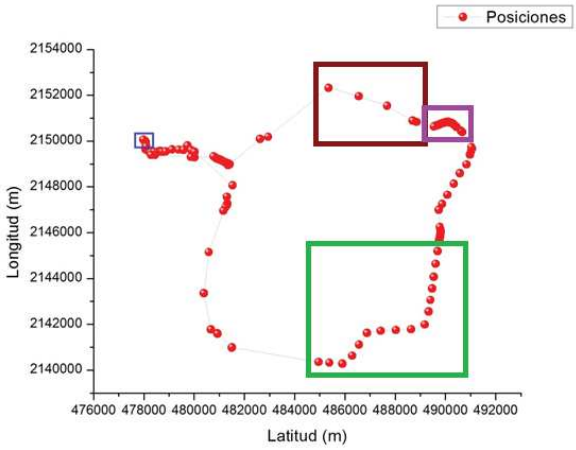

Fig. 10. Second path (mathematical model of A. Coticchia and L. Surace) in truck made in Mexico City.

Fig. 11. Second path (geographic coordinates in the Android mobile application) in truck made in Mexico City.

Comparing Fig. 10 (Fig. 8) with Fig. 11 (Fig. 9) can be observed a similitude between both graphics that indicate, that the mathematical model selected to convert the geographical coordinates to UTM has been the correct. In the route second is appreciated a ordinate sequence of geographical positions (red dots) with equals spacing (time period) in the route (green frame, Fig. 10), or an ordinated agglomeration and equally spaced between geographical positions (purple frame, Fig. 10) of that zone, the that indicating a traffic density that can be corroborated with the stored data on the SD memory card. The

equal spaces between geographical positions are due the sampling period set up in the electronic system, and the unequal spacing (brown frame, Fig. 8) are due to false contacts of the electronic system mounted in breadboard by the damage on the road during the route. Moreover, in the route first (Fig. 8) can be seen an unequal sequence on the register of geographical positions (red dots) due to the random sampling period. Finally, with data of geographical positions registered on the SD memory card of the electronic system, it can be calculated data as velocity and distance traveled in each part of the route to estimate the traffic density, or to evaluate the behavior of the driver to drive the truck in Mexico City.

VI. CONCLUSIONS

The geographical positions obtained by the GPS UBlox-NEO 6M module does not provide the current position of the truck with exactly because this module has an CEP accuracy of 50% that the current position of the truck is in a radius of 2.5 meters around. Therefore, the other 50% of probability to obtain a valid geographical position is found anywhere outside this radius, causing errors in the calculation and estimation of displacement and speed of the truck to move from one position to another, where the current position will be considered valid only if the distance in a time period of 30 seconds is more than 5 meters.

The electronic system developed did not take into account the compensation for the loss of information and the exact geographical position of the truck coming from the GPS UBlox-NEO 6M module, but it can to implement the CAN communication protocol and the Universal Asynchronous Receiver Transmitter (UART) protocol of the OBD II, to communicate data between the electronics system and the ECU and to monitor the sensors and actuators of the vehicles and/or trucks that implement this electronic system.

The electronic system developed can be applied to other world countries, changing the current Datum by geoid datum corresponding to the country of interest in the algorithm of the main microcontroller of the system.

Power consumption of the electronic system is optimized using microcontrollers of the Texas Instruments Company that employing different configuration modes for lower power consumption to 5 μA, ideal when the truck has finished its travel and it don't need to receive more data of the GPS module.

The displacement of the truck can be determined more precisely, if it is taken into account the vehicle speed through OBD2 connector as additional parameter to calculate the distance between two geographical points.

Electronic system design can be scalable because it provides all the necessary hardware and software architecture for the addition of other communication modules which can improve system performance in future works, as: the addition of a GPRS module and the development of a triangulation algorithm can help to improve the precision of the positioning geographical of a truck or a vehicle, to cover zones where this isn't signal of the GPS commercial module, to send text messages or to make call to the final user to report the current system status. The addition of a Wi-Fi module that makes a backup of information stored in the system in a web server to be displayed in a mobile device from anywhere. The data communication (of the main sensors and actuators) between the electronic system either with the truck by using the UART serial communication protocol, or a vehicle by using of the CAN communication protocol and the development an intelligent algorithm to make a preventive maintenance, among other functions that electronic system could need, as well as the use of the intelligent algorithms for it.

ACKNOWLEDGMENT

The authors thank to the National Polytechnic Institute - **IPN**, Research Center in Applied Science and Technology– **CICATA** Legaria, Computing School High– **ESCOM** and Conacyt for their support during the development of this work.

REFERENCES

[1] R. Bosch, “CAN Specification”, version 2.0, 1991.

[2] N.K.H. Davies, “Diagnostic at the roadside”, IEEE Colloq. Vehicle Diagnostics, London, Europe, pp. 1-7, February 1994.

[3] L. Baghli, A. Moussaoui, K. Benmansour, S. Delprat and M. Djemai, “Optimal hybrid vehicle, embeded data adquisition and tracking”, IEEE 2nd Int. Symp. Environment Friendly Energies and Applications (EFEA), Newcastle upon Tyne, pp. 68-73, June 2012.

[4] L. Baghli, K. Benmansour and M. Djemai, “Development of a data acquisition and tracking system for vehicles”, IEEE 3rd Int. Symp. Enviroment Friendly Energies and Applications (EFEA), St. Ouen, pp. 1-6, November 2014.

[5] B. Blanco and J. Romero, “Geolocation, monitoring and tracking vehicles and mobile users”, Interdisciplinary Professional Unit in Engineering and Advanced Technologies (UPIITA), National Polytechnic Institute (IPN), Mexico, 2010 [B. Blanco and J. Romero, “Geolocalización, monitoreo y rastreo de vehículos y usuarios móviles”, Unidad Profesional Interdisciplinaria en Ingeniería y Tecnologías Avanzadas (UPIITA), Instituto Politécnico Nacional (IPN), Mexico, 2010].

[6] E. Segura, G. Morán and C. Valdivieso, “Mass data storage of GPS positioning in an USB memory for later use with compatible path maps with Google Earh”, Research Center for Scientific and Technological (CICYT), Higher Polytechnic School of the Coast (ESPOL), Ecuador, 2011. [E. Segura, G. Morán and C. Valdivieso, “Almacenamiento masivo de datos de posicionamiento GPS en un pen driver para su posterior utilización con mapas de trayectoria compatibles con Google Earh”, Escuela Politécnica Superior del Litoral (ESPOL), Centro de Investigación Científica y Tecnológica (CICYT), editorial FIEC, Ecuador, 2011].

[7] R. Gonzáles, E. Benítez, N. Blanco and M. Villapol, “Using smart phones as a communication solution for route accounting applications in vehicle fleets”, Simon Bolivar University, Department of Computer and Information Technology, Venezuela, 2012. [R. Gonzáles, E. Benítez, N. Blanco and M. Villapol, “Uso de teléfonos inteligentes como una solución de comunicación en aplicaciones de seguimiento de rutas en flotas de vehhículos”, Universidad Simón Bolivar, Departamento de Computación y Tecnología de la Información, 5To Congreso iberoamericano de estudiantes de ingeniería eléctrica (V CIBELEC) Caracas, Venezuela, 2012].

[8] L. Pacheco, “GIS application for a control system of geo reference of orders and furniture delivery”, San Francisco de Quito University, Postgraduate College, Ecuador, 2014. [L. Pacheco, “Aplicación de GIS para un sistema de control geo referenciado de pedidos y entrega de muebles”, Universidad San Francisco de Quito, Colegio de postgrados, Ecuador, 2014].

[9] ARM, "Cortex-M4 Devices, generic user guide", ARM DUI 0553A, N° ID121610, 2010, pp. 1-4. Available online: http://infocenter.arm.com/help/topic/com.arm.doc.dui0553a/DUI0553A_cortex_m4_dgug.pdf.

[10] ATMEL, "ATmega48A/PA/88A/PA/168A/PA/328/P, ATMEL 8-bit microcontroller with 4/8/16/32 Kbytes in-system programable flash, datasheet", Atmel-8271J-AVR, 2015, pp. 1-2. Available online: http://www.atmel.com/images/atmel-8271-8-bit-avr-microcontroller-atmega48a-48pa-88a-88pa-168a-168pa-328-328p_datasheet_complete.pdf.

[11] MICROCHIP, "PIC16F87/88 datasheet, 10/20/28-Pin enchanced flash MCUs with nano watt technology", DS30487C, 2005. Available online: http://akizukidenshi.com/download/PIC16F87.pdf.

[12] Official gazzete, "AGREEMENT where the technical standard for the national geodetic system is approved", National Institute of Statistics and Geography (INEGI), First section, R. -318637, 2010. [Diario oficial, "ACUERDO por el que se aprueba la norma técnica para el sistema geodésico nacional", Instituto Nacional de Estadística y Geografía (INEGI), primera sección, R. -318637, 2010]. Available online: http://www.inegi.org.mx/geo/contenidos/normastecnicas/doc/norma_tecnica_sobre_estandares_de_exactitud_posicional.pdf.

[13] K. Betke, "The NMEA 0183 Protocol", Rev., pp. 1-14, August 2001. Available online: http://www.tronico.fi/OH6NT/docs/NMEA0183.pdf.

[14] U-blox, "GPS: Essentials of SatelliteNavigationCompendium", N° GPS-X-02007-D, p.p 51-138, 2009. Available online: https://www.u-blox.com/en/technology/GPS-X-02007.pdf.

[15] UBLOX (2011), "NEO-6 series, Versatile u-blox 6 GPS modules", Ref. GPS.G6-HW-09003-D, 2011. Available online: https://www.u-blox.com/images/downloads/Product_Docs/NEO-6_ProductSummary_%28GPS.G6-HW-09003%29.pdf

[16] Texas Instruments, "Tiva TM4C123GH6PM Data Sheet", Austin Texas 78746, DS-TM4C123GH6PM-15842.2741, N° SPMS376E, pp. 893-897, 997-1002, 2014. Available online: http://www.ti.com/lit/ds/spms376e/spms376e.pdf.

[17] ITead Studio, "HC-05 Bluetooth to serial port module", pp. 1-13, June, 2010. Available online: http://documents.mx/download/link/bluetooth-hc-05-558462162b02a.

[18] Texas Instruments, "MSP430x2xx Family User's Guide", Austin Texas 78746, N° SLAU144J, Rev. July 2013. Available online: http://www.ti.com/lit/ug/slau144j/slau144j.pdf.

[19] Texas Instruments, "MIXED SIGNAL MICROCONTROLLER: MSP430G2x53, MSP430G2x13 Datasheet", Austin Texas 78746, N° SLAS735J, Rev. May de 2013. Available online: http://www.ti.com/lit/ds/symlink/msp430g2553.pdf.

[20] Maxim integrated, "DS1307 64 x8, Serial I2C Real Time Clock Datasheet", Rev. 100208, pp. 1-14, 2015. Available online: http://datasheets.maximintegrated.com/en/ds/DS1307.pdf.

[21] J. Falla, "Map projections and Datum, What are they and what are they for?". Laboratory of Remote Sensing and Geographic Information Systems PRMVS-EDECA, National University, Colombia, pp. 9-14, 2013. [J. Falla, "PROYECCIONES CARTOGRÁFICAS Y DATUM ¿Qué son y para qué sirven?", Laboratorio de Teledetección y Sistemas de Información Geográfica PRMVS-EDECA, Universidad Nacional, Colombia, pp. 9-14, 2003]. Available online: http://ucv.altavoz.net/prontus_unidacad/site/artic/20110725/asocfile/20110725122826/proyecciones_cartograficas_y_datum__que_son_y_para_que_sirven___jorge_fallas.pdf.

[22] I. A. Fernández, "Geographical Locations. The geographic coordinates and the UTM (Universal Transverse Mercator) projection. The Datum", Department of Agricultural and Forestry Engineering, Higher Technical School of Agricultural Engineering. Palencia, Valladolid University, pp. 65-72. [I. A. Fernández, "Localizaciones geográficas. Las coordenadas geográficas y la proyección UTM (Universal Transversa Mercator). El Datum", Departamento de Ingeniería Agrícola y Forestal, Escuela Técnica Superior de Ingenierías Agrarias. Palencia, Universidad de Valladolid, pp. 65-72]. Available online: http://www.cartesia.org/data/apuntes/cartografia/cartografia-geograficas-utm-datum.pdf.

[23] Official gazzete of Federal District, "Regulation of metropolitan transit", Chapter II: general traffic rules, pp. 2-3, Mexico City, Mexico, 2007. [Gaceta Oficial del Distrito Federal, "Reglamento de tránsito metropolitano", Capitulo II: De las Normas Generales de Circulación, pp. 2-3, Ciudad de México, México, 2007]. Available online: http://www.ssp.df.gob.mx/OrgPolicial/Documents/REGLAMENTO%20DE%20TRANSITO%20METROPOLITANO.pdf

[24] A. Coticchia and L. Surace, "Troubleshooting geodetic with mini programmable electronic calculators", Boll. Geodesia e S.A., Italy, n.1, pp.111-113,1978 [A. Coticchia and L. Surace, "Rizoluzione di problemi geodetici con le minicalcolatrici elettroniche programmabili", Boll. Geodesia e S.A., Italy, n. 1, 1978].

[25] T. Leal, A. Juárez and L. Oliva, "Android mobile application for monitoring truck routes in the Mexico City", XI International Congress of Engineering Electronics and Advanced Technologies (CIETA), Pamplona University, Cúcuta, Colombia, november 2015, unpublished. [T. Leal, A. Juárez and L. Oliva, "Aplicación móvil en Android para el monitoreo de rutas de camiones en la Ciudad de México", XI Congreso Internacional de Ingeniería Electrónica y Tecnologías de Avanzada (CIETA), Universidad de Pamplona, Cúcuta, Colombia, noviembre de 2015].

Estimación de Función deTransferencia en Lazo de Temperatura

Proceso De Lorenzo DL 2314

Cortés Ramírez U.
Departamento de Mecatrónica
Universidad Tecnológica de Huejotzingo
Santa Ana Xalmimilulco, Huejotzingo, Puebla, México
e-mail: ulises@cortes.mitmx.net

Castañeda Espinoza A.
Departamento de Mecatrónica
Universidad Tecnológica de Huejotzingo
Santa Ana Xalmimilulco, Huejotzingo, Puebla, México
e-mail: angelly_42@hotmail.com

Domínguez Sanchez V. F.
Departamento de Mecatrónica
Universidad Tecnológica de Huejotzingo
Santa Ana Xalmimilulco, Huejotzingo, Puebla, México
e-mail: victork@outlook.com

Pérez Pérez J.
Departamento de Mecatrónica
Universidad Tecnológica de Huejotzingo
Santa Ana Xalmimilulco, Huejotzingo, Puebla, México
e-mail: visioncure@hotmail.com

***Resumen*—En este trabajo se muestra la metodología para obtener la función de transferencia por métodos computacionales de un proceso, partiendo de su respuesta en lazo abierto, como planta se utilizó el lazo de temperatura del módulo De Lorenzo DL 2314, la adquisición de variables se realizó con una tarjeta CompactDAQ para graficar los datos en el entorno de desarrollo LabVIEW, y posteriormente exportarlos a MATLAB para su caracterización. El objetivo de este trabajo es que el laboratorio de Mecatrónica de la Universidad Tecnológica de Huejotzingo, cuente con una plataforma didáctica en la que sea posible encontrar su modelo matemático de una forma rápida y fiable, con la finalidad de implementar de manera teórica técnicas de control, a partir de la función de transferencia del sistema; con lo que alumnos de primeros cuatrimestres del área de ingeniería, tengan la habilidad de elaborar modelos de control para un sistema real, sin tener un dominio total en el modelado de sistemas dinámicos.**

Palabras clave; PID control, Data adquisition, Transfer function.

I. INTRODUCCION

El control automático desempeña un papel sumamente importante en los procesos de manufactura, industriales, navales, aeroespaciales, robótica, económicos, biológicos, y una de las tendencias actuales es la de contar con plataformas didácticas en la que sea posible su rápida comprensión e implementación.

Las plantas didácticas permiten al alumno interactuar directamente con los procesos, con el objetivo de facilitar la comprensión de los sistemas de control y permitir la puesta en marcha de los conceptos adquiridos en el aula de manera acelerada, con lo cual, el alumno puede reafirmar sus conocimientos teóricos aplicándolos en la práctica [1].

Como el control automático va ligado a, prácticamente, todas las ingenierías (eléctrica, electrónica, mecánica, sistemas, industrial, química), este documento ha sido desarrollado sin preferencia hacia alguna disciplina determinada, de tal manera que permita al alumno obtener la función de transferencia y simular la estrategia de control de manera teórica.

Como primer instancia se obtiene la respuesta en lazo abierto a través de un sistema de adquisición de datos y el software de desarrollo LabVIEW, empleando el modulo "DL 2314 De Lorenzo" como planta [2].

Posteriormente, se hallará el modelo matemático del sistema con la ayuda del software MATLAB, y se ubicara el lugar geométrico de las raíces, el conocimiento de la función de transferencia y la ubicación de polos y ceros, darán las bases necesarias para implementar de manera teórica un control PID para el lazo de temperatura del proceso De Lorenzo DL 2314.

II. ENTERNADOR DE CONTROL DE PROCESOS DL 2314

El proceso DL 2314 De Lorenzo mostrado en la Figura 1, es un entrenador para el control de procesos, este panel didáctico cuenta con un depósito presurizado con una capacidad de 5 litros y un juego de sensores y actuadores de nivel, presión, temperatura y flujo; un módulo de control, que contiene los circuitos para los sensores y actuadores; y, circuitos de control ON/OFF, proporcional y proporcional+integral+derivativo (PID).

De los elementos que conforman al módulo DL 2314 De Lorenzo son:

- Termo-resistencia de platino Pt 100.
- Termómetro de lectura directa bimetálico.
- Sensor de nivel LVDT.
- Sensor ON/OFF tipo on-reed.
- Sensor de flujo 8000 pulsos/litro.
- Visualizador de flujo.

- Galga extensiométrica.
- Manómetro de lectura directa.
- Bomba de recirculación: 6 litros/min., 12V/1.5A.
- Válvula motorizada.
- 4 válvulas manuales.
- Resistencia para calentamiento de agua: 48V, 200W
- Válvula de seguridad ajustada a 2.4 bar.
- Termostato de seguridad.
- Tubería de latón-

Figura 1. Módulo Didáctico DL 2314 De Lorenzo.

III. OBTENCIÓN DE LA FUNCIÓN DE TRANSFERENCIA

A. Respuesta en lazo abierto

El modulo didáctico DL 2314 De Lorenzo cuenta con un sensor de temperatura tipo PT-100, con el que se mide la temperatura del tanque y se ha conectado a un módulo de entradas analógicas NI 9219, integrado en un chasis CompactDAQ 9174 como se muestra en el diagrama de la Figura 2, la resistencia para calentar el agua está conectada a 48Volts de DC

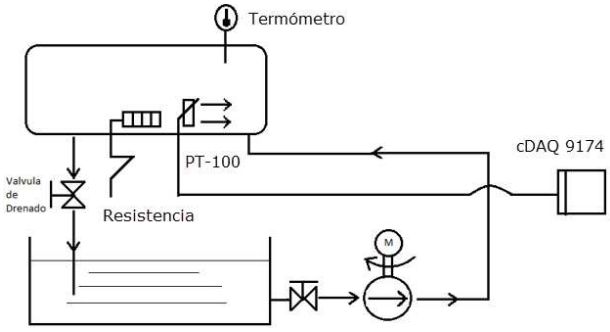

Figura 2. Diagrama de sensores y actuadores del proceso DL 2314.

La conexión del sensor a la entrada analógica se muestra en la Figura 3, la configuración del canal analógico se realizó a través de la aplicación NI-MAX, donde se indicó el modo de adquisición como "bajo demanda (On Demand)" ya que a través de software se establecerá el periodo de muestreo, y el tipo de sensor; es prescindible argumentar que este módulo ya tiene implementada la linealización del PT-100, por lo que ya no requiere circuitería adicional o programación para realizar este proceso

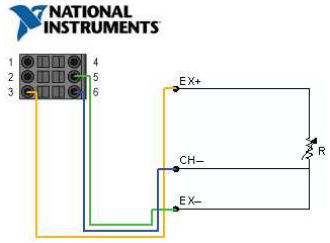

Figura 3. Conexión del sensor PT-100 al módulo NI 9219.

Para visualizar los datos obtenidos se desarrolló una interfaz de usuario mostrada en la Figura 4, la cual tiene dos gráficos, uno donde se muestra la valor de temperatura en tiempo real, y otro donde se visualiza la respuesta del sistema desde que empezó a correr la aplicación hasta que se pulsa el botón de "Stop"; además, cuenta con un indicador donde se muestra el periodo de muestreo, el cual se seleccionó de 0.5 segundos. Una vez finalizada esta aplicación los datos adquiridos serán exportados a Excel.

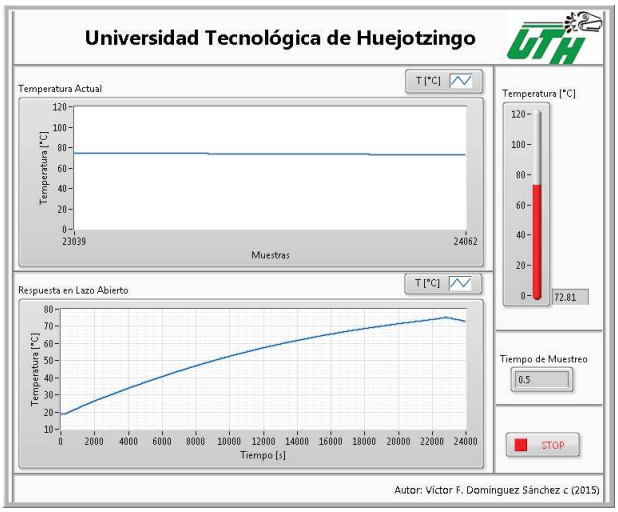

Figura 4. Interfaz de usuario para la adquisición de datos.

La temperatura máxima que alcanza el tanque es de 80 grados centígrados, el tiempo que le toma al sistema llegar desde la temperatura ambiente hasta la temperatura máxima es de aproximadamente 4 horas con 52 minutos.

B. Esteimación de la función de transferencia en Matlab.

Para obtener la función de transferencia del sistema, que para este caso en particular se trabajó con el lazo de temperatura, se designó un valor de entrada, el cual es el voltaje de alimentación de la resistencia de 48 Volts de DC equivalente a 80 grados centígrados ($U(s)$), y en el sensor se observó el cambio de temperatura con respecto al tiempo ($Y(s)$), como se ilustra en la Figura 5.

Para importar los datos almacenados de Excel a Matlab se empleó el código mostrado en la Figura 6, donde, *"Respuesta"* es el nombre del archivo que se exporto desde LabVIEW, *"y"* son los datos contenidos en el archivo y *"u"* es la temperatura máxima que alcanza el sistema, es prescindible denotar que tanto *"y" como "u"* son vectores que deben tener la misma dimensión.

$$G(s) = \frac{Y(s)}{U(s)} \qquad (1)$$

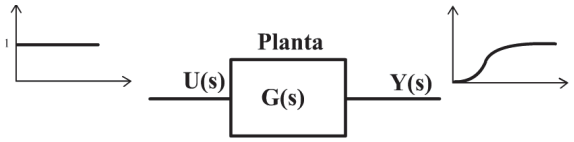

Figura 5. . Respuesta de la planta en Lazo Abierto.

```
Datos = xlsread('Respuesta');
%Datos del Sistema
y = Datos(:,2);     y = y(i:n+i-1);    %Respuesta en lazo abierto
u = linspace(80, 80, n)';
```

Figura 6. Código para extraer datos de Excel a MATLAB.

Una vez que la variables de entrada (u) y la salida (y) estén cargados en el Workspace de MATLAB, podemos graficar la respuesta del sistema como se muestra en la Figura 7.

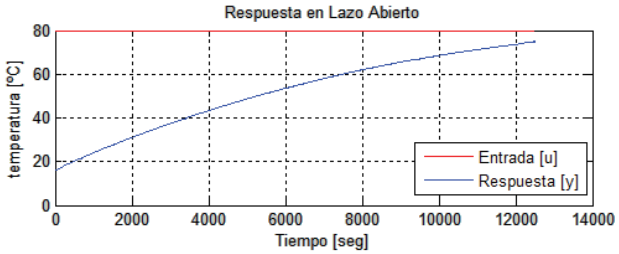

Figura 7. . Respuesta en lazo abierto del Lazo de Temperatura.

Para obtener la función de transferencia del sistema, se empleó la aplicación "System Identification Toolbox" de MATLAB, en la que necesitamos importar los datos en el dominio del tiempo de: la salida del sistema *y(t)*, la entrada de la planta *u(t)* equivalente al escalón unitario, el tiempo de inicio y el periodo de muestreo; como se muestra en la Figura 8 [3].

Para calcular la función de transferencia del sistema en la opción "Estimate" se elige la Opción "Transfer Function Models" en donde podremos elegir el número de polos y ceros, dependiendo del orden que tenga la función de transferencia será su aproximación con la respuesta real del sistema.

En la Figura 9, se muestra la respuesta de las funciones de transferencia estimadas, en el lado derecho con la leyenda *"Best Fits"* se enlista de la mejor aproximación a la peor ponderada con un valor porcentual, la respuesta del sistema pertenece al trazo de color negro, para la primera estimación identificada como tf1 se consideró un sistema de dos polos y ningún cero (80.9), en la segunda tf2 se tienen dos polos y un cero (97.93), para la tercera tf3 son dos polos y dos ceros (99.08), en la cuarta tf4 son tres polos y dos ceros (80.9), y para la quinta prueba tf5 son tres polos y tres ceros (99.08).

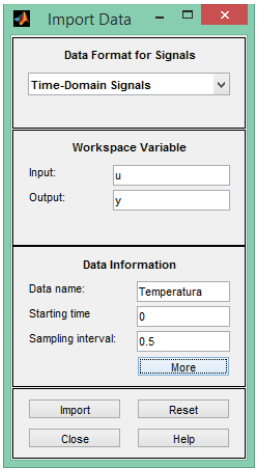

Figura 8. Datos importados en la aplicación System Identification.

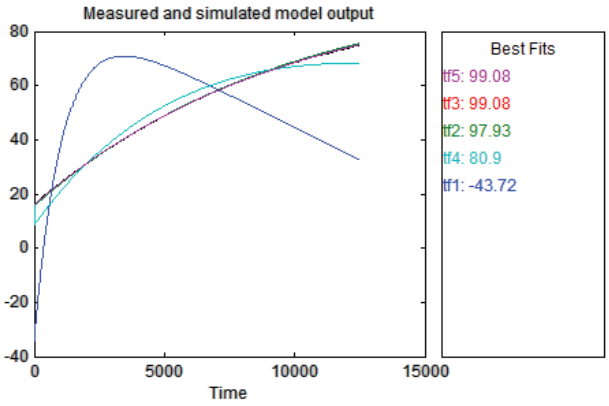

Figura 9. Funciones de Transferencia estimadas.

De la funciones de transferencia obtenidas podemos deducir que tf3 y tf5 tienen una mejor aproximación a la respuesta real del sistema, y corresponden a las que tienen dos y tres polos respectivamente, para lo que es posible argumentar que la función de transferencia equivalente al lazo de temperatura es tf3, dada como:

$$G = \frac{0.2025s^2 + 0.007951s + 4.96e-6}{s^2 + 0.03964s + 4.056e-6} \qquad (2)$$

En la Figura 10, se muestra la respuesta al escalón unitario de la función de transferencia estimada, y en la Figura 11, se muestran la ubicación de los polos y ceros, de lo que es posible observar que los polos están ubicados en el semiplano izquierdo, por lo que, el sistema es estable.

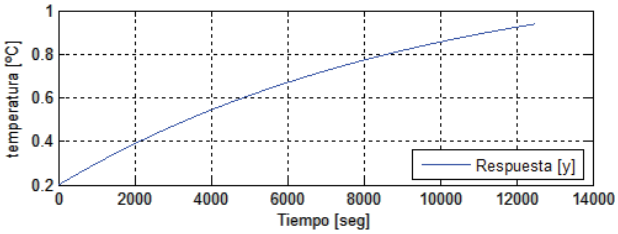

Figura 10. Respuesta al escalón unitario.

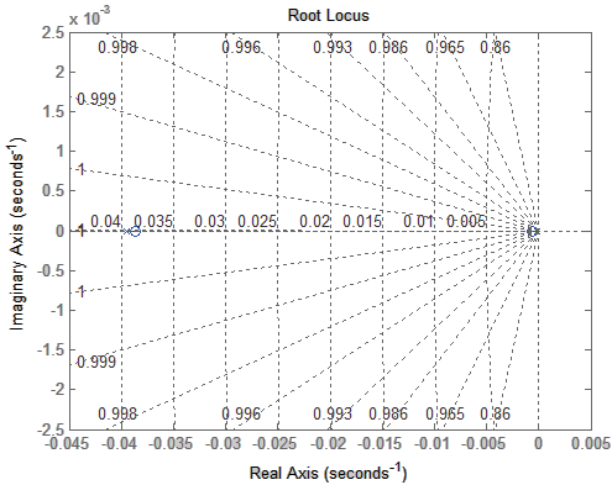

Figura 11. Ubicación de las raíces y polos.

IV. CALCULO DEL CONTROLADOR

A partir de la función de transferencia del sistema es posible calcular el control en lazo cerrado, por lo que se tendría un esquema como el que se muestra en la Figura 12, los tipos de controlador a considerar son: Proporcional (P), Proporcional + Integral (PI), y Proporcional + Integral + Derivativo (PID).

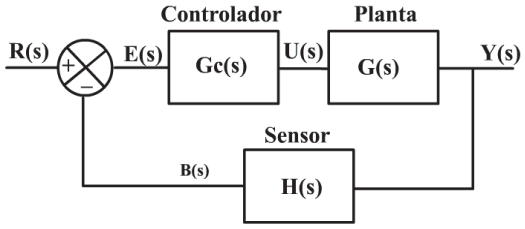

Figura 12. Sistema en lazo cerrado.

El cálculo del control puede realizarse con la aplicación PID Tuning de MATLAB, en la que tendremos que indicar la función de transferencia de la planta, y seleccionar el tipo de control a calcular, este toolbox.

De la teoría de control, el PID se puede expresar de dos maneras en su forma paralelo como [4]:

$$Gc(s) = K_p + \frac{K_i}{s} + K_d s \qquad (3)$$

O en su forma estándar como [5]:

$$Gc(s) = K_p\left(1 + \frac{1}{T_i s} + T_d s\right) \qquad (4)$$

Si en la aplicación System Identification de MATLAB se selecciona la opción "Estándar" el software calculara la ganancia proporcional, el tiempo de integración y derivativo; sin embargo, si se elige la opción "Paralelo" arrojara las ganancias proporcional, integral y derivativa. Para este caso en particular se trabajó la forma estándar, por lo que los tres controles quedan expresados como:

$$Gcp(s) = K_p = 1.221 \qquad (5)$$

$$Gcpi(s) = 0.48453\left(1 + \frac{1}{1319.0708}s\right) \qquad (6)$$

$$Gcpid(s) = 0.00097\left(1 + \frac{1}{0.093s} + 0.023s\right) \qquad (7)$$

donde: Gcp, pertenece al control proporcional; Gcpi, pertenece al control proporcinal + integral; Gcpid, es el control proporcional + integra + derivativo.

En la Figura 13, se muestra la respuesta teórica correspondiente al lazo de temperatura del proceso DL 2314 De Lorenzo, con los tres controles en lazo cerrado, es posible denotar que el control PID llega al valor deseado en un menor tiempo en comparación con el PI, y para el caso del control Proporcional tiene error en estado estable ya que no alcanza el valor deseado.

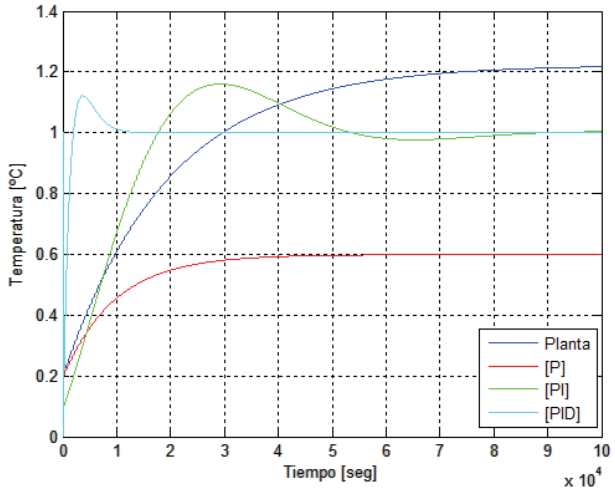

Figura 13. Respuesta de los controles calculados.

V. CONCLUSIONES

Del trabajo realizado podemos concluir que en efectos fue posible encontrar la funciona de transferencia del sistema por

métodos computacionales, ya que comparando el grafico de la Figura 7, correspondiente a la respuesta del sistema, con el grafico de la Figura 10 obtenido del escalón unitario de la función de transferencia, su aproximación es muy cercana, definido con un 99.08%.

Como principal aporte podemos resaltar que se ha realizado una modificación al proceso DL-2314 De Lorenzo, conectando el sensor de temperatura a la compactDAQ y la implementación de una interfaz de usuario, con lo que alumnos de primeros cuatrimestre se de la carrera de Mecatrónica podrán realizar el modelado de la planta usando métodos computacionales, como se realizó en este caso con MATLAB, con la finalidad de que puedan realizar de manera teórica la respuesta ante controladores PID, el cual puede ser realizado de forma continua o discreta.

Como trabajo futuro se contempla implementar el controlador de forma física al sistema, realizando la generación de señales a partir de la tarjeta de adquisición de datos CompactDAQ y poder controlar el voltaje de alimentación de la resistencia encargada de calentar el agua, además de contar con otras herramientas para la estimación de la función de transferencia como LabVIEW o Scilab.

VI. Referencias

[1] U. Cortés Ramírez, J. J. Vásquez Sanjuan y M. A. Alonso Pérez, «Plataforma didáctica de control automático basada en un reductor de tensión cd-cd,» *Pistas Educativas,* vol. XXXV, nº 108, pp. 389 - 411, 2014.

[2] De Lorenzo Of America Corp., «DE LORENZO,» 2015. [En línea]. Available: http://www.delorenzo.com.mx/. [Último acceso: 8 Septiembre 2015].

[3] MathWorks, «System Identification Toolbox,» The MathWorks inc., 2015. [En línea]. Available: http://www.mathworks.com/products/sysid/. [Último acceso: 09 Septiembre 2015].

[4] R. C. Dorf, Sistemas de Control Moderno, Madrid: Pearson, 2005.

[5] K. Ogata, Ingeniería de Control Moderna, Madrid, España: Pearson, 2010.

Design and Construction of a XY Cartesian Robot for Scanning Applications on Geological Studies

López-Pérez,Luis F
Universidad Autónoma de San Luis Potosí
San Luis Potosí, S.L.P.
Luis.perezperez2@hotmail.com

Rodríguez-Niño, Omar A.
Universidad Autónoma de San Luis Potosí
San Luis Potosí, S.L.P.
Alex.rdz.n@gmail.com

Madrigal-Méndez, Guillermo I.
Universidad Autónoma de San Luis Potosí
San Luis Potosí, S.L.P.ing.
isreal.madrigal@gmail.com

Solís-Saucedo, Gabriel S.
Universidad Autónoma de San Luis Potosí
San Luis Potosí, S.L.P.
sinuhe_skinhead@hotmail.com

Sanchez-Flores, Alejandra
Universidad Autónoma de San Luis Potosí
San Luis Potosí, S.L.P.
Alejandra.sanchez@uaslp.mx

González-Murillo, Luis. A.
Universidad Autónoma de San Luis Potosí
San Luis Potosí, S.L.P.
luis.murillo.uaslp@gmail.com

***Abstract*—This document describes the construction of a Cartesian robot whose goal is to perform scanning movement in a plane. The scanning paths are preset or can be defined in manual mode, both options are commanded using a teach pendant interfaced as a remote control. The full development includes: mechanical analysis and construction of the base structure, electronic interface, software development and tech pendant design.**

Keywords—cartesian robot; xy scanning; raspberry pi2.

I. INTRODUCTIÓN

In this paper is exposed the development of the "XY Cartesian Robot" project (based on a request from the Institute of Geology of UASLP) to perform studies on rough terrain or geological samples with a set of camera / scanner / laser. The most important user requirements are: flexibility structure to be placed vertically or horizontally; the weight must not exceed 40kg to maintain portability; it should have a load capacity of 2.5Kg to support a set of light and camera; the dimensions must be 1.3m x 0.4m; motion accuracy shall be +/- 0.265 mm with a maximum speed of 0.15m / min; and finally a teach pendant as the user control (i.e. independent of any PC). The construction of the robot was proposed within the framework of the course Integrator Project for the career of Engineering in Mechatronics (IMT) of UASLP.

The project was divided into three stages: design and construction of the mechanical structure, implementation of the electrical system and software development.

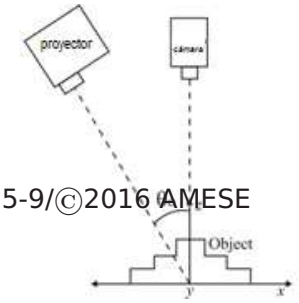

II. MECHANICAL DEVELOPMENT

The established goals of mechanical system are: to design a base of a steel support subject to the load cases considered; designing the size and shape of the structure for all positions required by the application; stand design of the camera or laser; selection of materials to ensure robustness; set the system to the movement of actuators that will support the terminal body.

A. Base structure

The configuration of the mechanical structure is selected as a fixed table because thus offer advantages of robustness in the system and a compact structure, noting that this should be as light as possible without exposing the stability of the same.

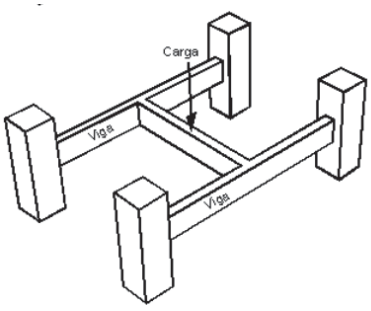

Fig. 1. Schematic diagram of critical force applied to the structure

Fig. 2. Fringe projection configuration

For practical purposes, we analyzed the structure only at its most critical point, with the maximum weight on it (even if the full weight is supported along the rails). Thus we corroborated if this is able to operate under different loads and positions effortlessly. Futhermore aluminum profiles BOSCH 22.5 mm x 180 mm, as it is widely used in CNC machining centers for its ability to hold pieces of different geometry was selected, its length and its lateral grooving, can simultaneously placing the projector and camera which are larger optical devices that will work with the robot.

B. *Optical devices support*

The support is formed of two parts (Fig. 2): a fixed support for a laser device (used in fringe projection application) and an articulated support for the camera (used at the same time to capture the image).

The laser device is very light, so the bracket was engineered using laser cut 12mm thick acrylic, drilled later they became the setting for both laser and for attaching it to the desk.

The placement of the camera is a bit more complex, as the camera Lumenera LT225 is much smaller in size and mobility should be adjusted at an angle θ. Therefore a profile section BOSCH 15mm x 180mm was used. To provide the camera angle 40x40 BOSCH an articulated support (Fig. 3) that can be used for joints mobile or fixed profiles at any angle, with an area of 180 ° is used and also features an auxiliary graduation of 15 °. User can tighten using a lever and adjust comfortably to the desired angle.

Fig. 3 Articulated support

Fig. 4. Complete mechanical structure

C. *Screw power*

It is a device that is responsible for transforming an angular movement into a linear shape and is usually used for power transmission. The function of this element is completed by including motors to control movement about two different axes. To solve the screw concerning our theoretical framework, we should question the torque that is required to raise and lower the load, being parallel to the screw axis loads. Considering a total weight of 10 Kg (base and optical devices and support weights), the torque analysis showed the torque rise is 0.32 Nm, and torque lowering is -0.315 Nm. The total torque is defined by the sum of torques, and the torque required supplied by the engine $T_{motor} > T_t$. So, a Nema engine with 1,9 Nm is selected. Complete mechanical structure is shown in Fig. 4.

The ball circulation system needs maximum geometric precision, to ensure smooth running at all speeds, with minimal friction.

Ground ball spindles are manufactured in two types of internal return, so that we get good compact nuts, without external projections.

III. ELÉCTRIC AND ELECTRONIC CIRCUITRY

This section set forth electrical, electronic and power "XY Cartesian Robot" circuits. The block diagram representing the electrical system is shown in Fig. 5. We briefly explain the whole analysis which consists of electronic systems and electrical power cabinet and how they were selected, resulting in generating the plans of circuits, in the armed electrical structure and the final assembly. It was determined that the project was suitable for assembling a cabinet without external wiring which gives us the following advantages: transporting more efficiently and comfortably, connection cables do not disturb for transportation, allows field use and isolate power systems.

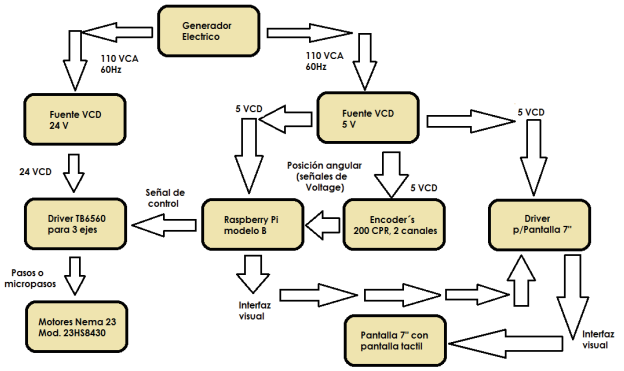

Fig. 5. Block diagram of electrical system

The specifications of Avago encoder devices are: 2 channels of square output waveforms (from the difference between these two signals the position of the effector in the two axes respectively is computed), 200 steps or counts per revolution, 5-pin input and output (figure), the supply voltage is 5 volts, two output communication channels "A" and "B", the ground ("GND").

"SYC semiconductors and components" limit switches were chosen, based on detectors beam or phototransistors, to avoid damage of the robot. The circuitry is installed by a small "PCB" which is bolted to the structure.

The engines used in the projects are bipolar stepper motors 200 steps per revolution, Nema 23, 1.8 A (shown in Fig. 6), 23HS8430 model, with this high accuracy is ensured.

To control engines a "TB6560AHQ" card of Toshiba was added per engine.

The fan is permanently activated to prevent heating of the 3-axis driver board, with a diameter of 120 mm and connected directly to the power cabinet by a supply of 5 volts.

For wiring feed and control signals (5 V) 18 AWG and 20 AWG wires are used. For connecting the generator, which transmits 127VCA, 14 AWG wire was used for heavy duty.

A. *Control case*

An ADC converter is included for the joystick interface. The coded readings form the converter are sent to the Raspberry Pi and interpreted as a plane position.

The housing was designed in CAD and printed using a 3D printer. The main goal was the user comfort and keep safe the electronics parts as the Raspberry Pi and the ADC. Also here are added buttons joystick, potentiometer and screen for handling the device.

Fig. 6. Engines and circuitry mounted in vertical position

B.

C.

Fig. 7. 3D Printed Case

D. *Screen*

In order to show options to user by a visual interface, it was resorted to using a touch screen (Fig. 5) 7 inches with a resolution of 800x480 pixels (WVGA). For the standards of today's resolution can be very poor but for this application is sufficient to display the required information.

Resistive touch interface is connected via USB to the Raspberry Pi, it is also fed through this port. The image is delivered via HDMI.

The panel brightness is controlled via PWM, but for the use it will be preferred to leave default.

IV. SOFTWARE

In this section the development of software for the raspberry pi 2 will be discussed. Since it is a robot manipulator can be driven without the need for other computer equipment.

A. *Programming language*

Software development depends entirely on the type of language used. During the project we chose C ++. The IDE selected to develop the software was Qt Creator for its ease of use and have been used previously with excellent results.

B. *Threads*

According to the nature of the applications certain processes will take a lot of time to be completed, this may cause the main thread of the program be blocked during execution and as a result cannot be used until the code run finish. To avoid the main thread being blocked, parallel threads process recursive tasks while main thread is dedicated only to display values and to attend events that occur at the interface.

Specifically yarns have been used provided by Qt in QThread class. Each instance of this class represents a program thread. Each thread performs a specific action program triggered by some event that occurs within the main thread. WiringPi

To access the GPIO pins of the Raspberry Pi was necessary to use the library WiringPi being a major developed for use in C and C ++. Among the advantages that can be found this quick configuration of ports as input or output and

enabling SPI communication that was used in the project to communicate with the ADC.

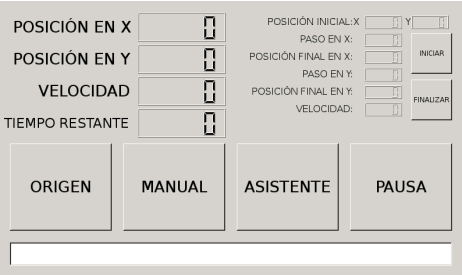

Fig. 8. Main window

Visual interface

Since the robot can be manipulated from a control box, manual or automatic mode can be used the GUI was designed looking for ease of use.

The visual interface is a touch-screen. The user can navigate into different windows; in the Main window (seen in Fig. 8) the program captures the functional options: manual or automatic mode; start position; end position. Speed and time remaining are displayed if used in automatic mode. The buttons placed on the inside function as selectors of basic functions; the first is the Origen button whose function is to lead the team to the position (0, 0). The button with the Manual option allows the free use of equipment with either analog or digital joystick buttons.

As mentioned, the source takes the robot to the absolute initial position, located in the lower left corner; this position was selected to avoid negative values be confusing to the end user. Moreover, while this option is selected the program waits until the robot reaches the absolute initial position is executed.

A simple state machine was implemented to deactivate the engines when a final position is detected by the input signals from GPIO 5 6 GPIO ports, which are connected to optical sensors and limit switches.

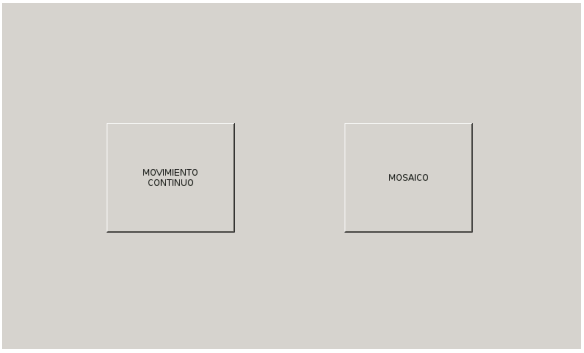

Fig. 9. Selection window

C. Manual mode

In manual mode, the user selects the program to manipulate the robot using the joystick manipulator and digital buttons. To get a correct reading of the values provided by the ADC a function that will convert the ADC value to adapted information for the Raspberry P. The x and y axes of the joystick and the speed value provided by potentiometer are the values that will be delivered to the ADC channels.

D. Wizard

The wizard is the main part of the software as it is here where movements are generated to be registered in memory and routes be setup to use, there are basically two movements; continuous movement, intended to be used in the laser scanning line and mosaic movement (*Fig. 9*), which seeks to photograph a previously configured user defined area, it is clear that this mode covers two of the three applications of the robot; with scanning fringe projection and digitization of images.

When user enters either mode, the values are inserted into the main window and refer to the limits of the rectangle is to scan or sweep the laser.

V. Conclusions

The Cartesian robot XY is located now in the Laboratory of Image Analysis and Analogical Modeling (LAIMA) of the Institute of Geology at the Autonomous University of San Luis Potosí. The first integration tests were performed using a PC (Fig. 10).

The work efficiency according to the customer specifications is around 85%. A brief description is below:

- The full weight is 10Kg, below the maximum required.
- In general, dimensions were correctly implemented. Mobility is accomplished since the structure can be transported on a big car.
- The robot structure has been tested in the Laboratory proposed in several configurations, keeping the desired scan movement.
- Speed is less than initially proposed by the customer.
- Fringe projection function runs correctly.
- User interface is functional, and easy to handle.

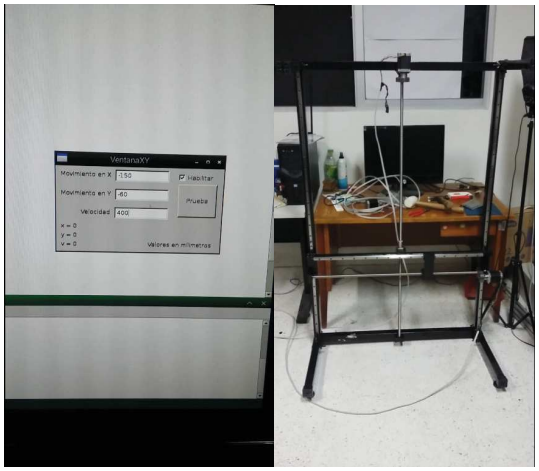

Fig. 10. Performing Integration tests

Some improvements needed are listed below:

- The closed loop for control implementation is missing. The system remains as an open loop system. Even this fault, the robot resolution and positioning, rest in acceptable error margins (because the speed required is slow and paths have not abrupt change of sense). A very important improvement will be the correction of output signals based on measuring from encoders (these are currently connected).
- Error detection implementation. The robot can be programmed to detect many physical problems (for example: obstacle detection, engine malfunction, overload, etc). This, for a safety operation.
- The teach pendant remains in mid construction. The customer asks for a more comfortable device. A probable solution should be to use a higher resolution 3D printer to avoid rough texture. The full ensemble is pending.

The testing results of the robot performance will be reported by the client as processes are carried out for which the robot was made. A more exhaustive evaluation could be based on the acquired image quality.

A. REFERENCES

1. Stephen J. Chapman. Maquinas Eléctricas. Mc Graw Hill. (2005).
2. Diseño de Ingeniería Mecánica. (mechanical engineering design); 9th edition; Editorial Mcgraw-Hill (2010)
3. Richard G. Budynas y J. Keith Nisbett. Diseño en ingeniería mecánica de Shigley. Mc Graw Hill. (2008)
4. J. A. S. Pachón. Implementación de un sistema posicional con motores paso a paso y servo controlado por computador. Bogotá. (2009)
5. H. H. R. Cubides y L. C. S. Heredia. Prototipo de maquinado para fabricación de circuitos impresos con fresadora. Colombia: XX. (2010)
6. Meier C.F, Ríos J. A., Pereyra H. Manual Czerweny, Motores Paso a Paso" Parte III. Gálvez Pcia de Santa Fe. (1980)
7. Silvia, Guardati, Buemo, *Estructura de datos orientada a objetos: Algoritmos con C++*. Pearson Educación. México, (2007)
8. Javier García de Jalón, José Ignacio Rodríguez, José María Sarriegui, Alfonso Brazalez., *Aprenda C++ como si estuviera en primero*. Universidad de Navarra. San Sebastián, abril 1998
9. Tornillos de bolas Recirculculantes: http://www.apiro.com/husilloscatalogo.html
10. Catalogo tornillos de potencia (Tablas de diámetros tornillos unificados) http://www.mecapedia.uji.es/catalogos/tornillo_de_potencia.com.htm
11. Guía y conceptos básicos para SolidWorks Pag (9-26) https://www.solidworks.com/sw/docs/Student_WB_2011_ESP.pdf
12. Productos ABB (botonera): http://www.abb.com.mx/cawp/seitp202/
13. Tarjeta Driver Toshiba TB6560: http://www.roboticacnc.com.mx/controladoras_cnc.html
14. Rexroth Bosch Group. Elementos básicos de mecánica, 57, 149, 155-156. Obtenido de: http://www.perfilesbosch.com.mx/
15. Lt225-datasheet. Obtenido de: http://www.lumenera.com/usb3/index.php
16. LC532-5-3-F (16x65). Obtenido de: http://www.picotronic.de/picopage/de/product/detail/id/2030
17. Brochure_1776w. Obtenido de: http://www.epson.com/cgi-bin/Store/jsp/Product.do?UseCookie=yes&sku=V11H476020
18. Canon-EF-28-135mm-f-3.5-5.6-IS-USM-Lens. Obtenido de: http://www.canon.com/c-museum/en/product/ef342.html

Integrando Múltiples Sensores RGBD en la Nube

Alberto Pacheco, Isidro Robledo, Elisabet González
División de Estudios de Posgrado e Investigación
Instituto Tecnológico de Chihuahua
Chihuahua, México
{apacheco, irobledo, egonzalez}@itchihuahua.edu.mx

***Abstract*— La creciente popularidad y disponibilidad de sensores de profundidad embebidos brindan una interesante oportunidad para diseñar innovadoras aplicaciones provistas con interfaces naturales donde un usuario interactúa por medio de comandos de voz y gestos corporales (cara, cuerpo y manos). El presente trabajo tiene por objetivo integrar en tiempo real la información de diversos sensores de profundidad, para lo cual se propone el diseño de un eficiente protocolo en red que permita generar personajes animados como resultado de dicha integración de información y ofrecerlo como un servicio en la nube de tal forma que cualquier cliente en red, independientemente de su dispositivo y sistema operativo pueda reproducir dichas animaciones en tiempo real, bajo un novedoso y compacto formato de *video streaming* basado en gráficos vectoriales escalables independientes de la resolución de la pantalla del dispositivo.**

Keywords—captura de movimiento humano; sensores RGBD; imágenes de profundidad; protocolo de tiempo real

I. Introduccion

Entre los elementos de comportamiento natural que pueden ser usados para interactuar con sistemas computacionales están: la interacción basada en gestos mediante interfaces multitáctil, el reconocimiento de voz, el seguimiento de los ojos, la identificación de expresiones faciales, el reconocimiento de las emociones, entre otros. En base a un sondeo de la literatura disponible en el área [1-6], sugerimos la siguiente clasificación para las interfaces de usuario (**fig. 1**):

- Interfaz basada en texto.
- Interfaz gráfica (GUI).
- Interfaz natural (NUI), que se subdivide en:
  - Interfaz tangible o multitáctil (TUI).
  - Interfaz de audio (AUI).
  - Interfaz de vision (VUI), subdivida en:
    - Procesando imágenes de color (RGB).
    - Com imágenes de color y profundidad (RGBD).

En una interfaz VUI (**fig. 1**) se interactúa recurriendo a un sistema de visión capaz de reconocer gestos y capturar movimientos (*motion capture*) ya sea procesando imágenes de color (RGB) de una cámara o usando imágenes compuestas de color y profundidad (RGBD), donde por cada pixel RGB además de su posición (x,y), hay una estimación de profundidad D.

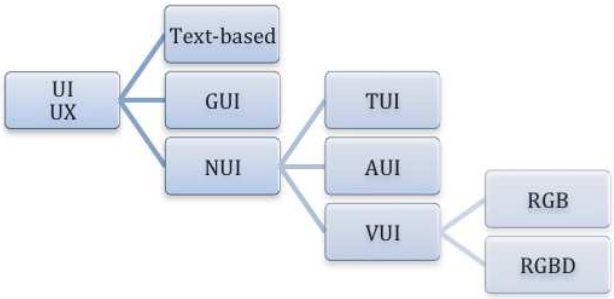

Fig. 1. Una clasificación de interfaces de usuario.

II. Planteamiento del Problema

A. Objetivo del trabajo

Se propone desarrollar una interfaz natural VUI, cuyo reto consiste en enlazar tres sensores RGBD para rastrear los gestos de la cara, manos y cuerpo de tres usuarios distintos (**fig. 2**), desarrollando un protocolo y un software para integrar de manera simultánea todos estos movimientos en un solo personaje animado que pueda consultarse desde cualquier dispositivo conectado a la red.

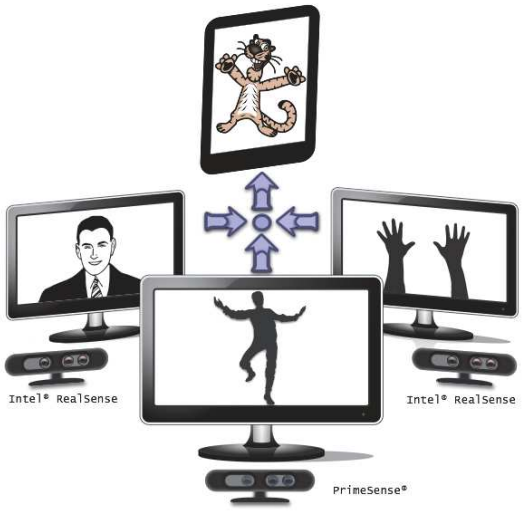

Fig. 2. Integrando datos de varios sensores RGBD en la nube para crear un personaje animado.

B. *Sensores de Profundidad RGBD*

A continuación se detallan las especificaciones de cada uno de los sensores RGBD utilizados. Teniendo en primer instancia el sensor de PrimeSense®, que resulta ser muy similar al sensor Kinect en su primer versión, que fue fabricado por el mismo PrimeSense® antes de cerrar a finales de 2013, debido a que fue adquirida por la compañia Apple. Este sensor RGBD es más pequeño, económico y más simple que un sensor Kinect, solo tiene que conectarse a una computadora a través de un cable USB y puede usar software de OpenNI, un driver de código abierto y no requiere del uso exclusivo del SDK de Microsoft limitado al sistema Windows®, sino por el contrario, puede programarse, como fue usado en este proyecto, con otros lenguajes como Java y Processing y otras plataformas como OS X para Apple Mac. El sensor de profundidad de PrimeSense® tiene un rango de alcance de 0.8 a 3.5m y una baja resolución en imágenes de profundidad (640x480). El sensor es capaz de detectar posturas del cuerpo sin incluir manos y detalles del rostro, razón misma por la que sólo se usó en el proyecto sólo para capturar movimiento del cuerpo; los gestos de la cara y las manos se detectaron con el sensor que se describe a continuación.

Fig. 3. Sensor RGBD PrimeSense® Carmine 1.08

El sensor RealSense® de Intel modelo F200 es pequeño, económico, de corto alcance (0.2 a 1.2m). Genera imágenes de profundidad de 640x480 y video de alta resolución 1080p. Este sensor resulta apropiado para capturar y reconocer expresiones faciales y gestos de la mano. Sin embargo, su SDK requiere de Microsoft Visual Studio® corriendo desde luego, bajo Windows® versión 8 ó 10. Existen ya disponibles en el mercado diversas dispositivos móviles que tienen embebido dicho sensor, como por ejemplo, las computadoras HP Spectre x2, Dell Inspiron 17 y 24, Lenovo IdeaPad Y700, entre otros.

Fig. 4. Sensor RGBD Intel® RealSense F200

III. DISEÑO DE UN API Y UN PROTOCOLO

A. *Metodología*

Tanto en el mercado de herramientas de software, repositorios de proyectos de código abierto y en la literatura técnica, no fue posible identificar un sistema que fuera capaz de integrar los datos capturados en una configuración de más de dos sensores RGBD distintos, motivo por el cual se decidió proponer un esquema propio y desarrollar las herramientas necesarias para lograr dicho objetivo. Para el desarrollo de este proyecto se plantearon las siguientes etapas de diseño:

- Diseño de un esquema de representación para una marioneta digital basada en gráficos escalables;
- Diseño de un API para generar animaciones con dichos personajes o marionetas digitales;
- Diseño de un protocolo de red en tiempo real para transferir datos capturados y reproducir cada animación.

Para la representación de los personajes animados se utilizaron gráficos vectoriales escalables SVG del estándar del consorcio Web [7]. Una vez establecidas las definiciones y estructura interna del archivo XML, estos personajes articulados fueron creados y desarrollados por varios estudiantes de licenciatura y posgrado como parte de un proyecto de generación de narrativas digitales educativas reportadas en [8].

Para que un programa pueda interactuar con estos personajes se definió un API genérico y reutilizable, independiente de la plataforma y del lenguaje de programación, trabajo que ha sido previamente publicado [9]. Este API abstracto fue representado en UML 2.5 (**fig. 5**) y nos permite animar y manipular cualquier personaje representado en SVG.

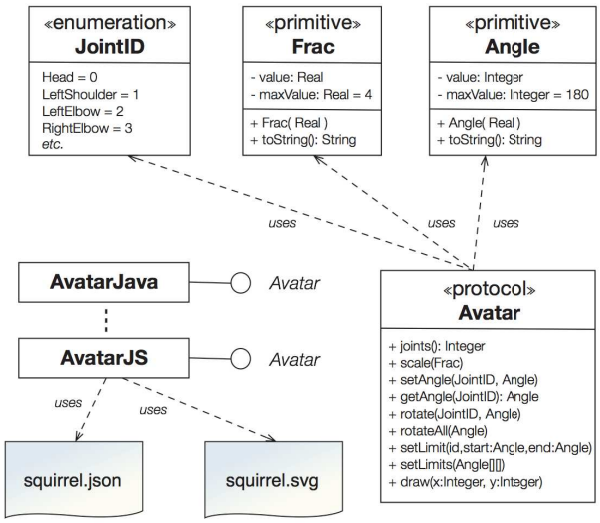

Fig. 5. Diseño del API representado en UML 2.5

B. *Arquitectura*

Para el diseño del protocolo, tomando como base el API de marionetas programables descrito, se estableció y publicó en [11] la siguiente arquitectura (**fig. 6**), misma que se compone de los siguientes módulos:

- **Módulos de captura:** Son clientes heterogéneos que por medio de un protocolo específico y muy ligero, inyectan de manera continua un flujo de datos de captura de movimiento proveniente de distintas estaciones con sensores RGBD operadas por distintos usuarios. En los módulos de captura de movimiento los usuarios registran sus gestos y movimientos frente a un sensor RGBD. Los datos son mapeados a una secuencia de descriptores específico para luego ser filtrados y compactados para ser enviados de manera eficiente a un servidor. El protocolo de tiempo real que enlaza los puertos A-B (**fig. 6**) tiene un diseño compacto, independiente de la plataforma, de datos estructurados y compactados a nivel binario, conteniendo además, un registro preciso del tiempo de captura. Como primera opción se ha considerado para ello, usar sockets.
- **Servidor para fusión RGBD:** Este servidor acopia todos los flujos de datos provenientes de los distintos sensores RGBD, para posteriormente integrar las variaciones de cada parte corporal captada para obtener cada cuadro de animación. Es importante notar que tanto los flujos de entrada como salida, no están atados a ninguna marioneta en específico, dejando así abierta la posibilidad de que cada cliente de animación designe el personaje deseado. Se cuenta además en el servidor un repositorio de metadatos descritos en JSON y los diseños de marionetas digitales representados en gráficos vectoriales SVG (**fig. 5**).
- **Reproductores para el flujo de cuadros de animación:** Clientes heterogéneos que se comunican entre los puertos C-D (**fig. 6**) con otro protocolo específico y ligero para transmitir descriptores y elementos estructurados para facilitar la animación vectorial de marionetas digitales articuladas. Este módulo forma parte de los clientes implementados en diversas plataformas móviles que son capaces de visualizar un personaje animado en base el flujo de datos (*streaming*) recibido desde la nube.

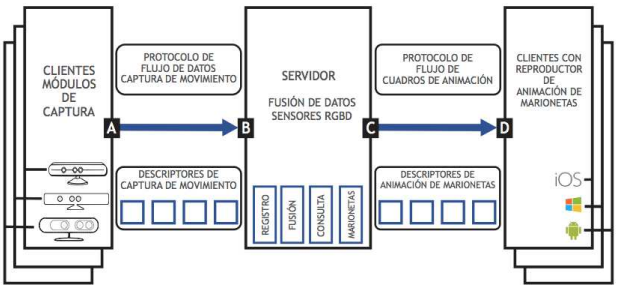

Fig. 6. Arquitectura propuesta para integrar los datos de los sensores RGBD.

IV. Resultados y trabajo futuro

Para el proceso de representación de una marioneta digital en SVG se ha establecido un procedimiento para elaborar una marioneta articulada, obteniéndose como resultado la edición de un manual de usuario y un conjunto de videos ilustrativos del proceso [8]. Esto ha permitido que un buen número de estudiantes haya realizado en sus proyectos de narrativas digitales sus propios personajes, teniéndose a la fecha un acervo y catálogo de más de 30 personajes disponibles tanto en los módulos de captura como en la adaptación del entorno de programación de Khan Academy publicado en [10]. Una limitante del diseño actual a ser superada en el futuro inmediato es cómo integrar las tres especificaciones de cara, manos y cuerpo en una sola, es decir, que en una marioneta programable podamos controlar cada elemento del cuerpo, cara y manos a través de un sólo API y gráfico vectorial.

Entre los beneficios obtenidos encontramos que, la especificación del API diseñada (**fig. 5**) ha permitido implementar de manera más ágil, efectiva y portable diversos prototipos, uno de los cuales, denominado marionetas programables [10], consistió precisamente en realizar la adaptación del editor en línea interactivo de Khan Academy (**fig. 7**) para manipular un personaje para la enseñanza de la programación, donde un estudiante a nivel principiante puede escribir sencillas instrucciones de Javascript en un editor interactivo dentro de una página web para crear sus propias animaciones usando cualquiera de los personajes disponibles. Actualmente se esta trabajando en diversas extensiones del API para realizar animaciones más complejas, tales como la detección de colisiones y la posibilidad de tomar y soltar objetos con las manos del personaje.

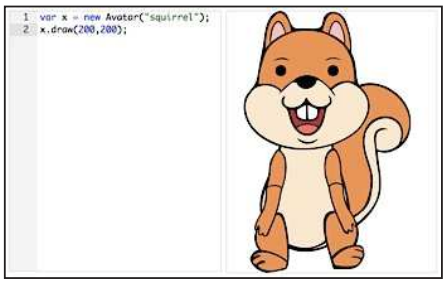

Fig. 7. Editor del entorno de programación de Khan Academy modificado para soportar el API propuesto para animar marionetas programables.

Actualmente ya se tienen implementados los módulos de captura para ambos sensores: para el sensor PrimeSense® se construyo el módulo en Java y Processing bajo OS X y para el sensor RealSense® de Intel se uso C# bajo Windows 10. También ya se tienen implementadas parcialmente las interfaces de usuario de los clientes para dispositivos móviles: el cliente web está escrito en HTML5 y ProcessingJS; el cliente de iOS está escrito en Swift 2.1; el cliente de escritorio esta desarrollado en Java y Processing para OS X, Windows y Linux. El prototipo del servidor está implementado en Python, Java y PHP, mismo que usa de momento, solo las primitivas de las librerías básicas de sockets. Para la codificación y decodificación del protocolo de datos de captura de gestos y movimientos se recurrió al uso de operaciones a nivel de bits,

teniéndose por ejemplo la codificación de un gesto facial en una secuencia de 64 bits. Este empaquetamiento es muy compacto y eficiente, pero al momento de portar el código para implementar por ejemplo, el cliente web en Javascript, se ha encontrado que dicho lenguaje no soporta enteros de 64 bits de manera nativa. Otro problema detectado es la carencia de soporte de enteros sin signo de 64 bits en Java, tanto a nivel de la representación de un tipo de dato, como de las operaciones de bits y estructuras de control de flujo, tales como el uso de la sentencia switch/case, por lo que se recurrirá al uso de librerías, conversiones y funciones en dichos lenguajes, lo cual decrementa la eficiencia y claridad del código resultante. Afortunadamente, los lenguajes de programación C# y Swift poseen un soporte nativo muy completo para enteros sin signo de 64 bits. Por otro lado, el protocolo de aplicación en red para los cuadros de animación es simplemente una representación numérica de las instrucciones y sus parámetros respectivos.

También a nivel de la representación del API diseñada en UML 2.5, hemos encontrado que todos los lenguajes adolecen, de una u otra forma, ciertos elementos para la especificación de APIs a un nivel elevado de abstracción. Destaca sin embargo, el nuevo lenguaje de programación Swift, el cual esta muy cercano a lograr un mapeo directo entre una especificación en UML 2.5 y el propio lenguaje, gracias a ciertos elementos del lenguaje, tales como los protocolos y extensiones, así como a la capacidad de renombrar con un *alias* cualquier definición de clase o tipo primitivo, e.g. para renombrar el Int de Swift al Integer de UML sólo se requirió declarar lo siguiente: `typealias Integer = Int.` Desafortunadamente, Java no ofrece algún mecanismo de abstracción similar. Por otro lado, todos los lenguajes utilizados (Java, C#, Swift, Javascript) no ofrecen un mecanismo nativo que permita especificar nuevos tipos de datos "primitivos" acotados a un dominio o rango de valores específico, e.g. `Angle: Integer = -180...180`

Finalmente, a nivel del análisis de los datos generados en los módulos de captura, se ha detectado que de manera intermitente se producen datos inconsistentes debido al ruido de la señal proveniente del sensor, mismos que tendrán que filtrarse en una etapa posterior. Por otra parte, consideramos que es posible serializar el flujo de datos a una representación aproximada más compacta. Por ejemplo, si representamos con las primitivas del API una porción del movimiento del codo izquierdo (primer columna en **fig. 8**), esta puede ser simplificada a desplazamientos angulares (segunda columna **fig. 8**) y también es factible analizar si existe una tendencia lineal y aproximarla (sección final **fig. 8**). Aplicando la programación funcional que soporta este nuevo lenguaje, sería interesante derivar para un cierto intervalo, su ecuación `fn()` de desplazamiento angular como parámetro, e.g. `setNext(2,fn)`

`avatar.angle(2,88.2)`	`avatar.angle(2,88.2)`
`avatar.angle(2,89.3)`	`avatar.rotate(2,1.1)`
`avatar.angle(2,90.2)`	`avatar.rotate(2,0.9)`
`avatar.angle(2,91.4)`	`avatar.rotate(2,1.2)`
`avatar.setNext(2,1.0)` `avatar.next(2)`	

Fig. 8. Análisis y simplificación de una secuencia de datos capturados.

V. Conclusiones

Se ha presentado el diseño de un sistema capaz de integrar en tiempo real de manera coherente la información proveniente de tres sensores de profundidad RGBD distintos para proveer posteriormente un servicio en la nube capaz de suministrar un *stream* de animaciones vectoriales. Este es un trabajo en proceso, del cual ya se tienen avances significativos, tales como: a) la implementación del API en diversos dispositivos móviles de distintas plataformas (iOS, Web, OS X, Linux, Windows); b) Los módulos de captura para los distintos sensores de profundidad RGBD, específicamente el sensor PrimeSense® implementado en Java bajo OS X y el sensor Intel RealSense® implementado en C# bajo Windows 10. A pesar de tener pruebas preliminares sobre el protocolo de red para la transferencia de descriptores, aún falta integrar los distintos APIs y protocolos (cara, manos y cuerpo) y realizar las pruebas de validación y rendimiento apropiadas para este nuevo protocolo de tiempo real para aplicaciones web de animación basada en gráficos vectoriales que ofrecerá sin duda la gran ventaja de transmitir video con un *bitrate* significativamente menor al esquema *streaming* convencional, incluso sin incorporar esquemas de compresión de datos.

Referencias

[1] M. R. Ogiela y T. Hachaj, "Natural user interfaces for exploring and modeling medical images and defining gesture description technology", en Natural user interfaces in medical image analysis: Cognitive analysis of brain and carotid artery images, Springer International Publishing, Switzerland, 2015, pp. 205-275.

[2] O. Schreer, P. Eisert, P. Kauff, R. Tanger y R. Englert, "Towards robust intuitive vision-based user interfaces", en IEEE Int. Conf. on Multimedia and Expo, 2006, pp. 62-72.

[3] D. Wigdor y D. Wixon, "Brave NUI world: Designing natural user interfaces for touch and gesture", Morgan Kaufmann, Burlington, MA, 2011.

[4] O. Shaer y E. Hornecker, "Tangible user interfaces: Past, present, and future directions", Now Publishers Inc. Delft, 2010.

[5] R. Steinmetz y K. Nahrstedt, "User interfaces", en Multimedia applications, Springer-Verlag Berlin, Heidelberg, 2004, pp. 151-172.

[6] M.H. Cohen, J.P. Giangola y J. Balogh, "Introduction to voice user interfaces", en Voice user interface design, Pearson Education Inc., Boston, MA, 2004, pp. 3-14.

[7] A. Pacheco y R. Cruz, "Animating 2D digital puppets using motion capture and vectorial graphics", The Graphical Web 2014, Winchester, UK, 2014.

[8] A. Pacheco, M. Ramírez, C. Guzmán y E. González, "Marionetas digitales: Tecnología emergente para narrar historias con personajes animados mediante la captura digital de movimiento", en R. Cruz, G. López y A. Pacheco, "Tecnologías emergentes en la educación", Pearson Educación, 2015, pp. 161-177.

[9] A. Pacheco, E. González e I. Robledo, "Diseño de un API de control para marionetas digitales", Memorias de la Electro 2015 – ISSN 1405-2172. Chihuahua, México, 2015.

[10] A. Pacheco y E. González, "Marionetas digitales programables: Un entorno interactivo en línea para la introducción a la programación", Memorias Encuentro Nacional de Computación. Ensenada, B.C., 2015

[11] A. Pacheco, I. Robledo y E. González, "Plataforma de fusión de sensores RGBD para la animación de marionetas digitales", Memorias del Encuentro Nacional de Computación. Ensenada, B.C., 2015

Domótica: Prototipo de vivienda para personas con déficit auditivo

La tecnología como apoyo a personas con capacidades diferentes

Torres-Frausto, David A., Villegas-Téllez Rodrigo, De los Reyes-Quiroz, Fernando,
Raya-Mata J. Salvador, Martínez-González, M. Elizabeth.
Coordinación de Ingeniería en Informática
Instituto Tecnológico Superior de Irapuato (ITESI)
Irapuato, Gto., México
datorres@itesi.edu.mx, rovillegas@itesi.edu.mx, fedelosreyes@itesi.edu.mx

***Abstract*— El propósito del proyecto es que, al construir un prototipo a escala simulando la vivienda de una persona con discapacidad auditiva, este brinde seguridad a través de sensores controlados por una aplicación móvil.**

El prototipo brinda seguridad a las personas con discapacidad auditiva a través de sus múltiples circuitos controlados por medio de tecnología Bluetooth; en conjunto con componentes electrónicos implementados en placas Arduino. Dichas tecnologías realizan la función de mantener informados a los habitantes de la vivienda cuando alguien entra en sus hogares sin permiso, mientras están ausentes y a distancia del peligro.

Keywords—domótica; discapacidad; securidad; vivienda; audición.

I. INTRODUCCIÓN

La Domótica tiene sus orígenes en la década de los 70's, con el auge debido al progreso de tres grandes sectores de la tecnología: telecomunicaciones, electrónica e informática.

Este es el término que se utiliza para denominar la ingeniería que integra el control y supervisión de los elementos existentes de una vivienda; surge de la unión de *domus* (casa) y *tica* (automática). En sus inicios, la domótica solo se utilizaba en lugares donde el consumo de energía era muy elevado, como es el caso de hospitales y hoteles. Con el tiempo, el desarrollo de la tecnología impulso e incremento la construcción de edificaciones inteligentes.

Implantada desde los años noventa, la domótica se ha desarrollado a gran escala desde que se desarrollaron las redes de comunicación, ya sea por cable o uso de Wi-Fi.

Con el avance de las redes de comunicación, la *Domótica* hace uso de los *Sistemas Ubicuos*. Un sistema ubicuo es un modelo de computación innovador en el que la tecnología se encuentra integrada en elementos de la vida real; generando así una interacción con el ambiente.

Ésta interacción en situaciones cotidianas, no siempre es posible; ya que pueden presentarse diversas complicaciones en las personas, tales como discapacidades temporales o permanentes.

De acuerdo con el censo de población y vivienda del 2010 realizado por el INEGI, se encontró que en México existen 5 ´739,270 personas con algún tipo de limitación o discapacidad; de las cuales 694,464 presentan algún tipo de problema para escuchar.

Las personas con algún grado de déficit auditivo se encuentran en constante riesgo de accidentes; ya que el perder su habilidad de escuchar hace que la experiencia visual desarrolle un papel importante para poder percibir los peligros de su alrededor. Por ésta razón, el presente proyecto se centra en construir un prototipo a escala de una vivienda automatizada que contenga sensores, controlados por una aplicación; permitiendo brindar seguridad a personas con déficit auditivo

II. DESARROLLO

A. Área de Desarrollo

El déficit auditivo o sordera es una degradación definitiva de la audición que proviene de una alteración del sistema auditivo. Una pérdida auditiva provoca repercusiones en la vida cotidiana y puede apartar rápidamente a las personas afectadas de toda vida social.

La pérdida de audición puede estar provocada por el envejecimiento lento y progresivo de la audición o por la sobre-exposición al ruido; sea cual sea el origen (profesional, escuchar música demasiado alta, tumor benigno del nervio auditivo, por medicamentos, entre otras causas).

La pérdida auditiva también se presenta en personas adultas como es el caso de las la personas de la tercera edad. La *presbiacusia*; es decir, un déficit auditivo causado por el envejecimiento del oído, es un padecimiento común en la población adulta mayor. Sin embargo, con los cuidados

necesarios y una detección temprana, se pueden tratar los efectos de la sordera.

Un padecimiento auditivo tiene importantes consecuencias sobre la vida de los adultos mayores. Las personas suelen experimentar cansancio físico, tensión muscular, estrés, problemas de alimentación y sueño. Lo anterior es producto del agotamiento que sufre un adulto mayor cuando se esfuerza por entender y darse entender a causa de la pérdida auditiva.

A nivel psicológico se produce ansiedad y estrés, mientras que a nivel social los adultos mayores sienten vergüenza porque tienen que pedir constantemente que les repitan las cosas. Esto a su vez, genera sentimientos de culpabilidad, depresión y aislamiento.

Ante esto, una opción ampliamente utilizada es el uso de algunas ayudas técnicas, como los avisos luminosos, que son dispositivos que se iluminan para dar información de alguna incidencia que, de manera habitual, se realiza de forma sonora. Por ejemplo, el timbre de la puerta de casa, el aviso de recreo en el colegio, entre otros.

B. *Requerimientos*

El Centro Estatal de Rehabilitación (INGUDIS), ofrece a las personas con discapacidad un espacio en el que puedan recibir tratamiento especializado, integral y humano. Se imparten programas especiales de intervención familiar para personas con discapacidad, se cuenta con el programa de *Inclusión Laboral para personas con discapacidad* y se realizan campañas de detección de discapacidad y promoción a la salud.

El centro atiende a 700 pacientes con problemas auditivos, de los cuales la mayoría son adultos de la tercera edad. Los principales problemas que el centro trata son: la Hipoacusia y la patología del lenguaje.

INGUDIS permitió realizar entrevistas a sus pacientes, de las cuales surgieron los siguientes requerimientos:

Timbre luminoso. Debido al problema que enfrentan las personas con déficit auditivo, no son totalmente capaces de determinar cuando alguien toque a su puerta. Es por esto que este timbre permite que las personas estén al tanto de la presencia de alguien en sus hogares.

Sensores de movimiento. Se encuentran ubicados en las habitaciones del prototipo, para que las personas estén al tanto de la presencia de alguien en su hogar. Se instaló un panel principal, además de contenerlo en una aplicación móvil. Dicho panel permite a la persona con déficit auditivo, visualizar el movimiento desde donde esté por medio de luces de distinto color. Las luces se determinan de acuerdo a la habitación.

Sistema de Seguridad - Sensor de Proximidad. Empleado para protección y seguridad de las personas que habiten la vivienda. La funcionalidad general de dicho sistema de seguridad involucra el uso de una pantalla y un sensor, el cual detecta la distancia entre distintos objetos y lo muestra en una pantalla. Esto permitirá a los habitantes de las viviendas estar enterados de la distancia de un posible peligro para sus vidas u hogares.

C. *Evaluación de Herramientas de Desarrollo*

Como parte del desarrollo del proyecto, se analizaron distintas plataformas con el fin de seleccionar la más adecuada para elaborar la aplicación necesaria para el proyecto, las cuales se presentan a continuación:

Arduino Software. Es una plataforma de prototipado electrónico de diseño abierto. Una placa arduino contiene un microchip que se puede programar. De forma adicional, se pueden conectar sensores para medir condiciones; con lo que se pueden controlar otros objetos para que reaccionen a esas condiciones, o que reaccionen cuando un interruptor es accionado.

Fritzing. Es un programa de automatización en diseño electrónico libre, que busca ayudar a diseñadores para pasar de prototipos (usando, por ejemplo, placas de pruebas) hacia los productos finales con una interfaz dinámica. El desarrollo en esta herramienta permite a los usuarios documentar sus prototipos, compartirlos con los demás, enseñar electrónica en el salón de clases, y crear un diseño para la fabricación de circuitos impresos de manera profesional.

MIT App Inventor. Es una herramienta de programación basada en bloques que permite iniciar la programación y construcción en menor tiempo que con lenguajes más tradicionales, basados en texto. Es una herramienta de código abierto que pretende realizar la programación y creación de aplicaciones accesibles a una amplia gama de audiencias.

En la Tabla I se enlistan las características bajo las cuales se realizó la comparativa con otras plataformas de desarrollo.

TABLA I. CARACTERÍSTICAS DE LA PLATAFORMA DE DESARROLLO

CARACTERÍSTICAS	MIT App Inventor	Modkit	Scratch	S4A	Minibloq	Ardublock
Librería de Block	X	X			X	X
Lenguaje de programación Kawa.	X					
Aplicaciones sencillas, aptas para el SO Android.	X				X	X
Fácil de utilizar	X				X	X
Software libre	X				X	X
Multiplataforma	X	X				
Generador de Código	X				X	X

D. *Desarrollo del Prototipo*

El diseño completo del modelo utilizado para el prototipo de vivienda domótica es el que se muestra en la Figura 1, utilizado una escala de 1:10 cm, para que resulte la equivalencia en metros.

Fig. 1. Modelo a escala de vivienda domótica

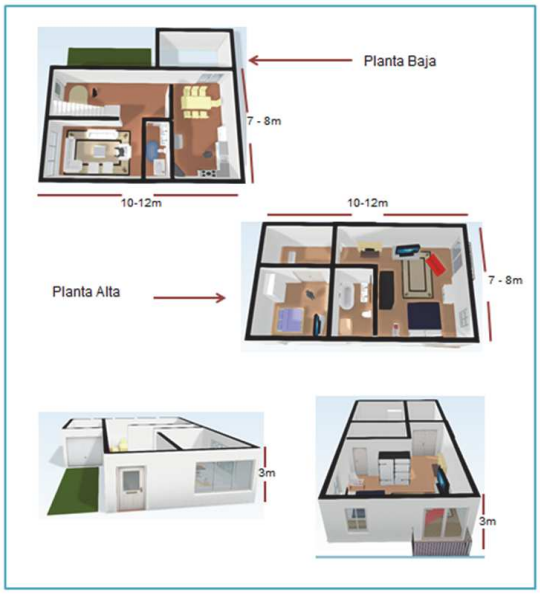

Durante la construcción de la maqueta se determinó el lugar donde se colocarían los componentes electrónicos para poder realizar las correspondientes modificaciones.

Posteriormente, se colocaron los componentes electrónicos y se probó su correcto funcionamiento individual.

En la Fig. 2 se muestra el esquema del timbre luminoso implementado en el prototipo. De igual forma, la Fig. 3 muestra el esquema del sensor de movimiento, la Fig. 4 el esquema del sensor de proximidad, y la Fig. 5 el esquema de la alarma laser.

Fig 2. Esquema timbre luminoso

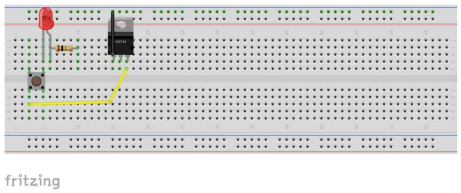

Fig. 3. Esquema sensor de movimiento

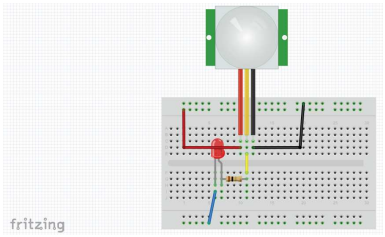

Fig 4. Esquema sensor de proximidad

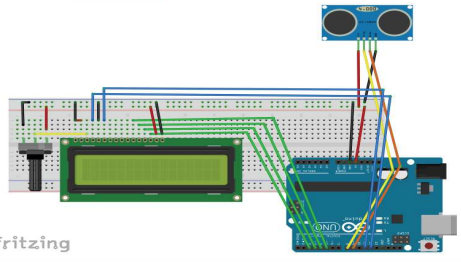

Fig 5. Esquema alarma laser

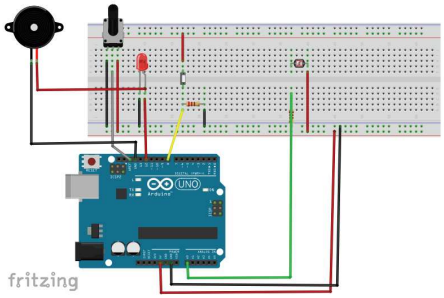

Una vez instalados los componentes, se realizaron diferentes pruebas para verificar el funcionamiento integrando todos ellos. Entre las pruebas efectuadas se encuentran:

- Funcionamiento con energía de 5V.
- Funcionamiento con diferente intensidad de luz (en el caso de los sensores).
- Conectividad Bluetooth (compatible con protocolo Bluetooth 2.0).
- Rango de distancia (en el caso de los sensores).

Posterior a la implementación de los componentes electrónicos, se desarrolló la parte de software en *MIT App Inventor*. La Fig. 6 muestra el bloque de instrucciones correspondiente.

Fig. 6. Codificación llamada de emergencia

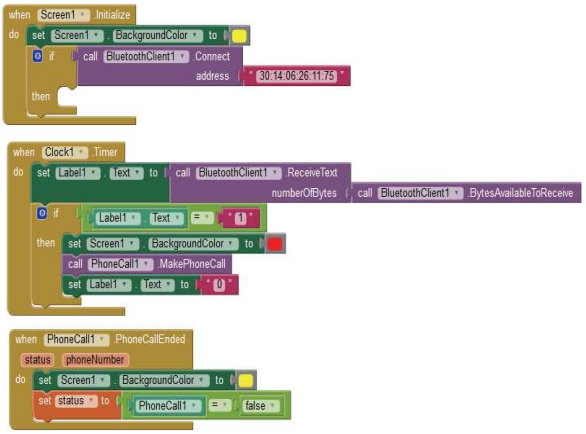

Como parte de la validación del Proyecto, el INGUDIS permitió mostrar a los pacientes el prototipo terminado; ante lo cual se obtuvo retroalimentación de éstos.

III. Conclusiones

El prototipo cumple con el uso de sensores de movimiento controlado por medio de una aplicación, desarrollada e instalada en un dispositivo móvil.

El prototipo permitió que las personas encuestadas dieran una opinión positiva, ya que para estas el prototipo brinda seguridad a las personas con déficit auditivo.

Con lo anterior, se obtiene que mediante un prototipo de vivienda automatizada es posible crear un entorno seguro para las personas con déficit auditivo, que les permita realizar sus actividades diarias.

De acuerdo a los datos recabados, los pacientes de INGUDIS perciben el prototipo con un nivel de seguridad del 90%. Además, de las cinco actividades presentadas a los encuestados, el 95% percibe que todas son de utilidad para ellos.

Como trabajo futuro, se tienen varias propuestas de mejora para el prototipo:

- Colocar los sensores en todas las habitaciones, pasillos o exteriores, y no solo en las recámaras.
- El panel de control que se manejó en la sala del prototipo puede ser instalado en algún otro sitio, o implementarse en la aplicación móvil
- La actividad *Llamada de emergencia* puede ser utilizada con más sensores, e implementar más de una de las actividades en su diseño.
- La actividad, *Alarma Láser* puede ser activada o desactivada desde otro tipo de interruptor, o implementarse en la aplicación móvil.
- A la actividad *Timbre Luminoso* puede implementársele un *buzzer*, para que adicional a la funcionalidad que ya tiene, ésta emita sonido.

Cabe mencionar que las mejoras anteriormente descritas van dirigidas a cualquier tipo de persona, y no solo a personas con algún tipo de discapacidad auditiva; ya que se busca que lo implementado sirva a cualquier persona que habite la vivienda.

Agradecimientos

Agradecemos al Centro Estatal de Rehabilitación (INGUDIS), por las facilidades prestadas para la realización de éste proyecto.

References

1. Arduino. (2015). Arduino. Obtenido de https://www.arduino.cc/en/pmwiki.php?n=Main/ArduinoBoardUno
2. Artigas. J, R. E.-N. (2008). Asociación Española de Pediatría. Obtenido de https://www.aeped.es/sites/default/files/documentos/24-lenguaje.pdf
3. Asociación Española de Domótica, I. p. (2008). Cómo ahorrar energía instalando domótica en su vivienda. Recuperado el Febrero de 2015, de http://www.idae.es/uploads/documentos/documentos_11187_domotica_en_su_vivienda_c7a81517.pdf
4. Bautista, L. A. (s/f). Blogger.com. Obtenido de http://data-collection-and-reports.blogspot.mx/
5. Bogado, P. E. (2012). Universidad Empresarial Siglo XXI . Recuperado en Febrero de 2015, de Prototipo de un sistema domótico. Seguridad y Confort .
6. Bonalde, G. (07 de Junio de 2009). slideshare. Recuperado el Febrero de 2015, de Computacion Ubicua: http://es.slideshare.net/gbonalde/computacion-ubicua
7. Candia, S. (Dirección). (2014). Domótica: Arduino & Android - Bluetooth [Tesis].
8. Center, T. I. (2012). i2cat. Recuperado el Febrero de 2015, de SENSORDROID: http://www.i2cat.net/es/proyectos/sensordroid
9. Centro Estatal de Rehabilitación . (2015). Acercamiento 01. [O. R. Terapeuta, Dirección] Irapuato, Guanajuato, México.
10. Citilab. (2013). S4A. Obtenido de http://s4a.cat/index_es.html
11. Confederación Española de Familias de Personas Sordas . (s.f.). Obtenido de http://www.fiapas.es/EPORTAL_DOCS/GENERAL/FIAPAS/DOC-cw47fa08e7c7e35/DOSSIERPADRES.pdf
12. Consejeria de Educación. Cultura y Deporte. (25 de septiembre de 2014). slideshare. Obtenido de http://es.slideshare.net/cantabrobots30/ardublock-39508070
13. Cuevas J, M. J. (2002). El Protocolo x10: Una solución Antigua a Problemas actuales. Recuperado el Febrero de 2015, de http://www.lcc.uma.es/~pedro/publications/566_art.pdf
14. Culkin, J. (s.f.). Arduino. Obtenido de http://playground.arduino.cc/uploads/Main/arduino_comic_v0004.pdf
15. D., B. (02 de JUNIO de 2014). blogsEQI. Recuperado el FEBRERO de 2015, de Songdo. La ciudad más inteligente y sostenible en el planeta: http://www.eoi.es/blogs/danielbarbosa/2014/06/02/songdo-la-ciudad-mas-inteligente-y-sostenible-en-el-planeta/
16. deMesa, J. A. (septiembre de 2005). academia.edu. Recuperado el Febrero de 2015, de Panorama de la Computación Ubicua: http://www.academia.edu/2748419/Panorama_de_la_Computaci%C3%B3n_Ubicua
17. Electronica, I. e. (Dirección). (2012). Casa Domotica con Arduino.
18. Gillig, J. U. (2012). Obtenido de http://multiplo.org/wp-content/uploads/2013/05/Minibloq.v0.8.Beta_.UserManual.20120125.pdf
19. González, H. G. (Dirección). (2013). Casa Ubicua Uaslp 2013 Computación Ubicua.
20. Informatica Hoy. (2007-2012). Informatica Hoy. Obtenido de http://www.informatica-hoy.com.ar/telefonos-celulares/Que-es-Bluetooth.php
21. Informatica, I. T. (2010). Inteligencia AmbientalL: El Futuro para la Computación Ubicua y MóvilL. Actualidad TIC, 10-13.
22. Lifelong Kindergarten en el MIT Media Lab. (s.f.). Scratch. Obtenido de https://scratch.mit.edu/about/

Sistemas Embebidos. Aplicaciones y Tendencias

ISBN 978-607-9394-05-9